1-2004

Manganese Toxicokinetics at the Blood-Brain Barrier

Robert A. Yokel
University of Kentucky, ryokel@email.uky.edu

Janelle S. Crossgrove
University of Kentucky

RESEARCH REPORT

HEALTH EFFECTS INSTITUTE

Number 119
January 2004

Manganese Toxicokinetics at the Blood–Brain Barrier

Robert A Yokel and Janelle S Crossgrove

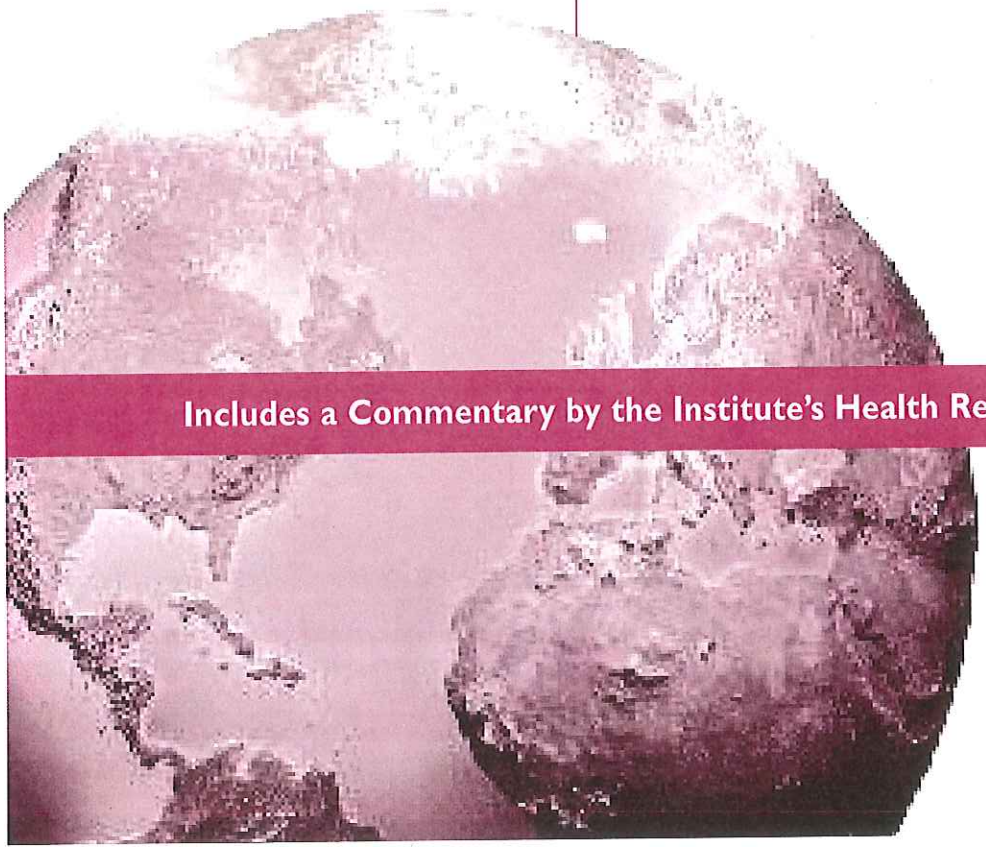

Includes a Commentary by the Institute's Health Review Committee

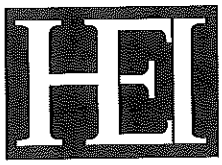

HEALTH
EFFECTS
INSTITUTE

The Health Effects Institute was chartered in 1980 as an independent and unbiased research organization to provide high quality, impartial, and relevant science on the health effects of emissions from motor vehicles, fuels, and other environmental sources. All results are provided to industry and government sponsors, other key decisionmakers, the scientific community, and the public. HEI funds research on all major pollutants, including air toxics, carbon monoxide, diesel exhaust, nitrogen oxides, ozone, and particulate matter. The Institute periodically engages in special review and evaluation of key questions in science that are highly relevant to the regulatory process. To date, HEI has supported more than 220 projects at institutions in North America, Europe, and Asia and has published over 160 Research Reports and Special Reports.

Typically, HEI receives half of its core funds from the US Environmental Protection Agency and half from 28 worldwide manufacturers and marketers of motor vehicles and engines who do business in the United States. Other public and private organizations periodically support special projects or certain research programs. Regardless of funding sources, HEI exercises complete autonomy in setting its research priorities and in reaching its conclusions.

An independent Board of Directors governs HEI. The Institute's Health Research Committee develops HEI's five-year Strategic Plan and initiates and oversees HEI-funded research. The Health Review Committee independently reviews all HEI research and provides a Commentary on the work's scientific quality and regulatory relevance. Both Committees draw distinguished scientists who are independent of sponsors and bring wide-ranging multidisciplinary expertise.

The results of each project and its Commentary are communicated widely through HEI's home page, Annual Conference, publications, and presentations to professional societies, legislative bodies, and public agencies.

HEI STATEMENT
Synopsis of Research Report 119

Manganese Transport at the Blood–Brain Barrier

Metals comprise a large group of elements. Many of these metals are essential to living systems because they participate in a variety of biological functions, but they can be toxic at concentrations above those needed in the body. Exposure to some metals has been found to cause neurologic damage—for instance, in children exposed to low levels of lead via ingestion and in workers exposed to moderate to high levels of manganese via inhalation. Metals are present as particles or particle components in emissions from vehicles and other sources and have been implicated as one possible reason for the adverse health effects associated with airborne particulate matter exposure.

As part of its research program to address the possible health effects of metal emissions from motor vehicles and fuels, an HEI workshop held in February 1998 focused in part on fuel additives containing cerium, iron, and manganese. One such additive, methylcyclopentadienyl manganese tricarbonyl (MMT), is an antiknock agent that also reduces emissions of nitrogen oxides. Because MMT contains manganese, controversy exists about whether its widespread use as a fuel additive may pose a health risk to the general population. MMT is currently used in Canada and parts of the United States. Pending completion of a mandated series of emissions and toxicity tests in 2004, the US Environmental Protection Agency will determine whether regulation of MMT as a fuel additive is necessary.

After the 1998 workshop, HEI issued a Request for Preliminary Applications, RFPA 98-4, *Research on Metals Emitted by Motor Vehicles*. In response, Dr Robert Yokel proposed to study the mechanisms by which manganese enters and leaves the brain across the blood–brain barrier and, in particular, whether transporter molecules are involved. The blood–brain barrier is a function of the walls of small blood vessels that shield the brain from possibly harmful molecules. Certain molecules may cross the blood–brain barrier via diffusion or via carrier-mediated transport. HEI funded Dr Yokel's study in part because it would be the first direct investigation of whether specific transporter molecules remove manganese from the brain. Evidence for carrier-mediated transport of manganese out of the brain would be particularly interesting in that it would indicate a possible mechanism for preventing manganese accumulation, thereby affecting the likelihood of neurologic damage from chronic low-level exposure.

APPROACH

In this study Drs Yokel and Crossgrove used in vivo brain perfusion in rats as well as in vitro tests in several cell lines to assess specific characteristics of manganese transport, such as pH and energy dependence. Manganese transport rates were compared with those of sucrose and dextran, which do not easily cross the blood–brain barrier. Experiments to identify putative transporters focused on known transport molecules, such as a divalent metal transporter, a monocarboxylate transporter, and calcium channels. The investigators used both a genetic approach (comparing results in rats with and without a functional divalent metal transporter) and a pharmacologic approach (evaluating manganese transport function in the presence of several selective inhibitors).

RESULTS AND INTERPRETATION

Yokel and Crossgrove have provided convincing evidence that manganese enters the brain via carrier-mediated transport, confirming and extending previous observations. They also are the first to have shown that manganese leaves the brain via diffusion only, a much slower process than carrier-mediated transport. Experiments conducted to identify the transporters involved in manganese uptake into the brain suggested that the divalent metal transporter DMT-1, which is specific for iron uptake, is not involved. However, the identity of the putative manganese transporters remains elusive.

This Statement, prepared by the Health Effects Institute, summarizes a research project funded by HEI and conducted by Drs Robert A Yokel and Janelle S Crossgrove at the University of Kentucky Medical Center, Lexington KY. The following Research Report contains both the detailed Investigators' Report and a Commentary on the study prepared by the Institute's Health Review Committee.

The finding that manganese transport out of the brain occurs via the slow process of diffusion, rather than via carrier-mediated transport, is important: it suggests that no mechanism exists to protect the brain from accumulating manganese. This finding has important implications for neurotoxicity resulting from chronic manganese exposure. Although Yokel and Crossgrove studied manganese transport rates in rats, their observations may be relevant to humans because transport mechanisms at the blood–brain barrier are similar in rodents and humans. Their results support the current understanding that the potential for manganese accumulation in the brain should be considered when assessing risk from exposure to manganese in the environment. Future studies and risk assessments should also consider susceptible populations (such as people with iron deficiencies or liver disease) who may be at greater risk from increased manganese uptake. New research would be useful to confirm the lack of a carrier-mediated transport system for removing manganese from the brain and to address the relevance of these findings to humans.

Library of Congress Catalog Number for the HEI Report Series: WA 754 R432.
The paper in this publication meets the minimum standard requirements of the ANSI Standard Z39.48-1984 (Permanence of Paper) effective with Report 21 in December 1988; and effective with Report 92 in 1999 the paper is recycled from at least 30% postconsumer waste with Reports 25, 26, 32, 51, 65 Parts IV, VIII, and IX, 91, 105, and 117 excepted. These excepted Reports are printed on acid-free coated paper.

HEALTH EFFECTS INSTITUTE

CONTENTS

Research Report 119

Manganese Toxicokinetics at the Blood–Brain Barrier

Robert A Yokel and Janelle S Crossgrove

College of Pharmacy and Graduate Center for Toxicology, University of Kentucky Medical Center, Lexington, Kentucky

HEI STATEMENT

This Statement is a nontechnical summary of the Investigators' Report and the Health Review Committee's Commentary.

PREFACE

This Preface describes the general regulatory and scientific background for the HEI Research Program that produced this and other reports on related topics.

INVESTIGATORS' REPORT

When an HEI-funded study is completed, the investigators submit a final report. The Investigators' Report is first examined by three ouside technical reviewers and a biostatistician. The report and the reviewers' comments are then evaluated by members of the HEI Health Review Committee, who had no role in selecting or managing the project. During the review process, the investigators have an opportunity to exchange comments with the Review Committee and, if necessary, revise the report.

Continued

COMMENTARY Health Review Committee

The Commentary about the Investigators' Report is prepared by the HEI Health Review Committee and staff. Its purpose is to place the study into a broader scientific context, to point out its strengths and limitations, and to discuss remaining uncertainties and implications of the findings for public health.

RELATED HEI PUBLICATIONS

Publishing History: This document was posted as a preprint on *www.healtheffects.org* and then finalized for print.

Citation for whole document:

Yokel RA, Crossgrove JS. January 2004. Manganese Toxicokinetics at the Blood–Brain Barrier. Research Report 119. Health Effects Institute, Boston MA.

When specifying a section of this report, cite it as a chapter of the whole document.

PREFACE

Metals comprise a large group of elements that can exist in several valence states and combine with a large number of organic and inorganic compounds. Many metals are critical for living systems because they participate in essential cellular, physiologic, and structural functions. For example, iron is part of the hemoglobin molecule that carries oxygen in the blood, and zinc is a component of insulin, body fluids, and many enzymes. At concentrations above those needed for essential biological functions, however, these metals are toxic. Other metals, such as arsenic and lead, are toxic to most living systems, even at low levels (US Agency for Toxic Substances and Disease Registry 1999, 2000a). Toxic effects caused by metals range from damage to the immune system, kidneys, heart, brain, reproductive organs, and fetus, to gene damage and cancer. Metal accumulation in the environment raises concern because metals are not biodegradable.

Metals can be emitted into the environment from a number of sources. From motor vehicles, emissions may come from components such as catalytic converters, lubrication oil, and brake pads and from fuels and fuel additives used to reduce certain emissions or improve engine performance. It is important to explore possible exposure to and the possible adverse effects of these metal compounds. In February 1998 HEI held a workshop to gather information about the use of metals as fuel additives and about other exposures to metals from mobile sources. A goal of the workshop was to help HEI define priorities for a research program on metals by gaining a better understanding of which additives were most likely to be used, how much was known about their chemical form and concentration in emissions, the toxicity of these emissions, and what research was being conducted. As a result of the workshop, HEI issued a Request for Preliminary Applications: RFPA 98-4, *Research on Metals Emitted by Motor Vehicles.*

Among other metals proposed for use in fuel additives, such as cerium and iron (used in ferrocene), HEI was interested in manganese as a component of methylcyclopentadienyl manganese tricarbonyl (MMT*), which was developed as an antiknock agent but also reduces emissions of nitrogen oxide. MMT has been used for more than 50 years, initially as an alternative to tetraethyl lead and currently as an alternative to fuel additives such as methyl *tert*-butyl ether (MTBE), which is being phased out due to groundwater contamination from leaking underground fuel-storage tanks.

Proposed increases in use of MMT have raised concerns that higher concentrations of manganese in ambient air may pose a threat to public health (Kaiser 2003). Some researchers have compared the risk of manganese exposure in the general population to that of exposure to lead in the environment, in part because both metals affect the nervous system. A large body of occupational data, dating back to the 1837, has provided strong evidence that high concentrations of manganese inhaled by miners and other workers cause neurologic symptoms similar to those of Parkinson disease. Whether or not manganese may cause neurologic damage at low concentrations, and the extent to which it may accumulate in the brain and thereby cause long-term effects, however, are unclear. As a prelude to addressing many of these questions, the study by Yokel and Crossgrove described here evaluated the mechanisms by which manganese may enter and leave the brain.

REGULATORY BACKGROUND

MMT was developed in 1954 by the producer of tetraethyl lead, and small-scale use of the additive in the United States began shortly thereafter. After new government regulations issued in 1970 required registration of all fuel additives, MMT was registered for use in both leaded and unleaded fuel. In 1977 the Clean Air Act Amendments spurred creation of a program to ensure the operability of automobile emission control systems in the United States, and as a result some additives suspected of being harmful to these systems—including MMT—were banned. In 1978, the sole producer of MMT, Ethyl Corporation, filed a request for a waiver with the US Environmental Protection Agency (EPA) to allow the sale and distribution of MMT to resume. EPA denied the waiver, citing insufficient evidence that the additive would not interfere with automobile emission control systems. As result, MMT was effectively banned from sale and use in unleaded fuel in the United States from 1978 until 1995. During this period Ethyl Corporation periodically reapplied to obtain a waiver for MMT, but each application was denied on grounds that further testing was necessary to determine whether MMT posed an operational threat to emission control systems.

In 1994 EPA agreed that recent studies suggested MMT had no significant adverse effects on automobile emission

*A list of abbreviations and other terms appears at the end of the Investigators' Report.

control systems. However, the agency again denied the Clean Air Act Section 211(f) waiver, citing uncertainties over possible adverse health effects of MMT. Ethyl Corporation filed suit against EPA, asserting that such action was outside the agency's authority. In 1995 the United States Court of Appeals for the DC Circuit ruled that MMT had not yet clearly been proven to be a danger to public health, and that according to Clean Air Act Section 211(b)(3), the EPA Administrator should grant the waiver once all required information from the manufacturer was made available. MMT was retroactively approved for use in all fuels as of late 1993.

In Canada, MMT was introduced into the marketplace in 1972 and officially approved for use in unleaded gasoline 2 years later. In 1997 the Canadian Parliament banned the import and interprovincial trade of MMT owing to concerns over possible public health effects and possible impairment of vehicle emission control systems. Ethyl Corporation sued the Canadian government under Chapter 11 of the North American Free Trade Agreement (NAFTA), claiming that the ban on MMT reduced the value of its Ethyl Canada plant (which blends and distributes MMT). Ethyl Corporation also argued that the ban precluded sale of MMT products already on the market. Furthermore, it argued that the Canadian government's actions would curtail future sales, and that the claim that MMT was an ineffective fuel additive and an unsafe product harmed the company's reputation. The Canadian government settled the dispute and rescinded the trade ban on MMT in 1998.

MMT is currently available in Canada and the United States, except in California and Nevada, where it is banned (State of Nevada 1999; California Air Resources Board 2003), but most US oil refiners do not add it to their products. The Alliance of Automobile Manufacturers, based on analyses it has conducted (Alliance of Automobile Manufacturers 2002; Benson and Dana 2002) is of the opinion that MMT can lead to failure of emission control systems of some vehicle models and has advised consumers against using gasoline containing MMT. Nonetheless, use of MMT is increasing throughout the world; in addition to Canada and the United States, MMT has been officially approved for use by the governments of Argentina, Bulgaria, Russia, South Africa, and New Zealand (Health Canada 2003).

Environmentalists and some scientists continue to raise concerns about the public health impact that might result from more widespread use of MMT through increased manganese particulate emissions in the environment (Kaiser 2003). Under the US Clean Air Act Section 211(c), EPA is mandated to assess risks posed by fuels and fuel additives and to take regulatory action to control the manufacture or sale of these products if they are reasonably anticipated to endanger public health or welfare. Pursuant to Clean Air Act Section 211(b)(2) and 211(e), EPA is authorized to require producers of fuel and fuel additives to fund further testing that will provide information on the potential risks associated with use of their products. The EPA has stated that in order to conduct a more accurate risk assessment, further scientific research is needed to fill in the knowledge gaps about mechanisms of manganese neurotoxicity (Davis 1998). Therefore, EPA issued Alternative Tier 2 Requirements for MMT, which include characterization of manganese emissions from vehicles utilizing fuels containing MMT and pharmacokinetic testing of manganese compounds (EPA 2000).

Because EPA has suggested that "differences in the valence state of inhaled manganese may result in differences in distribution or toxicity" (EPA 1994), the agency has stated that "it is important to determine the composition of actual manganese particles emitted by vehicles burning fuels containing MMT." Although Ethyl Corporation had performed emissions testing under Tier 1 requirements, EPA concluded that "there are important unresolved questions regarding the relative proportions of the various manganese species present in the vehicle exhaust" (EPA 2000). Information obtained from emissions testing would help determine the manganese particle atmosphere for future toxicologic studies. Pharmacokinetic studies in rats and nonhuman primates, specifically the development of a physiologically based pharmacokinetic model, may provide insight into which species of manganese are most problematic in terms of delivery to the brain and also shed light on the appropriate atmosphere for long-term animal toxicologic testing (EPA 2000).

As mandated by EPA, Ethyl Corporation has funded several studies of manganese emissions and toxicity. Studies on manganese toxicity are being conducted at the CIIT Centers for Health Research (eg, Vitarella et al 2000; Dorman et al 2001, 2002a,b), including 90-day inhalation toxicity studies in primates and rats, developmental toxicity studies in rats, and ongoing studies of manganese uptake in primate brain. Emission studies are being conducted at the Lawrence Livermore National Laboratory (Bhuie and Roy 2001; Nelson et al 2002) and the Southwest Research Institute. Results from this and other research on manganese emissions and toxicity will be evaluated in 2004. The EPA will then determine whether regulation of MMT is necessary. If uncertainties over health effects or exposure to emissions remain, EPA reserves the right to call for a second stage of research (for example, involving population exposure assessments or neurotoxicity testing on animals, including nonhuman primates).

In addition to guidelines for limits of exposure to manganese in the air (see Commentary Table), guidance exists for exposure to manganese in drinking water. Under the 1996 Amendments to the Safe Water Drinking Act, manganese was included in a list of candidate contaminants for which EPA must provide regulation or guidance. However, manganese concentrations detected in drinking water are frequently far below the average daily intake from dietary sources (1 to 10 mg/day), and manganese levels in public drinking water are not likely to pose a health risk (US Agency for Toxic Substances and Disease Registry 2000b; EPA 2001, 2002). Therefore, no National Primary Drinking Water Standard for manganese has been issued (EPA 2001). For aesthetic quality, the World Health Organization (1984) has issued a guideline manganese value of 0.1 mg/L for drinking water. At the same time, guidelines exist for minimum daily intake levels of manganese to prevent dietary deficiency of this essential trace element. The US Institute of Medicine (IOM) has recommended Adequate Intake levels of 2.3 and 1.8 mg/day for adult men and women, respectively, with a Tolerable Upper Intake Level of 11 mg/day as a no-observable-adverse-effect level for Western diets (IOM 2003).

MANGANESE NEUROTOXICITY

Abundant occupational evidence indicates that chronic exposure to high levels (1–450 mg/m^3) of inhaled manganese compounds can lead to a neurologic syndrome called *manganism* (World Health Organization 1981, US Agency for Toxic Substances and Disease Registry 2000b). Manganism is a progressive condition that usually begins with relatively mild neurologic symptoms but can evolve into impaired motor ability, altered gait, fine tremor, and psychiatric disturbances (see Levy and Nassetta 2003). Because their symptoms progress similarly, manganism has frequently been misdiagnosed as—or confused with—parkinsonism. The first signs of manganism are generalized feelings of weakness, heaviness, or stiffness of the legs, anorexia, muscle pain, nervousness, irritability, and headache. These feelings are often accompanied by apathy, dullness, impotence, and loss of libido. Further symptoms of the disease include halting or inflectionless speech, slow and clumsy movement of the limbs, and emotionless facial expressions (Rodier 1955; Mena et al 1967).

As the disease progresses muscles become hypertonic. Victims have difficulty walking, develop a staggering gait, and suffer from tremor. Once it has progressed to this middle stage, manganism is widely thought to be irreversible (Levy and Nassetta 2003), although some evidence suggests that recovery is possible when exposure ceases (Smyth et al 1973). Extreme neurotoxicity has been observed in manganese miners and, to a lesser extent, in industrial workers; the advanced condition known as *manganese madness* involves aggression, destructiveness, and bizarre compulsive and seemingly uncontrollable behavior (US Agency for Toxic Substances and Disease Registry 2000b).

The evidence of manganese neurotoxicity has driven research to elucidate the mechanism by which manganese may damage specific neural pathways. The similarities with parkinsonism have pointed to damage of the midbrain, specifically in the dopaminergic areas of the basal ganglia, part of the extrapyramidal motor circuitry. In humans with compromised liver function, who have increased manganese levels in blood despite normal dietary intake (Krieger et al 1995), manganese accumulation has been observed in the basal ganglia (Hauser et al 1996; Spahr et al 1996; Lucchini et al 2000). One study suggested that initial damage resulting from manganese exposure may occur in pathways that are postsynaptic to the nigrostriatal system, most likely involving striatal or pallidal neurons (Wolters et al 1989). Another study using magnetic resonance imaging showed manganese accumulation specifically in the globus pallidus (which is rich in neurons containing γ-aminobutyric acid), rather than the striatum (Lucchini et al 2000). Animal studies have investigated manganese accumulation in specific brain regions after inhalation exposure; some studies found evidence for manganese accumulation in the striatum, globus pallidus, and substantia nigra (Newland et al 1989; Tjälve et al 1996; Roels et al 1997; Vitarella et al 2000; Normandin et al 2002). These studies indicated that manganese accumulates in certain brain regions, prompting research into the mechanisms by which manganese may enter and be retained in the brain.

The current report describes a study by Yokel and Crossgrove that investigated how manganese may enter the brain across the blood–brain barrier, which protects the brain from harmful molecules that circulate in the blood. They also investigated how manganese may leave the brain across the barrier. Assessing rates of movement both into and out of the brain is important because they can be used to evaluate how manganese accumulates in the brain with prolonged exposure, even at much lower levels than found in occupational settings. Another study, by Gunter of the University of Rochester, investigated whether manganese exposure caused increased calcium transport into mitochondria, which may in turn lead to cell death. This study was initially funded by HEI and completed with funding from the National Institutes of Health (Gunter et al 2004).

REFERENCES

Agency for Toxic Substances and Disease Registry (US). 1999. Toxicological Profile for Lead. US Department of Health and Human Services, Public Health Service, Atlanta GA.

Agency for Toxic Substances and Disease Registry (US). 2000a. Toxicological Profile for Arsenic. US Department of Health and Human Services, Public Health Service, Atlanta GA.

Agency for Toxic Substances and Disease Registry (US). 2000b. Toxicological Profile for Manganese. US Department of Health and Human Services, Public Health Service, Atlanta GA.

Alliance of Automobile Manufacturers. 2002. The Impact of MMT of Vehicle Emissions and Durability. Alliance of Automobile Manufacturers, Washington DC. Available from *www.autoalliance.org/mmt_program.htm*.

Benson JD, Dana GJ. 2002. The Impact of MMT Gasoline Additive on Exhaust Emissions and Fuel Economy of Low Emission Vehicles (LEV). SAE Technical Paper, 2002-01-2894. Society of Automotive Engineers, Warrendale PA.

Bhuie AK, Roy DN. 2001. Deposition of manganese from automotive combustion of methylcyclopentadienyl manganese tricarbonyl beside the major highways in the greater Toronto area, Canada. J Air Waste Manage Assoc 51:1288–1301.

California Air Resources Board. 2003. The California Reformulated Gasoline Regulations: Title 13, California Code of Regulations, §2250–2273 (as of May 1, 2003). California Air Resources Board, Sacramento CA.

Davis JM. 1998. Methylcyclopentadienyl manganese tricarbonyl: Health risk uncertainties and research directions. Environ Health Perspect 106(Suppl 1):191–201.

Dorman DC, Brenneman KA, McElveen AM, Lynch SE, Roberts KC, Wong BA. 2002a. Olfactory transport: a direct route of delivery of inhaled manganese phosphate to the rat brain. J Toxicol Environ Health (Part A) 65:1493–1511.

Dorman DC, Struve MF, James RA, Marshall MW, Parkinson CU, Wong BA. 2001. Influence of particle solubility on the delivery of inhaled manganese to the rat brain: Manganese sulfate and manganese tetroxide pharmacokinetics following repeated (14-day) exposure. Toxicol Appl Pharmacol 170:79–87.

Dorman DC, Struve MF, Wong BA. 2002b. Brain manganese concentrations in rats following manganese tetroxide inhalation are unaffected by dietary manganese intake. Neurotoxicology 23:185–195.

Environmental Protection Agency (US). 1994. Reevaluation of Inhalation Health Risks Associated with Methylcyclopentadienyl Manganese Tricarbonyl (MMT) in Gasoline. EPA/600/R-94/062. Office of Research and Development, Washington DC.

Environmental Protection Agency (US). 2000. Final Notification of Alternative Tier 2 Requirements for Methylcyclopentadienyl Manganese Tricarbonyl (MMT). Fed Regist 65:44775–44776.

Environmental Protection Agency (US). 2001. Contaminant Candidate List Preliminary Regulatory Determination Support Document for Manganese. EPA/815-R-01-013. Office of Water, Washington DC.

Environmental Protection Agency (US). 2002. Health Effects Support Document for Manganese: External Review Draft. EPA-R-02-029. Office of Water, Health and Ecological Criteria Division, Washington DC.

Gunter TE, Miller LM, Gavin CE, Eliseev R, Salter J, Buntinas L, Alexandrov A, Hammond S, Gunter KK. 2004. Determination of the oxidation states of manganese in brain, liver, and heart mitochondria. J Neurochem. In press.

Hauser RA, Zesiewicz TA, Martinez C, Rosemurgy AS, Olanow CW. 1996. Blood manganese correlates with brain magnetic resonance imaging changes in patients with liver disease. Can J Neurol Sci 23:95–98.

Health Canada. 2003. Assessment of Toxicological Risks of Environmental Contamination by Manganese. TSRI-109. Toxic Substances Research Initiative, Montreal QC, Canada.

Institute of Medicine. 2003. Dietary Reference Intakes for Vitamin A, Vitamin K, Arsenic, Boron, Chromium, Copper, Iodine, Iron, Manganese, Molybdenum, Nickel, Silicon, Vanadium, and Zinc. National Academy Press, Washington DC.

Kaiser J. 2003. Manganese: A high-octane dispute. Science 300:926–928.

Krieger D, Krieger S, Jansen O, Gass P, Theilmann L, Lichtnecker H. 1995. Manganese and chronic hepatic encephalopathy. Lancet 346:270–274.

Levy BS, Nassetta WJ. 2003. Neurologic effects of manganese in humans: A review. Int J Occup Environ Health 9:153–163.

Lucchini R, Albini E, Placidi D, Gasparotti R, Pigozzi MG, Montani G, Alessio L. 2000. Brain magnetic resonance

imaging and manganese exposure. Neurotoxicology 21:769–775.

Mena I, Marin O, Fuenzalida S, Cotzias GC. 1967. Chronic manganese poisoning. Clinical picture and manganese turnover. Neurology 17:128–136.

Nelson AJ, Reynolds JG, Roos JW. 2002. Comprehensive characterization of engine deposits from fuel containing MMT. Sci Total Environ 295:183–205.

Newland MC, Ceckler TL, Kordower JH, Weiss B. 1989. Visualizing manganese in the primate basal ganglia with magnetic resonance imaging. Exp Neurol 106(3):251–258.

Normandin L, Panisset M, Zayed J. 2002. Manganese neurotoxicity: Behavioral, pathological, and biochemical effects following various routes of exposure. Rev Environ Health 17:189–217.

Rodier J. 1955. Manganese poisoning in Moroccan miners. Br J Ind Med 12:21–35.

Roels H, Meiers G, Delos M, Ortega I, Lauwerys R, Buchet JP, Lison D. 1997. Influence of the route of administration and the chemical form ($MnCl_2$, MnO_2) on the absorption and cerebral distribution of manganese in rats. Arch Toxicol 71:223–230.

Smyth LT, Ruhf RC, Whitman NE, Dugan T. 1973. Clinical manganism and exposure to manganese in the production and processing of ferromanganese alloy. J Occup Med 15:101–109.

Spahr L, Butterworth RF, Fontaine S, Bui L, Therrien G, Milette PC, Lebrun LH, Zayed J, Leblanc A, Pomier-Layrargues G. 1996. Increased blood manganese in cirrhotic patients: Relationship to pallidal magnetic resonance signal hyperintensity and neurological symptoms. Hepatology 24:1116–1120.

State of Nevada. 1999. Nevada Administrative Code (NAC) 590.065. Petroleum products and antifreeze: Gasoline: Adoption of specification guides by reference; exemption from strict compliance with standards; limitations on vapor pressure; limitations on contents. Nevada Legislative Publications, Carson City NV. Available from *www.leg.state.nv.us/NAC/NAC-590.html#NAC590Sec065*.

Tjälve H, Henriksson J, Tallkvist J, Larsson BS, Lindquist NG. 1996. Uptake of manganese and cadmium from the nasal mucosa into the central nervous system via olfactory pathways in rats. Pharmacol Toxicol 79:347–356.

Vitarella D, Wong BA, Moss OR, Dorman DC. 2000. Pharmacokinetics of inhaled manganese phosphate in male Sprague-Dawley rats following subacute (14-day) exposure. Toxicol Appl Pharmacol 163:279–285.

Wolters EC, Huang CC, Clark C, Peppard RF, Okada J, Chu NS, Adam MJ, Ruth TJ, Li D, Calne DB. 1989. Positron emission tomography in manganese intoxication. Ann Neurol 26:647–651.

World Health Organization (WHO). 1981. Manganese. Environmental Health Criteria 17. WHO, Geneva, Switzerland.

World Health Organization. 1984. Guidelines for Drinking Water Quality. Vol 1: Recommendations. WHO, Geneva, Switzerland.

INVESTIGATORS' REPORT

Manganese Toxicokinetics at the Blood–Brain Barrier

Robert A Yokel and Janelle S Crossgrove

ABSTRACT

Increased manganese (Mn) use in manufacturing and in gasoline has raised concern about Mn-induced parkinsonism. Previous research indicated carrier-mediated brain entry but did not assess brain efflux.

Using in situ rat brain perfusion, we studied influx across the blood–brain barrier (BBB*) of three predominant plasma Mn species available to enter the brain: Mn^{2+}, Mn citrate, and Mn transferrin. Our results suggested transporter-mediated uptake of these species. The uptake rate was greatest for Mn citrate. Our results using the brain efflux index method suggested that diffusion mediates distribution from rat brain to blood.

To characterize the carriers mediating brain Mn uptake, we used rat erythrocytes, an immortalized murine BBB cell line (b.End5), primary bovine brain endothelial cells (bBMECs), and Sprague Dawley and Belgrade rats. Studies with bBMECs and b.End5 cells suggested concentrative brain Mn^{2+} and Mn citrate uptake, respectively, consistent with carrier-mediated uptake. Mn^{2+} uptake positively correlated with pH, suggesting mediation by an electromotive force. Mn^{2+} uptake was not inhibited by iron or the absence of divalent metal transporter 1 (DMT-1) expression, suggesting an iron-transporter-independent mechanism. Mn^{2+} uptake inversely correlated with calcium and was affected by calcium channel modulators, suggesting a role for calcium channels. Rat erythrocyte results suggested monocarboxylate transporter 1 (MCT1) and anion exchange transporters do not mediate Mn citrate brain uptake.

Considering carrier-mediated brain influx (but not efflux), repeated excessive Mn exposure should produce brain accumulation. Further work is necessary to identify the specific transporter or transporters mediating Mn distribution across the BBB.

INTRODUCTION

Mn is an essential trace element for normal brain development and function throughout life for all mammals (Smith 1990; Keen et al 2000). It is a cofactor for metalloproteins in the brain, such as the glial-specific enzyme glutamine synthetase, which accounts for 80% of the brain concentration of Mn, as well as superoxide dismutase and pyruvate carboxylase (Wedler and Denman 1984).

Excess brain Mn produces a parkinsonian syndrome, manganism (Hudnell 1999; Iregren 1999). Neurotoxicity has been reported in miners exposed to manganese dioxide (MnO_2) by inhalation (Couper 1837), factory workers producing dry-cell batteries (Keen and Lönnerdal 1995), children receiving long-term parenteral nutrition containing 0.8 to 1 µmol Mn/kg body weight/day (Fell et al 1996), and people drinking well water contaminated by buried dry-cell batteries (Hudnell 1999). Mn accumulation is associated with damage to neurotransmitter function, particularly dopaminergic systems (Verity 1999). Mn poisoning results from damage to many of the basal ganglia structures (Agency for Toxic Substances and Disease Registry 2000). Higher Mn concentrations have been found in the caudate nucleus, lenticular nuclei, and substantia nigra of monkeys (Newland et al 1989), and basal ganglia of rats (Kabata et al 1989). T1-weighted magnetic resonance imaging of patients who exhibited parkinsonism-like symptoms after prolonged total parenteral nutrition has shown high density attributed to Mn in the basal ganglia (especially the globus pallidus), the tectum, and the tegmentum of midbrain and pons (Ejima et al 1992; Ono et al 1995; Fitzgerald et al 1999; Nagatomo et al 1999; Masumoto et al 2001).

* A list of abbreviations and other terms appears at the end of the Investigators' Report.

This Investigators' Report is one part of Health Effects Institute Research Report 119, which also includes a Commentary by the Health Review Committee and an HEI Statement about the research project. Correspondence concerning the Investigators' Report may be addressed to Dr Robert A Yokel, College of Pharmacy, University of Kentucky Medical Center, 511C Pharmacy Building, Rose Street, Lexington KY 40536-0082.

Although this document was produced with partial funding by the United States Environmental Protection Agency under Assistance Award R82811201 to the Health Effects Institute, it has not been subjected to the Agency's peer and administrative review and therefore may not necessarily reflect the views of the Agency, and no official endorsement by it should be inferred. The contents of this document also have not been reviewed by private party institutions, including those that support the Health Effects Institute; therefore, it may not reflect the views or policies of these parties, and no endorsement by them should be inferred.

Symptoms of manganism include reduced coordination, hallucinations, and hyperirritability (Schuler et al 1957; Mena et al 1967). With prolonged exposure, symptoms progress and the chances of recovery diminish, suggesting that cumulative neurotoxicity results from repeated Mn exposure. Subtle neuropsychiatric deficits have been attributed to Mn in people exposed to lower concentrations (Sjögren et al 1990, 1996; Mergler et al 1994; Lucchini et al 1995). Early signs of nervous system dysfunction, in the absence of clinical manifestations, have been detected in people with occupational and environmental Mn exposure (Mergler et al 1999). Occupational exposure for an average of 7 years was associated with significant decrements in neurologic function (Roels et al 1987), with higher prevalence of abnormal symptoms in individuals who had been exposed longer. Other epidemiologic studies of industrial workers showed a positive correlation between neurologic dysfunction and lifetime integrated or cumulative Mn exposure (Roels et al 1992; Lucchini et al 1995, 1999).

Production of Mn ore has increased approximately 20-fold during the 20th century to accommodate increased uses: production of aluminum cans, fungicides such as ethylenebis(dithiocarbamato)manganese (maneb), fertilizers, electronic devices, and mangafodipir trisodium, a contrast agent used in medical diagnostics. Currently concern focuses on airborne Mn exposure from the fuel additive methylcyclopentadienyl manganese tricarbonyl (MMT) (Hudnell 1999). MMT has been used in Canadian gasoline since 1976 (except for 1997 to 1998, when it was banned). In the United States MMT was approved as a fuel additive by court ruling in 1995 (District of Columbia Circuit Court 1995), and it is being used to some extent. Amendments in 1996 to the Safe Drinking Water Act directed the EPA to generate a list every 5 years of candidate contaminants for which a decision is to be made to regulate, not regulate, or provide guidance, once sufficient data are available to do so. Mn is on that list, suggesting further understanding of its toxicology will be helpful to the EPA.

Mn SPECIES

The primary chemical forms (species) of Mn released from the tailpipe after MMT combustion are Mn^{2+} phosphate and sulfate (Reynolds et al 1997; Health Effects Institute 1998; Lynam et al 1999; Zayed et al 1999). Emitted into the air, they create the potential for humans to inhale or ingest Mn. Mn phosphate and sulfate readily dissolve in aqueous solution, releasing Mn^{2+}. Upon absorption, some Mn^{2+} may oxidize to Mn^{3+}, which is quite reactive (Cotton and Wilkinson 1980) and rapidly associates with transferrin (Tf) to form a stable complex. The formal binding constants (log K) of Mn^{3+} are ~ 3 and 4 (Harris and Chen 1994) and of Mn^{3+}, corrected for carbonate effects, are 22.2 and 23.4 at Tf's two metal-binding sites (Harris 1998). Therefore, little free Mn^{3+} would be expected in plasma in vivo because nearly all of it associates with Tf. Mn^{2+} does oxidize in blood to Mn^{3+} within 1 to 5 hours (Scheuhammer and Cherian 1985; Critchfield and Keen 1992). HEI-supported research has suggested the presence of Mn as Mn^{2+} adenosine triphosphate (ATP) in neuron-like PC12 cells and possibly as Mn^{2+} and Mn^{3+} in Mn superoxide dismutase in brain mitochondria (Gunter et al 2002).

Normal Mn concentration in plasma is approximately 20 nM (Keen et al 2000). A small percentage of Mn^{2+} in plasma exists as species that may cross the BBB. Thermodynamic modeling of Mn^{2+} in serum suggests it exists in several forms: for example, as an albumin-bound species (84%), as a hydrated ion (6.4%), and in 1:1 complexes with bicarbonate (5.8%), citrate (2.0%), and other low molecular weight ligands (1.8%) (Harris and Chen 1994). Mn^{2+} forms weak complexes with these ligands. The calculations based on this model are consistent with the observation of low molecular weight species in plasma (Critchfield and Keen 1992). We found approximately 8% of Mn^{2+} in rat blood plasma to be in the free fraction (Study 2 of this report), also consistent with the model calculations. Similar modeling of Mn^{3+} in serum suggests that it is almost 100% bound to Tf (Aisen et al 1969; Harris and Chen 1994).

Introduction of manganese chloride ($MnCl_2$) into blood releases ionic Mn in plasma. Equilibrium is quickly achieved with Mn, resulting in similar Mn species after exposure to Mn phosphate, sulfate, and chloride. (See the Discussion and Conclusions section for more details on the rate of Mn–ligand exchange.) Therefore, $MnCl_2$ was used in the present studies as a model for readily dissociated Mn salts. The log K (stability constant) values of Mn^{2+} are 4.06 and 2.96 with Tf's two metal-binding sites, 1.2 with lactic acid, 3.1 with oxalic acid, and generally 2.5 to 3 for 1:1 complexes with amino acids (Martell and Smith 1974–1982; National Institute of Standards and Technology 1995). At the dilute Mn and citrate concentrations and pH (7.33) of extracellular fluid, the Mn citrate complex would be expected to be a monomer (Amico and Daniele 1979). The 1:1 Mn citrate complex involves coordination bonds between Mn and the central hydroxyl group and the two terminal carboxylates of citrate, forming a tridentate complex. The central carboxylate group is not involved in this complex (Glusker and Carrell 1973; Amico and Daniele 1979; Gregor and Powell 1986), but it may serve as the recognition moiety of Mn citrate for a

transporter. In the present studies, we used Mn citrate as a model low molecular weight Mn complex and Mn Tf, which is the predominant species of Mn^{3+}, as a representative large Mn protein complex. Although other Mn species might contribute to distribution of Mn across the BBB, their lower concentrations and stability constants suggest they are less likely to play a major role.

Mn DISTRIBUTION

After entering blood, Mn rapidly distributes to other compartments. The terminal elimination half-life of Mn in blood has been reported to be 1.83 hours after intravenous $MnCl_2$ injection in Sprague Dawley rats (Zheng et al 2000). The whole-body terminal Mn half-life after intravenous injection was 119, 146, 99, and 68 days in RF mice, Sprague Dawley rats, *Macaca mulatta* monkeys, and beagle dogs, respectively (Furchner et al 1966). Mn decreases were slower in brain than in most other tissues. After an intravenous tracer dose of ^{54}Mn, a half-life of 32 to 40 days was seen in rats that were followed for 112 days (Vitarella et al 2000). The rat whole-body Mn half-life was reported to be between 6 and 30 days (Dastur et al 1969; Manghani et al 1970; Lee and Johnson 1988, 1989); however, Mn elimination was studied for shorter durations than in the studies previously cited (Furchner et al 1966; Vitarella et al 2000). The whole-body half-life of ^{54}Mn in the rhesus monkey was found to be 95 days (Dastur et al 1971). Liver, kidney, and other organs eliminated Mn with a half-life of 10 to 15 days, whereas in bone a Mn half-life longer than 50 days was demonstrated (Furchner et al 1966). The whole-body Mn half-life in humans has been reported to vary from 6 to 43 days after oral administration and from 24 to 74 days after intravenous administration (Mena et al 1967, 1969; Mahoney and Small 1968; Sandström et al 1986; Davidsson et al 1989; Johnson et al 1991). Extending the duration of study of substance remaining in the body or a specific tissue enables identification of a longer, perhaps the terminal, half-life of elimination, which probably accounts for some of the differences among the cited studies. To rigorously determine a biological half-life, one should determine the declining concentration of the test substance for three half-lives. Not all of the above studies meet this criterion. The reported data on the elimination whole-body half-life of Mn indicate that the rat is a valid model for the human.

In the brain, Mn concentrates in the corpus striatum and globus pallidus and remains there for weeks or months. The ^{54}Mn content of the cerebrum has been shown to increase over the first 4 days after administration in the rat (Dastur et al 1969) and 50 days in the rhesus monkey (Dastur et al 1971). Cerebrum Mn concentration did not appreciably decrease over 34 or 64 days in the rat; a half-life of Mn elimination from the brain was not calculated (Dastur et al 1969; Manghani et al 1970). In rhesus monkeys Mn was higher in the brain after 150 days than in all other sampled tissues and only slowly decreased in various brain regions over 278 days, resulting in a half-life that was longer than 100 days but could not be calculated (Dastur et al 1971). Over 278 days the retention of ^{54}Mn in the cerebrum relative to that in the whole body increased, while that in most other tissues remained fairly constant, suggesting a selective retention of Mn in the brain (Dastur et al 1971). In rats the decline over 90 days of ^{54}Mn in the brain was slower than that in liver, kidney, and skeletal muscle (Drown et al 1986). In one study the half-life estimates of ^{54}Mn in 16 rat brain regions ranged from 52 days in interpeduncular nuclei to 74 days in hypothalamic nuclei (Takeda et al 1995), but this study determined brain ^{54}Mn for only 60 days after intravenous $^{54}MnCl_2$ injection.

Overall, these animal studies show a much slower elimination of Mn from the brain than from many other tissues. Comparable data are not available for the human. A principle of pharmacokinetics is that elevated (eg, double) exposure will elevate (eg, double) the steady-state Mn concentration. Steady state would be expected to be reached in the brain in four to five half-lives. If the findings of these reports of brain Mn half-life in animals were extrapolated to the human, elevated Mn exposure would not result in a higher Mn steady-state concentration for at least one-half year, but would certainly do so within the human life span.

In contrast to toxicokinetic endpoints, the rat is not a good model for the pharmacodynamic endpoints of human Mn toxicity. The Toxicological Profile for Manganese (Agency for Toxic Substances and Disease Registry 2000) notes that animal inhalation studies have not produced neurologic signs similar to those seen in humans and that only a few studies have reported clinical signs such as weakness, ataxia, or altered gait after oral exposure. The authors note that available evidence suggests rodents are less susceptible than humans to neurologic damage from Mn. Because the present report describes toxicokinetic studies, the reasonable similarity of toxicokinetic endpoints has greater importance.

Mn BRAIN INFLUX

Central to homeostatic regulation of brain Mn levels is the exchange of Mn between blood plasma and brain tissue. Mn can enter the brain from blood plasma by crossing the capillary endothelial cells of the BBB or the choroid plexuses into cerebrospinal fluid and then into the

brain (Bradbury 1997). Brain Mn influx and efflux occur by diffusion or by carrier-mediated processes with speed and volume depending on the size, charge, and shape of the molecule. At physiologic Mn concentrations, brain influx has been reported to be nonsaturable and to occur primarily through the capillary endothelium of the BBB. At high plasma concentrations in the same study, Mn influx was saturable and occurred primarily via the cerebrospinal fluid (Murphy et al 1991; Rabin et al 1993).

Mn can enter the brain as a complex with Tf via endocytosis, which is mediated by the Tf receptor (TfR) (Aschner and Aschner 1990; Aschner and Gannon 1994), but the role of TfR-mediated endocytosis in brain Mn uptake may be minor (Takeda et al 2000; Malecki 2001). Mn^{2+} not bound to protein enters the brain so much more rapidly than Mn^{3+} Tf that even if it were only 1% of total plasma Mn, it would still be the predominant species entering the brain from plasma (Murphy et al 1991).

Transport mechanisms other than TfR-mediated endocytosis also have been proposed (Murphy et al 1991; Malecki et al 1999; Takeda et al 2000). A second, more rapid, brain influx of Mn not bound to protein may be the main Mn species crossing the BBB (Murphy et al 1991; Aschner and Gannon 1994). The presence of albumin and Tf reduced brain Mn uptake (Rabin et al 1993). This suggests low molecular weight Mn species are rapidly taken up into the brain, because albumin would not cross the intact BBB and TfR-mediated endocytosis is quite slow (Cole and Glass 1983). A recent review recognized that carrier-mediated systems appeared to be involved in Mn transport across the BBB but that the transporters responsible for non-Tf-mediated Mn transport were unknown (Takeda 2003).

Some have concluded that Tf does not play a major role in Mn efflux from brain to blood (Bradbury 1997). The concentration of Tf in brain extracellular fluid is less than 0.25 μM. The Tf metal-binding sites may be occupied by iron, leaving them unavailable for Mn binding.

Whether there is a predominant Mn species crossing the BBB is unclear. We proposed studies to test the hypothesis that Mn citrate is the predominant non-protein-bound Mn^{2+} species crossing the BBB. An extensive literature search and a discussion in 1999 with chemists who conduct metal speciation studies failed to reveal an available method to directly determine Mn species in vivo. One of the projects funded through HEI's Request for Preliminary Applications 98-4, "Research on Metals Emitted by Motor Vehicles," did develop a method to identify Mn^{2+} and Mn^{3+} in vivo in liver and heart mitochondria (Gunter et al 2002); however, these investigators did not develop methods that would differentiate Mn ions from Mn citrate or other low molecular weight Mn species. The lack of methods to directly determine Mn species in vivo led us to use in situ brain perfusion to provide better control over Mn species in the influx studies.

Mn is actively transported across cell membranes by several types of cells. Biliary excretion accounts for more than 95% of Mn excretion. Mn concentration in bile can exceed that in plasma by 100-fold, suggesting active transport (Klaassen 1974). The carrier has not been characterized (Schramm and Brandt 1986) other than by its independence from glutathione (Sugawara et al 1994; C Klaassen, personal communication, January 1998). Mn is actively transported into and out of astrocytes (Aschner et al 1992). Although the transporter has not been identified, introduction of $MnCl_2$ into the cell medium stimulated efflux from astrocytes, suggesting transstimulation, "consistent with efflux and influx mediated by the same system" (Aschner et al 1992). Carrier-mediated Mn transport was shown into Caco-2 cells from the apical side (absorption from gut), but perhaps not from the basolateral side (exsorption from blood) (Leblondel and Allain 1999). This unidentified carrier might mediate Mn absorption from the gastrointestinal tract. The authors found evidence that Mn uptake depended on sodium, did not depend on ATP, and occurred in competition with calcium, suggesting to them that Mn uptake from the gastrointestinal tract may be mediated by the same type of channel that is involved in calcium uptake.

Mn BRAIN EFFLUX

Efflux of Mn from cells and the brain has received little attention. Work in vitro showed Mn efflux from cultured chick glial cells (Wedler et al 1989), but the same process would not result in Mn efflux out of the brain. Prior to the present work, no studies investigating Mn efflux from the brain had been reported. As all organisms have systems for the export of toxic cations (Ketchum 1999), we hypothesized that the neurotoxicant Mn is effluxed from the brain by a carrier. Numerous facilitative diffusion carriers and active transporters exist at the BBB (shown in Table 1). Some of these transporters are capable of effluxing neurotoxicants from the brain: for example, azidothymidine or AZT (by the nucleoside transporter); cyclosporin, vinca alkaloids, etoposide, and taxol (by P-glycoprotein and multidrug-resistance-associated protein); iodine and thiocyanate; theophylline; atenolol; acetaminophen; fluconazole; baclofen; valproate; methotrexate; β-lactam antibiotics; and quinolones and fluoquinolones. Thus, brain efflux of a wide variety of substances occurs by many mechanisms. Carriers for nonmetabolizable substrates, such as metals, protect the organism against toxicity, just as P450 metabolism detoxifies metabolizable substrates.

Table 1. Some Carriers at the Blood–Brain Barrier[a]

Carrier[b]	Locus Symbol[c]	Distribution[d] L	Distribution[d] A	Type[e]	Substrates	Transport Rate (nmol/g/min)
Hexose (glutamate transporter 1)	*SLC2*	x	x	FD	Glucose	700
Monocarboxylate	*SLC16*	x	x	FD	Lactate, pyruvate	60
Anion exchange (band 3)	*SLC4*			FD	Lactate, Cl^-/HCO_3^-, metal-anion complexes	
Large neutral amino acid (L-system)	*SLC3*	x	x	FD	L-DOPA, phenylalanine	12
Small neutral amino acid (A-system)	*SLC5*		x	SAT	Alanine, serine, cysteine	
Neutral amino acid (ascorbate-system)	*SLC7*		x		D-serine	
Basic amino acid		x	x		Lysine	3
Acidic amino acid			x		Glutamate, aspartate	0.2
N-system		x		FD	Glutamine & glutamate	
Excitatory amino acid (EAAT1-3)	*SLC1*		x		Glutamate	
Amine (cation, y^+)	*SLC7*	x	x		Choline	0.2
β-Amino acid		x	x		Taurine	
Low-affinity γ-aminobutyric acid	*SLC6?*	x				
High-affinity γ-aminobutyric acid	*SLC6?*		x			
Saturated fatty acids					Octanoate	
Urea	*SLC14*			FD		
Purine		x	x		Adenine	0.006
CNT2 (Na-coupled nucleoside transporter, member 2)					Adenosine	
Nucleoside	*SLC28/29?*	x	x		Purine nucleosides	0.004
Na/K-ATPase	*ATP1*		x	AT	Potassium	
Ca-ATPase	*ATP2*	x	x	AT	Calcium	
Sodium		x		AT	Sodium	200
Potassium	*SLC12*		x	AT		12
Chloride	*SLC12?*					140
DMT-1, DCT1, Nramp2	*SLC11*				Fe^{2+}, Zn, Mn, Cu, Cd, Ca, Ni, Pb	
P-glycoprotein Multidrug resistance transporter (MDR)	*ABC*, subfamily *B*	x		AT	Organic cations with high lipophilicity: vincristine	
Multidrug-resistance-associated proteins (MRP1, MRP5, MRP6)	*ABC*, subfamily *C*			AT	Organic anions & glutathione, glucuronate & sulfate conjugates	
Organic anion transporting polypeptide (Oatp2)	*SLC21*				Negatively charged amphipathic organics	
BBB-specific anion transporter type 1 (Oatp14)						
Peptide transporter	*SLC15?*				Thyrotropin-releasing hormone, α-melanocyte-stimulating hormone, interleukin 1	
Transferrin receptor transport	*TFRC*	x	x	RM	Transferrin	0.003

[a] From *Aluminium and Alzheimer's Disease: The Science That Describes the Link* (C Exley, ed), RA Yokel, Aluminum toxicokinetics at the blood-brain barrier, pp 233–260, copyright 2001, with permission from Elsevier Science. Compiled from Locus Link (*www.ncbi.nlm.nih.gov/LocusLink*); from *Basic Neurochemistry: Molecular, Cellular and Medical Aspects*, 6th ed (GJ Siegel, RW Albers, BW Agranoff, SK Fisher, MD Uhler, eds), J Laterra, R Keep, A Betz, G Goldstein, Blood-brain-cerebrospinal fluid barriers, pp 671–689, copyright Lippincott-Raven Publishers, 1999, with permission from Lippincott Williams & Wilkins and Dr Betz; and from other sources. The substrates and transport rates listed are typical.

[b] Other carriers are leptin-receptor-mediated transport, many carriers for vitamins and cofactors, and several carriers for hormones.

[c] Locus symbols are from LocusLink. SLC = solute carrier.

[d] Distribution: L, luminal; A, antiluminal.

[e] AT indicates active transport; FD, facilitated diffusion; RM, receptor-mediated transport; and SAT, secondary active transport.

Studies with metabolic inhibitors have suggested that lead is transported from brain to blood by Ca-ATPase (Bradbury and Deane 1993), presumably revealing an efflux mechanism at the BBB for this neurotoxicant. We have found evidence for efflux of aluminum (Al), presumably as Al citrate, from the brain (Ackley and Yokel 1997; Ackley and Yokel 1998). For all of these substances, the ratio of brain extracellular fluid concentration to blood extracellular fluid (plasma) concentration was significantly less than 1, suggesting each is a substrate for carrier-mediated efflux from the brain.

METHODS TO ASSESS Mn TRANSPORT

Considering both the essentiality of Mn in the brain and its potential to damage the brain when present in excess, we hypothesized that there may be mechanisms to maintain brain Mn homeostasis by mediating both the influx and efflux of Mn in the brain. The present research describes studies conducted to determine the rates of Mn influx and efflux across the BBB. There are many methods to assess the influx of substances into the brain and to elucidate the properties of transporters at the BBB. In situ brain perfusion is accurate and sensitive, and it allows the investigator to choose the perfusion medium in which to administer the test substance (Smith 1996). Injection and infusion techniques allow substances to interact with blood and to travel throughout the body, where they can change chemical species (including changes in oxidation states), be metabolized, or be eliminated. Plasma concentrations may change over time with injections, whereas infusions can be used to achieve steady-state concentrations. In situ perfusion has been used to determine influx in mice and rats (Murakami et al 2000) for small compounds and for proteins (Deane and Bradbury 1990; Rabin et al 1993; Bonate 1995; Deguchi et al 2000; Allen and Smith 2001). We chose this technique to maintain control over Mn species in our studies.

In contrast, few experimental approaches are available to study efflux from the brain across the BBB. Early work used efflux from brain slices. Whole-animal techniques have included measuring the decrease in brain content over time after a bolus intracarotid injection (Oldendorf et al 1982; Cornford et al 1985); comparing the ratios of coinjected substances over time (Leininger et al 1991); and microdialysis (Deguchi and Morimoto 2001; Yokel 2001). A more recent method involves determination of the brain efflux index, which is designed to determine efflux from brain to circulating blood across the BBB (Kakee et al 1996).

The brain efflux index has been used to identify efflux of water, 3-*O*-methyl-D-glucose, azidothymidine, dideoxyinosine, *p*-aminohippurate, quinidine, taurocholate, BQ-123 (an anionic cyclic pentapeptide), γ-aminobutyric acid (GABA), L-aspartate, L-glutamate, dehydroepiandrosterone, estrone, and estrone-3-sulfate (Kakee et al 1996, 1997, 2001; Kusuhara et al 1997; Takasawa et al 1997; Kitazawa et al 1998; Hosoya et al 1999, 2000; Zhang et al 1999; Asaba et al 2000). Studies using this method have also shown the absence of efflux of L-glucose, octreotide (a cationic cyclic octapeptide), and D-aspartate (Kakee et al 1996; Kitazawa et al 1998; Hosoya et al 1999). The lack of difference in recovery of inulin from the brain of living rats versus that from nonliving rats (Kakee et al 1996) and the lack of significant loss of carboxyinulin, inulin, mannitol, and high molecular weight dextran from brain over time (Kakee et al 1996, 1997; Takasawa et al 1997; Kitazawa et al 1998; Zhang and Pardridge 2001) suggest these substances diffuse through the BBB very slowly. Each of these substances is useful as a marker compound that crosses membranes extremely slowly. The brain efflux index is used to compare the amounts of test substance and marker compound remaining in the brain after coinjection. The brain efflux index (Kakee et al 1996) was the method used in the present work.

The most likely candidate transporter for Mn^{2+} efflux from the brain was hypothesized to be DMT-1, which has been described in the brain (Gunshin et al 1997) and in the cells that comprise the BBB (Burdo et al 2001). DMT-1 transports metals across the cell membrane (Garrick et al 1999). Candidate transporters for Mn citrate brain efflux are the monocarboxylate transporters for lactate, pyruvate, and small carboxylate molecules (Price et al 1998). Most membrane transporters are well conserved across species; the monocarboxylate transporters have homologues that are believed to be present from yeast to human (Price et al 1998).

We used two approaches to ascertain the properties of Mn transporters at the BBB with the ultimate goal of identifying the carriers mediating Mn transport across the BBB. The first approach was to conduct uptake studies in single-cell preparations of rat erythrocytes, an immortalized murine brain endothelial cell line (b.End5), and bovine brain microvascular endothelial cells (bBMECs). The bBMECs were used because they are the classical single-cell preparation for in vitro study of the BBB (Audus et al 1996). They form the tight junctions that provide the barrier property of the BBB. They were studied as primary cells isolated from cow brain. The second approach was to characterize transporter properties using in situ brain perfusion in Sprague Dawley rats. Additionally, Belgrade rats were studied. The homozygous recessive Belgrade rat (*b/b*) expresses an inherited form of DMT-1 that is not functional for cation uptake. The heterozygous littermates (*+/b*) are phenotypically normal. Brain Mn uptake was compared among *+/b* and *b/b* Belgrade rats and Wistar rats.

The results of the present studies have implications for risk assessment and risk avoidance. An understanding of the absence or presence of carrier-mediated brain Mn influx and efflux processes indicates whether elevated Mn exposure represents a potential risk to the brain, or if there are protective processes to maintain a healthy brain Mn concentration under high-exposure conditions. An understanding of the characteristics of the carriers at the BBB might provide the opportunity to avoid exposure to agents or conditions that would enable excessive Mn to enter the brain. Identification of Mn carriers at the BBB might reveal inherited traits that alter the risk of brain Mn exposure compared to that of the general population and might identify conditions that increase or decrease, through up-regulation or down-regulation, the ability of Mn to cross the BBB.

SPECIFIC AIMS

The main aim of the present work was to address the hypothesis that the brain is protected both by processes of carrier-mediated influx that provide essential Mn and by processes of carrier-mediated efflux that shield it from excessive Mn accumulation. The findings could indicate whether homeostatic mechanisms exist that maintain a healthy brain Mn concentration in situations of low or elevated Mn intake. Identification of the properties of the carriers that maintain brain Mn concentration may provide guidance on conditions that could disrupt transport by these carriers.

We proposed to investigate three chemical species of Mn: Mn^{2+}, Mn citrate, and Mn Tf, which represent the unbound, small ligand-complexed, and protein-bound fractions of Mn in plasma, respectively. To estimate the rates at which these three Mn species would cross the BBB by diffusion, we determined their lipophilicity and their molecular weight (Study 1). We hypothesized that a brain influx rate significantly greater than the calculated diffusion rate would provide evidence of the influence of one or more carrier-mediated processes on brain Mn uptake.

To seek evidence for Mn transport across the BBB, we had conducted preliminary studies (prior to the studies funded by HEI) using intravenous injection of Mn species into rats (Study 2). These studies employed the microdialysis method to sample unbound extracellular Mn in brain and blood plasma of injected and control rats. To quantify influx rates of Mn^{2+}, Mn citrate, and Mn Tf into the rat brain (Study 3), we proposed to acquire and master the in situ brain perfusion technique, as developed by Takasato and coworkers (1984) and subsequently modified and currently utilized in the laboratories of Drs Quentin Smith and David Allen at Texas Tech University in Amarillo. The influx transfer coefficients (K_{in}) could then be compared with the diffusion rates of the three Mn species across the BBB. We also proposed to determine brain efflux rates (Cl_{efflux} or K_{out}) of the three Mn species to test the hypothesis that brain Mn efflux is carrier-mediated (Study 4). K_{out} is a term describing the rate of efflux from the brain, is comparable to K_{in}, and can be considered the efflux transfer coefficient. It is a product of the brain efflux index and the brain distribution volume of the test substance. We proposed to master, validate, and use a reported method (Kakee et al 1996) to determine the brain efflux index and brain distribution volumes of these three Mn species in the rat.

The final major aim of the proposed work was to characterize, and ideally identify, the transporters responsible for carrier-mediated Mn flux across the BBB (Study 5). As we did not find evidence for carrier-mediated brain Mn efflux in Study 4, characterization of transporters was limited to studies addressing brain Mn influx. In vitro and in vivo models were used to evaluate the roles of specific processes in the uptake of Mn^{2+} and Mn citrate to rule out or reveal evidence consistent with candidate transporters of Mn uptake. Toward this goal we determined the characteristics of Mn uptake into rat erythrocytes, which express the MCT1 and anion exchange carriers; uptake into b.End5 cells, an immortalized murine brain endothelial cell line; and uptake into bBMECs, which are primary bovine cells that express most of the barrier properties of the BBB. We also addressed this aim with studies of brain Mn influx in the whole animal, including a rat strain that does not express a functional form of one of the putative Mn transporters, DMT-1. Pharmacologic manipulations were conducted using cells as well as the whole animal to determine whether Mn uptake depends on sodium or pH and to determine the influence of competitive substrates and inhibitors of putative transporters.

METHODS AND STUDY DESIGN

All use of animals complied with the provisions of the Animal Welfare act and the guidelines set forth in the *Guide for the Care and Use of Laboratory Animals* (US National Research Council 1996). The protocols for these studies were approved by the University of Kentucky Institutional Animal Care and Use Committee.

STUDY 1. ESTIMATION OF CEREBRAL CAPILLARY DIFFUSION PERMEABILITY OF Mn SPECIES

The rate of diffusion of small molecules through a plasma membrane, such as the BBB, can be predicted from their molecular weight and lipid solubility, measured as

the partitioning between an octanol and an aqueous phase (Levin 1980; Laterra et al 1999). Deviations from the predicted relation have been attributed to carrier-mediated transport (Laterra et al 1999). For example, the brain influx rate of D-glucose is approximately 1000-fold greater than that of L-glucose, owing to glucose transporter 1 (GLUT1), which mediates the rate of glucose uptake required to support brain metabolism. The brain uptake rates of L-leucine and L-dopa are similarly greater than would be predicted if they crossed the BBB by diffusion, which has been attributed to their transport across the BBB by the large neutral amino acid (L-system) carrier. Conversely, the rate of brain uptake of phenytoin is slower than would be predicted for membrane permeation by diffusion. This difference is due to its efflux from the brain or brain endothelial cells by P-glycoprotein, which exports substances from the brain to protect it against xenobiotic toxicity. If there is a carrier for one or more Mn species, the rate at which they cross the BBB will be greater than that attributable to diffusion. Therefore our first step in identifying potential transport mechanisms for Mn was to estimate the rate of diffusion of Mn species through the BBB. This was calculated from the product of diffusion permeability and surface area ($P_{diffusion}S$), which is estimated from the octanol-to-aqueous partitioning coefficient ($D_{o/a}$). Therefore we determined the $D_{o/a}$ of the three Mn species. To conduct these and subsequent studies with Mn citrate and Mn Tf required demonstration and validation of our ability to form these Mn species (described in Appendix A).

The distribution (partitioning) of nonradioisotopic $^{55}Mn^{2+}$, ^{55}Mn citrate, and ^{55}Mn Tf between octanol and an aqueous phase was determined as previously described (Yokel and Kostenbauder 1987). The aqueous phase was modified to exclude bicarbonate (HCO_3^-) in the $^{55}Mn^{2+}$ and ^{55}Mn citrate systems, because it is a potential ligand for Mn. Bicarbonate was included when Mn Tf was studied because it is necessary for Mn Tf formation. Octanol/aqueous systems were agitated overnight at 37°C to establish equilibrium. Mn concentrations in the octanol and aqueous phases were determined by electrothermal atomic absorption spectrometry (ETAAS) (see Appendix A).

The calculation of permeability through the BBB by diffusion ($P_{diffusion}$, in centimeters/second) is described in the Statistical Methods and Data Analysis section. The product of rat brain cerebral capillary diffusion permeability and rat brain capillary surface area ($P_{diffusion}S$) has the same units as K_{in} and K_{out}, which are measures of influx and efflux at the BBB, respectively. This enabled their comparison. Sucrose was included in these calculations for comparison because it was used as a vascular marker in the determination of Mn influx (Study 3) and in the brain efflux index method to study brain Mn efflux (Study 4). Dextran was included because it also was used in Study 4 as a marker that exhibits poor membrane permeability. Sucrose and dextran cross the BBB by diffusion.

STUDY 2. Mn TOXICOKINETICS AFTER INTRAVENOUS INJECTION AND BRAIN–BLOOD RATIO

We determined the toxicokinetics of Mn after an intravenous bolus injection of $MnCl_2$ or Mn citrate at 25 µmol/kg body weight in anesthetized Sprague Dawley rats. Blood samples were collected for approximately 2 hours after Mn injection. From the clearance and volume of distribution, we calculated a bolus $MnCl_2$ injection (50 µmol/kg) and infusion rate (75 µmol/kg/hr) to achieve and maintain Mn steady state, which we used in microdialysis studies. These conditions rapidly produced a steady-state Mn concentration of approximately 185 µg/L (3.4 µM) in plasma, which is considerably above the approximate physiologic concentration of 20 nM.

Microdialysis is a sampling method utilizing semipermeable membrane tubing that is sealed on one end and mounted on the end of a needle-like probe with two channels. This produces a closed system except for diffusion across the membrane. The probe is implanted into a tissue. Extracellular unbound substances in the tissue that are able to diffuse through the membrane enter the dialysate, which is continuously perfused through and collected from the probe for analysis. For the microdialysis studies a cannula constructed from Silastic tubing, with 0.20-inch internal diameter and 0.037-inch outer diameter, was inserted into the femoral vein in 13 anesthetized Sprague Dawley rats. The tubing was expanded to accommodate polyethylene (PE-50) tubing, which was connected to the infusion syringe. The overlapping area of Silastic tubing and PE-50 tubing was inserted into the vein. The cannula was held in place with a suture over the overlapped tubing. The cannula enabled bolus injection and infusion of Mn-containing test solution. A similarly constructed cannula was inserted in the jugular vein to enable blood withdrawal. Microdialysis probes CMA/20 and CMA/12 were implanted, respectively, in the jugular vein and the brain (cortex or striatum). The brain microdialysis probes were implanted using a stereotactic instrument to hold the head in a defined position. A rat brain atlas was used to identify the coordinates to guide insertion of the probe in the desired brain location (Paxinos and Watson 1986). The cortex, often considered to be representative of brain tissue, was selected as a typical brain region for microdialysis studies. The striatum was selected because of its role in Mn neurotoxicity.

Indicators of microdialysis probe recovery and BBB integrity, antipyrine and 4-trimethylantipyrine, respectively, were included in the intravenous perfusate (Allen et al 1995). The dialysates from the microdialysis probes were analyzed to quantify Mn (by ETAAS) and antipyrine and 4-trimethylantipyrine (by high-pressure liquid chromatography [HPLC]), as described elsewhere (Allen et al 1995). An aliquot of the blood plasma from 5 of the 13 rats was centrifuged through an Amicon Centrifree Ultrafiltration System, containing a membrane with a molecular weight cutoff of 30 kDa, to determine the free (non-protein–bound) Mn fraction, by comparing Mn concentration in the plasma ultrafiltrate with that in the blood plasma.

STUDY 3: DETERMINATION OF Mn BRAIN INFLUX

Radioisotopic ^{54}Mn was employed in the studies of Mn brain influx (and efflux) because it enabled investigation of Mn distribution across the BBB at concentrations that do not exceed the reported Michaelis-Menten constant (K_m) of Mn influx into the brain, which is approximately 1 μM (Murphy et al 1991). It also allowed studies at more physiologically relevant Mn concentrations than could be achieved using nonradioisotopic Mn (^{55}Mn). The microdialysis technique used in preliminary studies allowed limited recovery of Mn and involved nonradioisotopic ^{55}Mn, which is normally present in the brain and blood; therefore, we had to establish Mn concentrations in the rat that were considerably higher than physiologic concentrations. In contrast, in later studies we used ^{54}Mn species, which are not normally present, so that their presence was unequivocally due to the administration of the ^{54}Mn test dose. A further disadvantage of microdialysis is that it typically requires sampling intervals of 5 to 20 minutes, which is sufficient time for Mn respeciation, in blood for example. Use of the in situ brain perfusion technique enabled us to study Mn influx over much shorter times after its administration than would be possible with microdialysis. The in situ brain perfusion technique also enabled control over Mn chemical species in the perfusate. Ligands that might associate with Mn could be excluded, reducing Mn respeciation.

Brain Influx Transfer Coefficients for Mn Species

We measured the brain influx rates of Mn^{2+}, Mn citrate, and Mn Tf to determine whether their influx rates differed significantly from their estimated diffusion rates. Greater influx than that which could be explained by diffusion was taken as evidence of one or more carrier-mediated influx processes. The unidirectional influx transfer coefficient (K_{in}) was determined for Mn^{2+} (after $MnCl_2$ administration), Mn citrate, and Mn Tf using the in situ brain perfusion technique (Takasato et al 1984), as modified by Drs Quentin Smith and David Allen (Smith 1996; Allen and Smith 2001). K_{in} is a measure of clearance from blood into one compartment containing endothelial cells, brain cells, and brain interstitial space. We coupled the determination of K_{in} described here with determination of the fractional distribution of isotope between the endothelial cells and the brain proper (brain cells and interstitial space) using the capillary depletion technique, as described later. This allowed us to report the corrected clearance from blood into the brain proper.

The in situ brain perfusion technique is a type of intravenous administration. Such techniques can be up to 100 times more sensitive than techniques based on indicator diffusion and can be modified to describe the K_{in} of substances with a wide range of BBB permeabilities (Smith 1989). In situ brain perfusion allows for more control over the chemical species of Mn than is possible with other techniques. Using this technique Dr Quentin Smith's group (Rabin et al 1993) found rapid uptake of Mn (when administered as $MnCl_2$) into the brain. The single-pass technique that employs bolus intracarotid arterial injection followed by decapitation in 15 seconds (Oldendorf method) was used to measure Mn uptake in the presence of Tf, at Mn concentrations up to 1000 μM (Aschner and Gannon 1994). This presumably demonstrated that 15 seconds is sufficient time to measure brain Mn uptake by TfR-mediated endocytosis, which is slower than the uptake process for low molecular weight Mn species (Murphy et al 1991). Therefore, we expected to be able to determine the K_{in} of Mn^{2+}, Mn citrate, and Mn Tf using the in situ brain perfusion technique. Longer incubation of Mn in the presence of Tf, which presumably increased Tf binding of Mn, increased the initial rate of brain uptake (Aschner and Gannon 1994). The extent of Tf binding of Mn was not determined. These results seem to conflict with the finding of reduced brain influx of Mn (introduced as $MnCl_2$) in the presence of blood, which was attributed to protein binding of Mn (Rabin et al 1993). We determined the K_{in} of Mn ion (introduced as $MnCl_2$,), Mn Tf, and Mn citrate, under similar conditions. We initially determined the K_{in} of Mn^{2+} and compared the results to those obtained using a saline perfusate (Rabin et al 1993), as part of the validation of this method in our hands.

In Situ Brain Perfusion Technique in Rats

The in situ brain perfusion technique is a surgical method used to study influx of substances across the BBB. A known concentration of radiolabeled test and reference materials perfuses the brain for a specific length of time (Figure 1). The animal is then decapitated, the brain is removed and dissected, and the tissues are weighed and

assayed for labeled test substances. The reference material, which has a very slow influx rate and does not appreciably cross the BBB during the time course of the experiment, serves as a marker of vascular volume and diffusion into the brain in a given tissue sample. For this study, $^{54}Mn^{2+}$, ^{54}Mn citrate, and ^{54}Mn Tf were used. The vascular marker reference compound included in the perfusate was ^{14}C-labeled sucrose.

Male Sprague Dawley rats were anesthetized with 75 mg/kg ketamine and 5 mg/kg xylazine. They were prepared for brain perfusion using described methods (Takasato et al 1984) that have been subsequently modified (Smith 1996; Allen and Smith 2001). The right common carotid artery was exposed near the branch of the internal and external carotid arteries. The external and common carotid arteries were ligated, and a perfusion catheter (PE-50 tubing) was inserted into the common carotid artery, with the outlet facing rostrally and terminating at the bifurcation. The pterygopalatine artery, which branches off the internal carotid artery and perfuses nonbrain tissue, was not ligated—a modification of the original technique. To compensate for this loss of perfusion fluid to the brain due to the perfusate flowing into the pterygopalatine artery, the perfusion rate was increased to maintain pressure, as described (Smith 1996; Allen and Smith 2001).

The cannula was attached to a syringe containing the perfusion fluid. $^{54}Mn^{2+}$, ^{54}Mn citrate, and ^{54}Mn Tf were administered in a perfusate (described in Appendix A) that also contained ^{14}C-sucrose to indicate the vascular and extravascular space of the brain occupied by the perfusate, as described under Statistical Methods and Data Analysis. The animal's chest cavity was opened, and the heart ventricles were cut open. Perfusion was started within 3 seconds and maintained at a constant delivery rate. The animal was decapitated at the completion of the perfusion duration (30–180 seconds). The brain was removed, surface blood vessels and meninges were removed, and the brain was dissected to harvest a number of regions from the perfused and contralateral hemispheres (see Table 4). After being weighed in tared tubes, the brain samples (usually 30 to 60 mg) were assayed for radioactivity in a γ counter to quantify ^{54}Mn, and the samples were digested (described in Appendix A). ^{14}C-sucrose was quantified by ^{14}C determination in a liquid scintillation counter (LSC), using established procedures (described in Appendix A). Two samples of the perfusion solution (20 to 50 µL) were obtained to determine the concentrations of ^{54}Mn and ^{14}C-sucrose. At least four brain perfusion durations were studied with each of the three Mn species. Perfusion durations were selected to ensure that entry of ^{54}Mn into the brain was sufficient for reliable determination of K_{in}; that the time was insufficient for brain ^{54}Mn to exceed 10% of blood ^{54}Mn, to minimize any contribution of Mn efflux to the determination of K_{in}; and that perfusion times would yield linear distribution volumes versus perfusion time curves (calculated as described under Statistical Methods and Data Analysis).

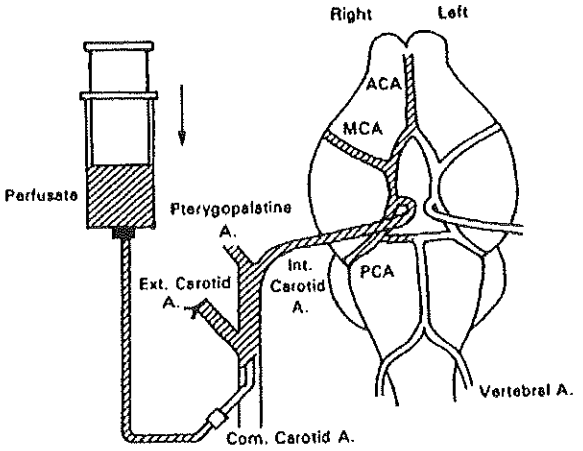

Figure 1. The in situ brain perfusion technique used to determine Mn influx. ACA is anterior cerebral artery; MCA, middle cerebral artery; PCA, posterior cerebral artery; Ext., external; Int., internal; Com., common; A., artery. Reproduced from Smith (1996), with permission of Kluwer Academic/Plenum Publishers and Dr Quentin Smith.

Flow Rate Dependency of Mn Influx Rate

This study examined the effect of perfusion flow rate on brain Mn influx rate. Flow-rate-dependent uptake is a property of some carrier-mediated uptake systems, but is not a property of diffusion. Animals were prepared for in situ brain perfusion and paired to receive the $^{54}Mn^{2+}$ or ^{14}C-sucrose perfusate at flow rates of 10 or 20 mL/min for 30, 60, 90, or 180 seconds.

Isolation of Brain Capillary Cells

The objective of this study was to differentiate ^{54}Mn reaching brain extracellular fluid from ^{54}Mn adsorbed onto or localized within endothelial cells. The capillary depletion method (Triguero et al 1990) separates brain tissue from capillary tissue. In this study, the brains were perfused, using the in situ brain perfusion technique, prior to separation into capillary and brain fractions. A detailed protocol of the capillary depletion is provided in Appendix A.

Animals were prepared as described previously and perfused at 10 mL/min through the right carotid artery. Perfusion durations of 90, 45, and 90 seconds for Mn^{2+}, Mn citrate, and Mn Tf, respectively, were chosen to maximize uptake while remaining within the linear portion of the uptake curves for all brain regions. The forebrain was isolated and the right lateral ventricle choroid plexus was

removed. The brain tissue (0.4 to 0.6 g) was homogenized in 3.5-mL ice-cold buffer with 8 to 10 strokes in a 15-mL tissue grinder (Tenbroeck, Wheaton Scientific, Milville NJ). The buffer contained (in mM): Na^+ (142), K^+ (4), Ca^{2+} (2.8), Mg^{2+} (1), Cl^- (151), $H_2PO_4^{2-}$ (1), SO_4^{2-} (1), D-glucose (10), and 4-(2-hydroxyethyl)-piperazine-1-ethanesulfonic acid (HEPES) (10), at pH 7.4. Dextran (70,000 g/mol) was added to a final concentration of 18% w/v, and the solution was homogenized with five additional strokes.

After centrifugation at 5400g for 15 minutes at 4°C, the supernatant (capillary-poor fraction containing neurons, glia, and contents of the vascular lumen) and pellet (capillary-enriched fraction containing the vascular network and nuclei of ruptured cells) were separated and counted for radioactivity. One disadvantage of this method is that the isotopes may redistribute between fractions during the isolation process. Care was taken to work rapidly and on ice to limit any redistribution of ^{54}Mn between the vascular and neuronal or glial compartments. We also examined the distribution of the relatively impermeable marker ^{14}C-sucrose, which did not appear to redistribute between fractions. Our values for the distribution volume of ^{14}C-sucrose in each fraction were 8.3 ± 1.0, 6.8 ± 1.3, and 0.20 ± 0.08 μL/g (mean ± SD), for the homogenate, supernatant (capillary-poor), and pellet (capillary-rich) fractions, respectively. These agree with reported values (Triguero et al 1990). If we assume that ^{54}Mn and ^{14}C-sucrose would redistribute similarly, then our lack of evidence for ^{14}C-sucrose redistribution implies that we were successful in limiting the redistribution of ^{54}Mn.

Effect of Nonradioactive Mn on Radioactive Mn Uptake

The objective of this study was to differentiate carrier-mediated from diffusional uptake processes. The diffusion rate, a function of membrane and substrate properties, is concentration-independent. Transporters, like enzymes, have limited capacities and can be saturated. Nonradioactive substrate competes with radioactive substrate for transporter binding sites and ultimately for transport across the membrane. If uptake is carrier-mediated, then $^{55}Mn^{2+}$ should inhibit the uptake of $^{54}Mn^{2+}$ and ^{55}Mn citrate should inhibit ^{54}Mn citrate uptake. This inhibition should be concentration-dependent.

Using the in situ brain perfusion technique, we measured the influx of 7 nM $^{54}Mn^{2+}$ in the presence of 0 and 1 × 10^2, 10^3, 10^4, 10^5, 10^6, and 10^7 nM $^{55}Mn^{2+}$ over 90 seconds. The influx of 7 nM ^{54}Mn citrate was measured in the presence of 0 and 1 × 10^2, 10^3, 10^4, 10^5, and 10^7 nM ^{55}Mn citrate over 45 seconds. Isolated brains were cleaned and dissected into nine brain regions and the choroid plexus, and tissue samples were prepared for radioactivity determination, as described previously.

STUDY 4. DETERMINATION OF Mn BRAIN EFFLUX

The experimental approach utilized determinations of the apparent elimination rate constant (K_{el}) and volume of distribution of Mn in the brain (V_{brain}), as initially described (Kakee et al 1996) and subsequently used (Kakee et al 1997, 2001; Kusuhara et al 1997; Takasawa et al 1997; Kitazawa et al 1998; Hosoya et al 1999, 2000; Zhang et al 1999; Asaba et al 2000). The brain efflux index (BEI) is the percentage of substance injected into the brain that has effluxed from brain to blood across the BBB. Therefore the percentage of Mn remaining in the brain is calculated as 100% (injected Mn) minus percentage of effluxed Mn (BEI); the term *100−BEI(%)* is used to represent this quantity. K_{el} is determined from 100−BEI(%), as described in the Statistical Methods and Data Analysis section. V_{brain} is determined from Mn uptake into brain slices. The brain capillary efflux rate (K_{out}) is calculated from the product of V_{brain} and K_{el}. It can be considered a clearance term with the units of volume/time/weight of brain. K_{out}, the influx transfer coefficient (K_{in}), and the product of brain capillary permeability and surface area ($P_{diffusion}S$) have comparable units of volume/time/mass brain.

Brain Efflux Index

The BEI method incorporates a reference compound that does not appreciably cross the BBB during the time course of the experiments, filling the same function as ^{14}C-sucrose in the in situ brain perfusion technique. We used both ^{14}C-sucrose and ^{14}C-dextran for this purpose. The BEI of Mn was determined from the coinjection of $^{54}Mn^{2+}$ or ^{54}Mn citrate and ^{14}C-sucrose or ^{14}C-dextran. The results obtained suggested that after their injection $^{54}Mn^{2+}$ and ^{54}Mn citrate respeciated to common species within the brain; therefore, we decided not to study Mn Tf efflux. Additionally, no evidence for Mn efflux from the brain was observed. Finally, it is suggested that there would be no Mn Tf in brain extracellular fluid, as reviewed in the Introduction section, to efflux from the brain.

Prior to conducting this study, we validated our ability to perform the intracerebral microinjection (described in Appendix A). Using these methods, the BEI was determined. A coin toss determined whether the right or left hemisphere was to be injected. The injected solution contained approximately 0.02 μCi (0.7×10^{-10} mol) ^{54}Mn and 0.008 μCi (1.6×10^{-11} mol) ^{14}C-sucrose or 0.008 μCi (approx. 1.3×10^{-7} mol) ^{14}C-dextran. When the time from injection to termination was longer than 5 minutes, 0.2 μCi ^{54}Mn and 0.005 μCi ^{14}C-sucrose or ^{14}C-dextran were injected. The amounts of ^{54}Mn and ^{14}C injected were chosen such that ^{54}Mn would be sufficient for its reliable quantification but would contribute no more than 10% to

the ^{14}C determination (described in Appendix A). Two injection solutions were studied: one contained (in mM) Na^+ (150), K^+ (5), Ca^{2+} (2), Mg^{2+} (1), Cl^- (141), HCO_3^- (20), and D-glucose (10), at pH 7.4; the other contained (in mM) Na^+ (147), K^+ (3.8), Ca^{2+} (1.4), Mg^{2+} (1.2), Cl^- (128), HCO_3^- (25), PO_4^{3-} (0.4), SO_4^{2-} (1.2), HEPES (10), and D-glucose (10), at pH 7.4, as previously used (Kakee et al 1996).

At a predetermined time after injection, the rat was decapitated, and the brain was removed and dissected into six equal sections. It was first bisected along the midline. Each hemisphere was then cut into rostral, medial, and caudal portions of approximately equal size, as described (Kakee et al 1996). ^{54}Mn was quantified in each weighed sample. The sample was then digested for ^{14}C determination (described in Appendix A). ^{54}Mn and ^{14}C were also quantified in an aliquot of the injection solution.

The BEI method provided the possibility to study brain efflux over shorter times than would be possible with microdialysis. It also provided control over the chemical species of Mn introduced into the brain, rather than having to speculate on the chemical species of Mn present in the brain after it entered the brain from blood.

Brain Distribution Volume

The distribution volume of Mn in the brain (V_{brain}) was determined by in vitro brain slice uptake experiments with $^{54}Mn^{2+}$, ^{54}Mn citrate, and ^{54}Mn Tf. Brains were removed from unanesthetized and anesthetized, decapitated rats. Anesthesia was achieved with 75 mg/kg ketamine and 5 mg/kg xylazine given intraperitoneally. The brains were dissected in ice-cold oxygenated tracer-free uptake solution and sectioned, using a McIlwain tissue chopper, to produce 300-μm-thick slices weighing approximately 10 mg from the Par2 region of the parietal cortex. The slices were immersed in freshly prepared tracer-free uptake solution at 37°C for 5 minutes prior to transfer to 12.5 mL of uptake solution at 37°C containing the radioisotopes. Two uptake solutions were employed, as described previously for the brain efflux index studies. For the uptake studies 0.05 μCi (1.7×10^{-10} mol) $^{54}Mn^{2+}$, ^{54}Mn citrate, or ^{54}Mn Tf and 0.01 μCi (2×10^{-11} mol) ^{14}C-sucrose were added. Uptake studies were conducted at 37°C. Sucrose indicated the extracellular space of the uptake solution.

At various times between 0 and 180 minutes (see Figure 7), three brain slices and an aliquot of the uptake solution were removed. The slices were rapidly rinsed twice in ice-cold tracer-free uptake solution and transferred to a tube. Each rinse was followed by removal of remaining liquid through capillary action by touching absorbent paper to the internal wall of the dish without contacting cells. Remaining uptake solution was removed from the slice, and the slice was weighed and counted to quantify ^{54}Mn, then digested in 500 μL 10% piperidine for ^{14}C quantification (described in Appendix A).

Initially, short uptake times (up to 11 minutes) were studied during which the V_{brain} value did not reach steady state. Longer incubation times, up to 180 minutes, were then studied (as shown in Figure 7). It was hypothesized that the considerable ^{54}Mn citrate uptake was due to incorporation of citrate in the tricarboxylic acid cycle, thereby enhancing dissociation of the ^{54}Mn citrate complex, promoting further uptake into the brain slice. To test this, 1 mM aconitine, 1 or 10 mM monofluoroacetate, or 0.2, 1, or 5 mM oxalomalate was added to the uptake solution. Aconitine, monofluoroacetate, and oxalomalate inhibit the enzyme aconitase that converts citrate to isocitrate, thereby reducing intracellular ATP (Festa et al 2000; Shinoda et al 2000). The effect of addition of sodium azide (1 mM), a respiratory chain inhibitor acting at complex I, was also assessed. Uptake of ^{54}Mn into slices was determined at 5, 30, 60, and 120 minutes in the presence of these inhibitors, using the methods described above.

STUDY 5: CHARACTERIZATION OF Mn TRANSPORTERS AT BBB

Results of the above studies revealed transporter-mediated brain uptake of Mn^{2+}, Mn citrate, and Mn Tf. We found no evidence of carrier-mediated Mn efflux from the brain. Experiments were then conducted with the aim of characterizing the properties, and ultimately identifying the transporters, mediating brain Mn uptake. Both single-cell and whole-animal models were utilized. Experiments were initially conducted with the rat erythrocyte, which expresses two transporters, and with two sources of BBB-derived cells, an immortalized murine cell line and primary cells obtained from bovine brain. The results of the experiments conducted in cell cultures were then used to design experiments in whole animals. This approach was taken because manipulations could be more rapidly conducted in cell cultures than in whole animals, enabling us to determine more rapidly some of the characteristics of Mn transporters and to rule out some candidates. However, the cell culture uptake studies provided only a partial model of the BBB because they were used to investigate uptake into cells, whereas BBB transport involves movement of substances both into and out of brain endothelial cells. We then returned to whole-animal studies to pursue this aim.

Cell culture models included the rat erythrocyte, which expresses MCT1 and the anion exchanger and could be used to assess their roles in Mn transport. The effects of

pharmacologic manipulation on Mn uptake were ascertained in immortalized (b.End5) and primary (bBMEC) BBB cells. Whole-animal experiments in Sprague Dawley rats used the in situ brain perfusion technique to inhibit putative Mn transporters through pharmacologic manipulations. Experiments were also conducted in homozygous Belgrade (*b/b*) rats, which do not express a functional form of DMT-1, one of the putative Mn transporters.

Experiments with primary cultures of bBMECs, a classical model of the BBB (Audus et al 1996), tested the effect of many pharmacologic probes on Mn^{2+} uptake. These cells are often studied as a monoculture in containers with a membrane on which the cells are grown (transwells). This enables the study of transport in both directions through the cell layer, modeling influx into and efflux from the brain through the BBB.

The BBB consists of endothelial cells with tight junctions, surrounded by a basement membrane of collagen and collagen-like protein. These endothelial cells constitute approximately 0.1% of the total volume of the brain (Pardridge 2003). Approximately 30% of the abluminal surface of these cells is surrounded by pericytes. Astrocyte foot processes cover a high percentage, variably estimated to be 80% to 100%, of this complex (Maynard et al 1957; Wolff 1963; Ambrosi et al 1995; Virgintino et al 1997). The bBMECs are used to grow a relatively pure population of brain capillary cells. Cells are plated and grown on a collagen matrix to study either uptake or transport.

One disadvantage to this in vitro model is that tight junctions between endothelial cells do not form as well as they do in vivo. This allows for greater movement between cells via diffusion. The gaps that can be found between cells in confluent bBMEC cultures are wide enough to allow significant paracellular passage of small ions (such as Mn^{2+}) and small complexes (such as Mn citrate). From the size of Mn^{2+} and Mn citrate and the rates of paracellular diffusion of comparable molecules in confluent bBMECs (Johnson and Anderson 2000), the amount of Mn transport through these cells would be expected to be relatively small compared with a large amount of diffusion. The studies of in situ influx rates suggested that Mn^{2+} (92%), Mn citrate (90%), and Mn Tf (75%) that initially entered the endothelial cells had already passed through the endothelial cells and crossed into brain extracellular fluid or brain cells during perfusion (see Isolation of Brain Capillary Cells, Study 3). This suggests that Mn entry into endothelial cells is equal to or slower than its export into brain space. That is, Mn uptake into bBMECs is the rate-determining step of Mn transport across the endothelial cell during influx. Therefore, Mn uptake studies were conducted.

Isolation of bBMECs

Janelle Crossgrove traveled to the University of Utah to learn the procedures to isolate bBMECs. She was trained by Jian Chen, a graduate student of Dr Brad Anderson. They successfully isolated endothelial cells in Utah, and Jian shared his protocols. At the University of Kentucky, the procedures were slightly modified to accommodate our different centrifuges and rotors. This enabled us to obtain sufficient yields of purified cells. The protocol for bBMEC isolation has been described in detail in a review (Audus et al 1996). The isolation procedures used also generally followed those described (Audus et al 1996). Two differences from the procedures in the review were that our isolation solutions of minimum essential medium contained sodium bicarbonate ($NaHCO_3$, 26 mM) and did not contain polymixin B. The cell culture medium used was similar to that described, with substitution of the antibiotics penicillin and streptomycin (100 U/mL and 100 µg/mL) for gentamicin (50 µg/mL).

In summary: bBMECs were isolated from fresh bovine brains using an established method (Bowman et al 1983), as described (Johnson and Anderson 1996) and reviewed (Audus et al 1996). Cow heads inspected and approved by the US Department of Agriculture were obtained immediately after slaughter, and the brains were removed. The meninges and surface blood vessels were removed, and the cortex was minced into millimeter-sized pieces. This brain dispersion was digested enzymatically with dispase (0.5% w/v). Microvessel fragments were collected by density centrifugation in 13% dextran before a second enzymatic digestion with collagenase-dispase (1 mg/mL) and purification through a Percoll gradient. The microvessel fragments and endothelial cells (bBMECs) were stored under liquid nitrogen until cultured. Approximately 25,000,000 cells were obtained from each bovine brain.

Approximately 500,000 cells were plated on each plastic 35-mm-diameter culture dish that had been collagen-coated and treated with fibronectin. Cells were grown at 37°C in 5% CO_2 with media containing 10% horse serum. Confluence was achieved around day 10 to 12. These bBMECs have the following characteristics of endothelial cells: (1) They are positive for γ-glutamyltransferase and alkaline phosphatase activity. (2) They do not have the processes or shapes associated with neurons and glial cells according to morphologic analysis of transmission electron microscopy (TEM) images. (3) They take up L-histidine, as do other isolated brain microvascular endothelial cells (Yamakami et al 1998). (Details of these validation procedures are in Appendix A.) Cultured, primary, nonpassaged bBMECs maintain excellent BBB characteristics (Weber et al 1993).

Polarity of the cultured cells, grown on a collagen matrix that resembles the abluminal basement membrane, is achieved and maintained. When the cells attach the abluminal face to the collagen, the observed differences in rates of unidirectional transport correlate with the expected differences (Borges et al 1994; Audus et al 1996).

Uptake Studies in bBMECs

^{54}Mn uptake was determined using procedures similar to those we had used previously (Yokel et al 2002). The uptake medium contained the following (in mM): Na^+ (122), K^+ (4.2), Ca^{2+} (1.5), Mg^{2+} (0.9), Cl^- (131), HEPES (10), and D-glucose (10), at pH 7.4. Briefly, each dish was rinsed three times in wash solution. This was a solution containing all the components of the uptake solution except the ^{14}C-sucrose and the $^{54}Mn^{2+}$ at the temperature of the uptake experiment. The third rinse remained on the cells for 10 minutes to equilibrate them to the reaction temperature. The cells were then incubated with 0.75 mL uptake media containing $^{54}Mn^{2+}$ at approximately 1.1 μCi/mL and at 184 nM total Mn (^{54}Mn and ^{55}Mn). Also, the media contained ^{14}C-sucrose at 1 μCi/mL (0.2 μM). The cells were incubated at their reaction temperature for the duration of the uptake study (10 to 120 minutes). After the completion of the incubation, the medium was removed and the cells were rapidly washed five times with ice-cold wash solution. Cells were removed and lysed with 0.75 mL sodium hydroxide (1 M) and neutralized with 0.75 mL equimolar hydrochloric acid (HCl). Cell lysates were collected for analysis of radioactivity. After γ radiation was determined, aliquots of the lysate were taken for scintillation counting and for protein determination via the bicinchoninic acid method.

Time Course of Mn Uptake in bBMECs

The initial experiment using bBMECs was to define the parameters to use in subsequent uptake experiments and identify a suitable time for those experiments prior to saturation of uptake. Total Mn uptake into bBMECs in culture dishes includes adsorption onto cells, exposed collagen, and the exposed plastic dish, as well as uptake via diffusion, pinocytosis, and carrier-mediated processes. To examine carrier-mediated Mn uptake processes, we had to account for these passive contributions to total ^{54}Mn uptake. Cell viability throughout the experiments was also measured, because carrier-mediated uptake is likely to be diminished in dead or unhealthy cells. Uptake was studied at two pH values to ascertain if it was linear at normal and reduced pH.

$^{54}Mn^{2+}$ adsorption onto collagen-coated dishes in the absence of cells was measured, because $^{54}Mn^{2+}$ does associate with collagen over the time course of the experiment. Collagen-only dishes were treated using the same procedures as cell dishes, from the initial three prerinses through the base-digestion and acid steps. Plastic cell culture dishes without collagen were similarly treated to measure the adsorption of Mn to any exposed plastic. Nonspecific binding of ^{54}Mn and ^{14}C-sucrose to all components of the collagen-coated dishes was determined as uptake for 15 seconds into ice-cold cells in culture dishes with ice-cold uptake media. Cells were lysed and lysates were analyzed as described previously.

Cell viability was measured in parallel dishes exposed to the same treatments. Cell membrane integrity was measured by determining the amount of lactate dehydrogenase released into the uptake media. Lactate dehydrogenase is a cytosolic enzyme. Cell redox potential was measured by the conversion of methylthiazoletetrazolium (MTT) to its formazan product as an indication of cell health (Mossman 1983).

Pharmacologic Manipulations of Uptake in bBMECs

Once we had determined a suitable time for uptake experiments, we determined the effects of various pharmacologic manipulations on Mn^{2+} uptake. Many of the major characteristics that differentiate transporters are shown in Figure 2. We used this scheme as a guide to the selection of pharmacologic manipulations to characterize Mn uptake processes. Each experiment compared the uptake achieved with one or more pharmacologic manipulations and the control uptake; collagen-only dishes were used and nonspecific binding controls were included for each treatment. Manipulations included uptake time, pH differences, sodium replacement, and the presence of inhibitors of energy production or of transporters.

Proton Dependence We studied the effect of pH on $^{54}Mn^{2+}$ uptake to test the hypothesis that the Mn carrier is proton-dependent. Many transporters are dependent on proton gradients. There are proton cotransporters for inorganic ions, sugars, amino acids, dipeptides, lactate, and other substances. There are also many proton-independent transporters. For proton-dependent transporters, such as the monocarboxylate transporter, substrate uptake inversely correlates with extracellular pH (Rosenberg et al 1993; Garcia et al 1994). This is presumably also true for DMT-1. Mn^{2+} was shown to be a substrate for DMT-1 at pH 5.5 when it was transfected into oocytes (Gunshin et al 1997). DMT-1 is expressed at some cell membranes, including the intestine and BBB (Burdo et al 2001). DMT-1 is a proton-dependent pump (cotransporter). It transports several divalent metals, including Fe^{2+}, Zn^{2+}, and Cu^{2+}, and may work in conjunction with the TfR. For metal transport

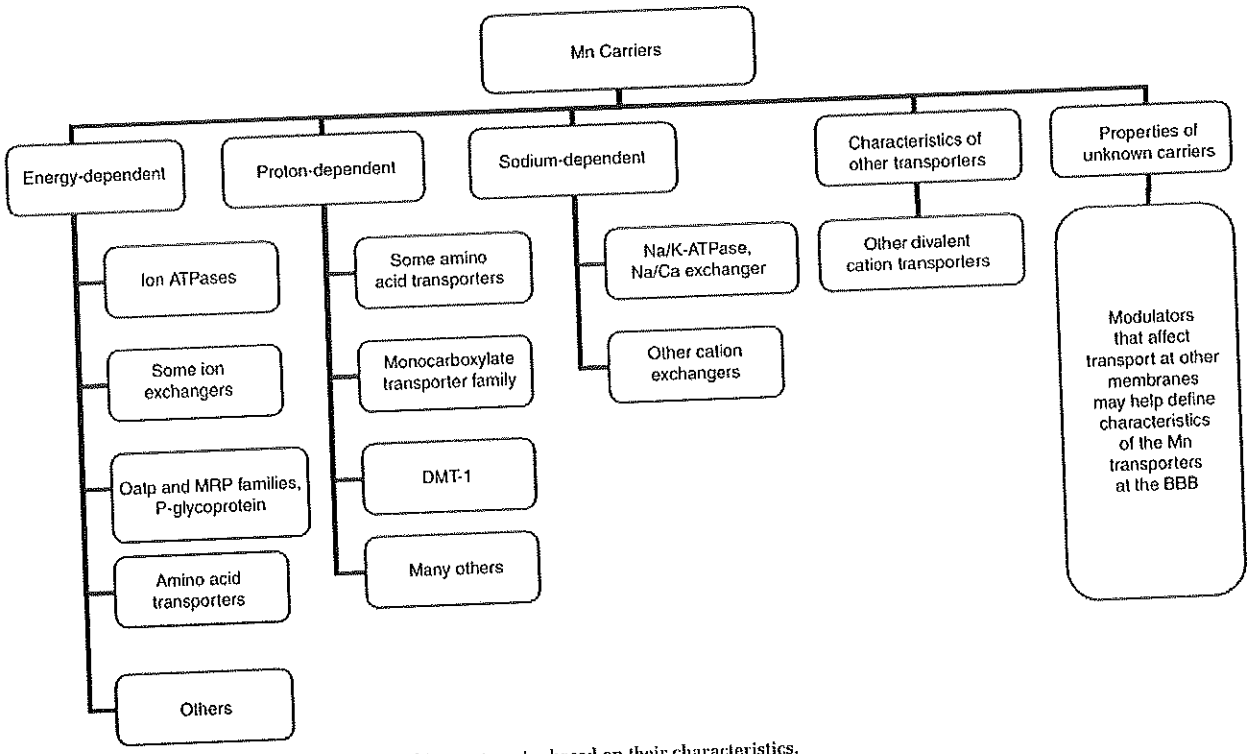

Figure 2. Possible Mn carriers at the BBB, divided into categories based on their characteristics.

via DMT-1, the optimum pH is 5.5. We hypothesized that Mn^{2+} brain entry at the BBB, in the absence of Tf, was mediated through DMT-1 at blood pH. To test the hypothesis that the Mn carrier is a proton cotransporter (symporter), $^{54}Mn^{2+}$ uptake at 30 minutes was measured in media buffered with sulfonic acids to pH 6.4 (10 mM piperazine diethanesulfonic acid [PIPES]), 6.9 (10 mM 4-morpholine propanesulfonic acid [MOPS]), 7.4 (10 mM HEPES), and 7.9 (10 mM HEPES). In one experiment, $^{54}Mn^{2+}$ uptake was measured in potassium hydrogen phthalate buffer at pH 5.4, but cell viability was reduced to only 6% of control viability, and that experiment was not repeated.

Sodium Dependence We conducted experiments in which sodium was partially or totally deleted from the uptake medium to test the hypothesis that it has a role in Mn^{2+} uptake at the BBB. On the one hand, sodium plays a role in the cotransport or exchange of several substrates. Many transporters are dependent on sodium or proton gradients. There are sodium cotransporters for inorganic ions, sugars, amino acids, nucleosides, bile acids, lactate, and other substances. On the other hand, there are many sodium-independent transporters. The role of sodium in Mn^{2+} uptake into bBMECs was measured by replacing 50% or 100% of the sodium in Mn^{2+} uptake media with choline or lithium.

Energy Dependence Using metabolic inhibitors, we tested the hypothesis that the Mn carrier is energy-dependent. Some transporters actively import substrates while expending energy, while others facilitate influx without depleting energy stores. We found that the intracellular Mn concentration in bBMECs after a 30-minute incubation exceeded the extracellular concentration by at least 10-fold (see Results section). This is evidence of concentrative uptake. It is expected that a source of energy is required to produce and maintain this concentration gradient. Energy may be provided by ATP hydrolysis or the movement of electrons. We hypothesized that blocking ATP hydrolysis would inhibit Mn^{2+} uptake into bBMECs. Cells were treated with Mn^{2+} in the presence of several energy inhibitors. 2,4-Dinitrophenol (0.25 mM) releases proton gradients and causes Ca^{2+} release from mitochondria to prevent the driving force of ATP production (Lynch and Deth 1984; Patel et al 2001). Azide (10 mM) inhibits complex IV in the electron transport chain (Cheng et al 2001). 2-Deoxyglucose (10 mM) produces a metabolically inactive metabolite that inhibits glycolysis (Newman et al 1990; Cheng et al 2001).

ATPase Membrane Channels We determined whether Mn uptake occurred via a P-type ATPase. P-type ATPases are membrane channels that pump ions across the cell

membrane and use ATP as an energy source (Carafoli and Brini 2000). Because Mn^{2+} has the same charge and relative size as Ca^{2+}, we hypothesized that Mn^{2+} brain entry may involve one or more Ca^{2+} channels or transporters. Ca^{2+}-ATPase is a plasma membrane calcium pump, reviewed in Carafoli and Brini (2000), which is located on brain capillary cells (Keep et al 1999; Manoonkitiwongsa et al 2000). We hypothesized that Ca^{2+}-ATPase may mediate Mn^{2+} transport at the BBB. Vanadate is a nonspecific inhibitor of p-type ATPases, including Ca^{2+}-ATPase (Tiffert and Lew 2001). It was added to the uptake media at 0.003 and 1 mM. To address the concern that vanadate might not enter bBMECs rapidly enough to be available to inhibit Mn uptake, it was added 30 minutes prior to Mn uptake study and then washed out. This also tested the reversibility of the vanadate effect on Mn uptake. Ouabain selectively inhibits Na^+/K^+-ATPase by competing for the K^+ binding site. It was added at 100 μM.

Uptake Studies in Intact Rats, Erythrocytes, and b.End5 Cells

In order to elucidate the properties and possibly identify Mn transporters at the BBB, we also conducted experiments in intact rats using in situ brain perfusion. Results of our bBMEC experiments supported the hypothesis that brain Mn uptake is mediated by a Ca^{2+}-ATPase: Mn^{2+} uptake was significantly and irreversibly inhibited by 1 mM vanadate, a concentration sufficient to block Ca^{2+} movement in red cell suspensions (Tiffert and Lew 2001). Therefore, we conducted in situ perfusion experiments in which vanadate (1 mM) was included in treatment perfusates. Perfusates with 10 mM vanadate were also studied because vanadate may not be extracted from the uptake media to a great extent. For example, Mn extraction is less than 10% during a 90-second perfusion.

p-Hydroxyhippuric acid is a specific inhibitor of Ca^{2+}-ATPase (Jankowski et al 2001). It was hypothesized that Mn^{2+} may enter the brain via a Ca^{2+}-ATPase, as both are divalent cations. In human erythrocytes, *p*-hydroxyhippuric acid (100 μM) inhibited Ca^{2+}-ATPase activity to 30% of basal activity (Jankowski et al 2001). In our experiments, *p*-hydroxyhippuric acid (200 or 400 μM) was added to the perfusate.

Iron Competition We tested the hypothesis that uptake of Mn and a similar divalent metal ion, ferrous iron (Fe^{2+}), are mediated by a common transporter. Since Mn and Fe are chemically similar, we hypothesized that they may be transported into the brain by the same process or processes and that Fe would compete for Mn uptake transporters. Fe and Mn are known to compete at the intestinal lumen (Simpson and Peters 1985). To test this hypothesis the effect of Fe^{2+} on $^{54}Mn^{2+}$ uptake was determined. Sprague Dawley rats were perfused with a perfusate containing 184 nM $^{54}Mn^{2+}$ and 0 or 100 μM ferrous sulfate ($FeSO_4$) for 90 or 180 seconds. Experiments were completed without antioxidant present or with 0.01% (5.3 mM) sodium bisulfite or 0.1 mM ascorbic acid. Control animals were completed for each experiment with Fe-free perfusate in the absence or presence of antioxidant.

DMT-1 Transporter To test the hypothesis that Mn is transported into the brain by DMT-1, we conducted experiments in a rat model that does not express a functional form of this transporter, the *b/b* Belgrade rat. The transport of iron, zinc, copper, cadmium, calcium, nickel, lead, and manganese by oocytes transfected with DMT-1 messenger RNA at pH 5.5 has been shown (Gunshin et al 1997). Fe and Mn compete for uptake via DMT-1 in human leukemia and kidney cell lines (Conrad et al 2000). DMT-1 is present in brain capillary cells (Burdo et al 2001). We hypothesized that Mn^{2+} brain uptake may be mediated by DMT-1.

Homozygous (*b/b*) Belgrade rats do not express functional DMT-1. Genotyping of the *b/b* and *+/b* Belgrade rats is described in Appendix A. A preliminary experiment was conducted to determine the rates of $^{54}Mn^{2+}$ brain uptake in *b/b* and *+/b* rats. For at least 2 weeks prior to study, all rats were maintained on a rodent chow (Harlan Teklad 2016) containing approximately 215 mg Fe/kg body weight. Brain $^{54}Mn^{2+}$ uptake was determined in five *b/b* female rats 135 to 220 days old, one female and five male *+/b* rats 140 to 560 days old, and six female Wistar rats 115 to 130 days old. The in situ brain perfusion technique was used. The perfusate solution contained ^{54}Mn (375 nm total Mn) as either $^{54}Mn^{2+}$ or ^{54}Mn Tf. Perfusion lasted 90 seconds. The rats were not paired. In a subsequent experiment conducted under more controlled conditions, rats were assigned to squads consisting of a *b/b* Belgrade rat 65 to 92 days old, a *+/b* littermate of the same sex, and a Wistar rat that was on the average 24 days older. All subjects within the squad were randomly assigned to receive in situ brain perfusion containing $^{54}Mn^{2+}$ or ^{54}Mn Tf.

To determine the distribution of Mn that was associated with the brain, squads of rats were randomly assigned to receive in situ brain perfusion containing $^{54}Mn^{2+}$ or ^{54}Mn Tf in the absence or presence of a cerebrovascular washout. The Belgrade rats were 71 to 82 (mean, 77) days old, the paired Wistar rats were 60 to 90 (mean, 69) days old, and with two exceptions, the rats were the same sex. The first objective was to determine whether ^{54}Mn adsorbed onto the endothelial cells during in situ cerebrovascular perfusion without further entering the endothelial cells, brain extracellular fluid, or brain cells. The brain ^{54}Mn influx

transfer coefficient (K_{in}) was determined in the perfused cerebellum, midbrain/colliculus, and pons/medulla and in nine brain regions contralateral to the perfused hemisphere. To remove ^{54}Mn and ^{14}C-sucrose adsorbed onto the luminal surface of the brain endothelial cells that constitute the BBB, a wash solution containing a Mn chelator was perfused through the brain after the ^{54}Mn-containing perfusate. It was hypothesized that if ^{54}Mn simply adsorbed onto the capillary membranes, then brain uptake of ^{54}Mn would be lower in rats that received the cerebrovascular washout after perfusion. The second objective was to ascertain if the brain Mn was primarily associated with the brain endothelial cells, or if a significant fraction had distributed through these cells into brain extracellular fluid and brain cells. After ^{54}Mn perfusion in the absence or presence of a cerebrovascular washout, the brain endothelial cells were separated from the remainder of the cerebrum.

Mn Citrate Transporters To determine the ability of Mn citrate to serve as a substrate for MCT1 and the band 3 (anion exchange) transporter, we used the rat erythrocyte, which expresses both MCT1 and the band 3 (anion exchange) transporter. This enabled us to test the hypothesis that Mn citrate is a substrate for one or both of these carriers. The rat erythrocyte is a classical preparation for the investigation of these carriers. Lactate and pyruvate are substrates for the monocarboxylate transporter. Therefore, pyruvate competes for lactate uptake. Band 3 exchanges chloride for bicarbonate. Two experiments were conducted to determine if Mn citrate serves as a substrate for one or both of these transporters. In the first experiment Mn citrate (5 and 10 mM) and 2 mM pyruvate were compared for their ability to inhibit uptake of 1 mM ^{14}C-lactate at 6°C after 20, 60, and 300 seconds. The second experiment was conducted at room temperature using a buffer containing sulfate (rather than the usual chloride) to remove the chloride gradient that might drive MCT1 and the anion exchanger to efflux Mn from erythrocytes if it enters those cells. This ensures that the transporters are acting as influx carriers. This experiment assessed the ability of 1 mM ^{14}C-citrate and 5 and 10 mM Mn ^{14}C-citrate to be taken up by the erythrocyte. Both of these experiments were conducted with triplicate observations.

We used an immortalized cell line, b.End5, to determine both the ability of Mn citrate to serve as a substrate for transporters and the pH dependence of its uptake. These cells were established from murine brain endothelial cells (the cells that constitute the BBB) and were obtained from the European Collection of Cell Culture. These cells express many of the properties of brain endothelial cells, including the endothelial-specific proteins PECAM-1, endoglin, MECA-23, and Flk-1, according to the supplier. We utilized them in uptake experiments in conjunction with uptake studies of Al citrate (Yokel et al 2002). We determined the time course and pH dependence of Mn citrate uptake.

In an initial study we determined the time course over 4 hours of Mn ^{14}C-citrate uptake by b.End5 cells. The cells were grown in 35-mm plastic dishes until nearly confluent. They were bathed in a physiologic medium containing 1 mM ^{14}C-citrate, Mn ^{14}C-citrate, or Al ^{14}C-citrate for 15, 60, 120, or 240 minutes at room temperature in one experiment conducted with triplicate observations. Uptake was normalized to cell volume, which was estimated from protein determination of the cells, assuming intracellular volume of 2 µL/1 mg protein. Uptake from media with pH 6.9 and 7.4 was also determined after 1 hour in three experiments, each conducted with triplicate observations.

An experiment was conducted to test the hypothesis that the Mn citrate carrier is a member of the family of organic anion transporters. Citrate is an endogenous metal chelator. At the dilute Mn and citrate concentrations and pH (7.33) of brain extracellular fluid or blood plasma, Mn citrate complex would be expected to be a monomer (Amico and Daniele 1979). Each citrate ion forms a tridentate complex with Fe, Mn, or Al involving the hydroxyl group and two terminal carboxylates, leaving a noncoordinated central carboxylate, as reviewed in the Introduction, which may serve as the recognition moiety of Mn citrate for the monocarboxylate transporter. As a 1:1 complex, Mn citrate has a negative charge and may serve as a substrate for an organic anion transporter. To examine the characteristics of Mn citrate uptake, rats were perfused with ^{54}Mn citrate for 45 seconds at 10 mL/min in the near absence of sodium, which is a potential cosubstrate of some transporters, and in the presence of quercetin, an inhibitor of the monocarboxylate transporter family.

Calcium Transport Pathways After the results of the above studies, we generated the hypothesis that the Mn^{2+} carrier is a Ca^{2+} carrier. Brain Mn^{2+} influx may occur via one or more calcium transport pathways. Calcium inhibits Mn entry into Hep-G2 cells (Finley 1998). Inhibitors of calcium entry also decrease Mn influx into thymic lymphocytes (Mason et al 1993), human erythrocytes (Lucaciu et al 1997), and a subclone of HEK293 cells (Kerper and Hinkle 1997a). Therefore, Mn ion entry could occur through calcium carriers at the BBB. Mn uptake into cells has been reported to occur via voltage-gated calcium channels, the sodium-calcium exchanger, the sodium-magnesium antiporter, and the active calcium uniporter (for review, see Takeda 2003).

Normal Ca^{2+} cycles include the release of endoplasmic Ca^{2+} stores into cytosol during Ca^{2+} oscillations or waves,

which are produced by a variety of events. Ca-ATPases pump intracellular free Ca^{2+} from the cytoplasm into the endoplasmic reticulum (sarco-endoplasmic reticulum Ca-ATPase) or out of the cell (plasma membrane calcium pump) to recover from the flood of cytosolic calcium. When intracellular stores are depleted of calcium, an unknown signal opens the plasma membrane store-operated channel to allow Ca^{2+} entry from extracellular fluid.

BBB cells express Ca^{2+}-ATPase, receptor-operated calcium channels, and store-operated calcium channels. The endothelial cells, which provide the initial barrier from blood to brain, are considered nonexcitable and would not be expected to have voltage-sensitive calcium channels. The perfusate and uptake solutions we used did not include receptor ligands, so activation of these pathways was not expected, assuming a minimal role for paracrine or autocrine factors. The store-operated calcium channel has not been specifically identified or crystallized but is thought to be homologous to the transient receptor potential (*TRP*) gene family. Mn entry through store-operated calcium channels increases in response to thapsigargin and cyclopiazonic acid, chemicals that deplete Ca^{2+} stores. Mn^{2+} has been shown to enter rat peritoneal mast cells through the store-operated calcium channel (Fasolato et al 1993a,b).

To test the hypothesis that Mn^{2+} influx is mediated by one or more calcium carriers, we conducted experiments using the in situ animal model. K_{in} values were determined at three perfusate calcium concentrations (0, 1.5, and 9 mM) and in the presence of calcium influx inhibitors. Inhibitors included nifedipine, amiloride, and verapamil (for voltage-gated calcium channels) and lanthanum nitrate [$La(NO_3)_3$, 50 µM] or nickel chloride ($NiCl_2$,1 mM). Lanthanum and nickel are inhibitors of a variety of calcium channels. In cell culture studies, Mn uptake into bBMECs was measured in the presence of $La(NO_3)_3$ (50 µM) or $NiCl_2$ (1 mM). Also, intracellular calcium stores were depleted by pretreatment with cyclopiazonic acid (10 µM) or thapsigargin (1 µM) for 5 to 10 minutes, after a published protocol for bBMECs (Kerper and Hinkle 1997b). Mn uptake in the continued presence of these Ca^{2+}-depleting chemicals was measured. The inhibitors used are relatively nonspecific, but the number of probes and preparations increased our confidence in the results.

STATISTICAL METHODS AND DATA ANALYSIS

ESTIMATION OF BRAIN UPTAKE RATES OF Mn SPECIES BY DIFFUSION

Rat brain cerebral capillary diffusion rates were estimated from the results of Study 1 based on the relation between molecular weight (MW) and the $D_{o/a}$, as described elsewhere (Ohno et al 1978; Levin 1980):

$$\log P_{diffusion} = -4.605 + (0.4115 \times \log [D_{o/a} \div MW^{1/2}]) .$$

The product of permeability and surface area ($P_{diffusion}S$ in mL/sec/g brain tissue) was then calculated by multiplying diffusion permeability by rat brain capillary surface area (240 cm^2/g; [Crone 1963]) as described elsewhere (Smith 1989).

CALCULATION OF TOXICOKINETIC PARAMETERS

The toxicokinetic parameters describing the results obtained after bolus intravenous injection of Mn into the rat were determined using a noncompartmental toxicokinetic modeling program (Fox and Lamson 1989). The area under the curve, area under the moment curve, initial blood concentration, and elimination half-life were determined from plots of Mn concentration versus sample collection time. Clearance (Cl_s) and volume of distribution (V_d) were calculated as described (Rowland and Tozer 1995).

ESTIMATION OF INFLUX PARAMETERS

For each brain region harvested from each animal after in situ brain perfusion, γ counts were converted to ^{54}Mn disintegrations per minute (dpm) per gram brain tissue. The ratio of ^{54}Mn in brain tissue to that in perfusate (which resolves to milliliters per gram) was calculated and plotted against time. From the linear portion of the graph, the slope was determined as the regression of the points for each tissue and each Mn species. The unidirectional influx transfer coefficient (K_{in}) is represented by the slope of the graph. K_{in} is a measure of the rate of influx of a substance in a given time into a given amount (space) of brain. It is the quotient of uptake space and time, and reflects the volume of perfusate cleared of substrate that is transferred into 1 g of brain over a given time period. The slope and its SEM were calculated using Microsoft Excel. The slope (K_{in}) has the units of milliliters per second per gram brain tissue.

The distribution volume, or uptake space (Q), is the amount of brain tissue into which the substrate distributes during a given perfusion duration. Q values (in milliliters per gram brain tissue) of ^{54}Mn and ^{14}C were calculated as

Q = Radioactivity per weight tissue (dpm/g)
/Radioactivity per volume perfusate (dpm/mL).

The ^{54}Mn uptake space results were corrected for the sample's vascular and extracellular space by subtracting the ^{14}C-sucrose uptake space; that is,

Corrected $Q_{Mn} = Q_{Mn\ total} - Q_{sucrose}$.

Thus,

$$\text{Corrected } Q_{Mn} = (^{54}Mn_{brain}\ [dpm/g] \div {}^{54}Mn_{perf}\ [dpm/mL]) - ({}^{14}C\text{-}Sucrose_{brain}\ [dpm/g] \div {}^{14}C\text{-}Sucrose_{perf}\ [dpm/mL]).$$

The second fraction ($Q_{sucrose}$) had a mean of 0.011 mL/g brain at 90 seconds. The corrected uptake spaces were plotted against perfusion time. Extreme values were tested by the Dixon criterion to determine whether they were outliers. To test for linearity, analysis of variance (ANOVA) of the uptake space versus time was conducted for each tissue and each Mn species. The F test determined linearity. If uptake was not linear throughout the four perfusion durations, then the lower three perfusion durations (30, 60, and 90 seconds for Mn^{2+} and Mn Tf; 15, 30, and 45 seconds for Mn citrate) were tested for linearity. The linear least-squares regression of the data points was plotted using Microsoft Excel. For ^{54}Mn Tf data, the ^{54}Mn activity in dpm was corrected for the contribution of $^{54}Mn^{2+}$, which accounted for 19% of the ^{54}Mn in the perfusate (described in Appendix A). For perfusate samples, the correction simply decreased total dpm by 19%. In tissue samples, this correction is the product of the tissue K_{in} for $^{54}Mn^{2+}$, the perfusion time, and the concentration of $^{54}Mn^{2+}$ as follows:

$$^{54}Mn\ Tf\ (dpm/g) = \text{Total } {}^{54}Mn\ (dpm/g) - (K_{in}\ [mL/sec/g]) \times (\text{Time [sec]}) \times (\text{Total } {}^{54}Mn\ [dpm/mL] \times 0.19).$$

K_{in} values were then converted to PS (the product of cerebrovascular permeability and surface area) using the Renkin-Crone model values according to the equation (Smith 1989):

$$PS = -vF \times \ln (1 - K_{in}/vF)$$

where P is permeability, S is the surface area of the perfused capillaries, F is the regional flow, and v is the fractional distribution of tracer in blood (for perfusate, $v = 1$). S is 240 cm^2/g brain (Crone 1963). P has units of distance per time. PS has units of volume per time per brain weight and is expressed as milliliters per second per gram. Influx (J) was calculated as the product of PS and Mn concentration and had the units of nanomoles per second per gram. The graphs of mean J versus concentration (C) were plotted and fit to the following Michaelis-Menten equations where J_0, J_1, and J_2 each represent a fit of the same J data set as defined below, K_d is the diffusional constant, C is concentration of total Mn (in nanomoles), V_{max} is the maximum velocity of the putative transporters, and K_m is the Michaelis-Menten constant of saturable uptake.

$$J_0 = K_d \times C$$
$$J_1 = V_{max} \times C/[K_m + C] + K_d \times C$$
$$J_2 = V_{max2} \times C/[K_{m2} + C] + V_{max} \times C/[K_m + C] + K_d \times C$$

The product of K_dC represents the nonsaturable component of uptake. The F test was used to determine the best-fitting model for each tissue and each Mn species. The K_m and V_{max} values were determined by nonlinear regression analysis of Mn influx versus concentration using SAAM II and GraphPad Prizm computer software programs.

Differences between tissue K_{in} values and predicted diffusion rates were compared by t tests, using the Bonferroni correction for multiple testing. In single-time-point experiments, the K_{in} values were determined by directly dividing each uptake space (milliliters per gram) by its perfusion duration (seconds). Comparisons were made by t test with the Bonferroni correction factor or with the Dunnett test.

Comparisons of the K_{in} values among the b/b, $+/b$, and Wistar rats were made by one-way ANOVA tests followed by a Bonferroni multiple comparison test.

To assess the results of in situ brain perfusion studies of the effect of $^{55}Mn^{2+}$, Fe^{2+}, vanadate, p-hydroxyhippuric acid, the absence of functional DMT-1 expression, and quercetin on ^{54}Mn uptake, influx rates were calculated as previously described with considerations for the diffusion of ^{54}Mn and the amount of ^{54}Mn remaining in the vasculature (sucrose space). The rates obtained in the presence of a treatment were then converted to percentages of control rates. The data were compared for any differences by a two-tailed t test with GraphPad Prizm.

COMPUTATION OF BRAIN EFFLUX INDEX

In Study 4, which investigated the efflux of Mn from the brain, brain efflux index (BEI) was calculated from the sum of the ^{54}Mn and ^{14}C-sucrose in the six brain sections compared to the amount injected, as described (Kakee et al 1996):

$$100\% - \text{BEI} = ({}^{54}Mn \text{ in brain}/{}^{14}C \text{ in brain}) / ({}^{54}Mn \text{ injected}/\text{Amount of } {}^{14}C \text{ injected}) \times 100$$

The ^{14}C-sucrose associated with the brain slices of Study 4 was graphed versus time to enable calculation of tissue extracellular space occupied by the uptake solution at time zero, from the y-intercept of the graph. The ^{54}Mn associated

with the slices was graphed versus time to enable determination of the apparent distribution volume (V_{brain}) of the Mn species. The ^{54}Mn values were corrected for the extracellular space occupied by the uptake solution, as estimated from the ^{14}C-sucrose results. The V_{brain} results represent a ratio of slice (tissue) to solution (medium).

A one-way ANOVA was used to compare all V_{brain} values followed by two-tailed unpaired t tests to compare the three Mn species to sucrose. The V_{brain} values obtained at the last two times studied for each Mn species were compared by two-tailed paired t tests.

STUDIES WITH CELL CULTURES

The γ radioactivity of bBMEC lysates and aliquots of uptake media from studies of Mn uptake into bBMECs was measured. The sample was then split to determine protein content and β radioactivity.

Total ^{54}Mn in the bBMEC lysate includes that of carrier-mediated and diffusional uptake as well as nonspecific adsorption to cells and collagen, as represented in the following equation.

$$\begin{aligned}\text{Lysate } ^{54}\text{Mn} = {} & \text{Carrier-mediated uptake into cells} \\ & + \text{Diffusion-mediated or pinocytotic uptake into cells} \\ & + \text{Nonspecific adsorption to cells} \\ & + \text{Nonspecific adsorption to collagen}\end{aligned}$$

Within-experiment determinations of nonspecific binding and diffusional or pinocytotic uptake were measured to account for these contributors. Uptake into dishes without cells (collagen-only dishes) and uptake into cells for 15 seconds on ice were determined as a measure of nonspecific adsorption to collagen and cells. We included ^{14}C-sucrose in the uptake media to measure diffusional and pinocytotic uptake from the uptake media. The nonspecific adsorption of Mn to the dish was also determined several times and was found to be negligible.

Subtracting the ^{54}Mn due to nonspecific binding and diffusional or pinocytotic uptake from the total amount of ^{54}Mn in the lysate estimated carrier-mediated uptake of Mn into bBMECs as picomoles per milligram protein. If one applies the estimation of 2 µL intracellular space per 1 mg total protein (Edlund and Halestrap 1988; Poole et al 1989), one can calculate the intracellular Mn concentration. One can then compare intracellular Mn concentration among treatments or versus media concentration.

For the cell culture experiments described in Study 5, each condition was examined in duplicate or triplicate within each experiment. Results of the time course of Mn uptake at pH 6.4 and 7.4 were analyzed by regression analysis using GraphPad Prizm to determine if uptake was best fit by a first-order or second-order relation. Uptake in the presence of treatments was converted to a percentage of control uptake for that experiment. The mean and relative standard deviation were calculated. To test for treatment differences, t tests or one-way ANOVAs were conducted. When found, post hoc comparisons were conducted after the ANOVAs to determine significant differences among treatment groups.

For all studies, a difference of $P < 0.05$ was accepted as statistically significant.

RESULTS

STUDY 1. CEREBRAL CAPILLARY DIFFUSION PERMEABILITY OF Mn SPECIES

In the absence of competing ligands for citrate or Tf (other anions or complexing proteins that have a comparable or superior stability constant with Mn and are present in sufficient concentration), Mn would be anticipated to associate with citrate and Tf. Our results suggest Mn citrate was successfully formed and that a high percentage of Mn was associated with Tf. The unbound fraction of Mn, in the presence of Tf, was estimated. (The methods we used to prepare Mn citrate and Mn Tf and the results we obtained are reported in Appendix A.)

The $D_{o/a}$ of Mn Tf was corrected to account for the contribution of the unbound fraction of Mn. Nineteen percent of Mn was found to be unbound and was assumed to have the same partitioning coefficient as Mn^{2+} in solution. The $D_{o/a}$ values for Mn^{2+}, Mn citrate, and Mn Tf, corrected for the contribution of the unbound Mn, are shown in Table 2.

The calculated rat brain capillary diffusion rates of Mn, Mn citrate, and Mn Tf are also shown in Table 2. All values were estimated to be less than 3×10^{-5} mL/sec/g brain. For comparison, the diffusion rates of sucrose and dextran were also estimated from their published permeability or their octanol/aqueous partitioning coefficients and molecular weights, and were found to be less than 5×10^{-5} mL/sec/g brain.

STUDY 2. Mn TOXICOKINETICS AFTER INTRAVENOUS INJECTION AND BRAIN–BLOOD RATIO

The results of the toxicokinetic determination of Mn after its intravenous administration (Table 3) show similar clearances and steady-state volumes of distribution for Mn^{2+} and Mn citrate. These results, obtained after intravenous injection of 25 µmol/kg $MnCl_2$, are compared to results of a study that administered larger doses to rats and was therefore able

Table 2. Octanol/Aqueous Partitioning Coefficients and Predicted Rat Brain Capillary Diffusion Rates for Three Mn Species and Two Diffusion Markers[a]

Mn Species or Diffusion Marker	$D_{o/a}$	$P_{diffusion}$	$P_{diffusion}S$ Shown × 10^5 (mL/sec/g)
Mn^{2+}	3.6×10^{-6}	6.3×10^{-8}	1.5 ± 0.1
Mn citrate	1.0×10^{-5}	6.8×10^{-8}	1.7 ± 0.2
Mn Tf	8.0×10^{-4}	1.2×10^{-7}	2.8 ± 0.5
Sucrose[b]	—	1.2×10^{-7}	2.9
Dextran[c]	2.1×10^{-3}	2.0×10^{-7}	4.8

[a] $D_{o/a}$, determined experimentally, is the octanol-to-aqueous partition coefficient. $P_{diffusion}$ is the diffusion permeability. S is the capillary surface area of the rat brain (240 cm^2/g). Manganese values shown are means ± SEM for $n = 5$ or 6.

[b] $P_{diffusion}$ determined directly from Levin (1980) and Pardridge (1998).

[c] $D_{o/a}$ determined by Huang (1990).

to follow blood Mn concentrations for a longer time after Mn dosing (up to 12 hours) (Zheng et al 2000).

A steady-state Mn brain-to-blood ratio was achieved within the first 20-minute dialysis sample after the bolus Mn injection and initiation of Mn infusion, as evidenced by consistent Mn concentrations over time in the dialysates flowing out of the microdialysis probes implanted in the jugular vein and brain frontal cortex. The mean (± SD) Mn brain-to-blood ratio at steady state was 0.15 (± 0.11). The Mn free fraction in five rats was 7.8% ± 2.0%. The rapid achievement of steady state suggests Mn was able to rapidly enter brain extracellular fluid through the BBB.

STUDY 3: Mn BRAIN INFLUX

Influx transfer coefficients (K_{in}) of $^{54}Mn^{2+}$, ^{54}Mn citrate, and ^{54}Mn Tf, determined by in situ brain perfusion, were plotted graphically for each tissue and each Mn species. Figure 3 shows uptake space versus time for the parietal cortex, a representative brain region, over the time course of the experiment. For comparison, the uptake rates predicted by diffusion are plotted on each graph. For the nine brain regions studied, the K_{in} values ranged from 5 to 13, 3 to 51, and 2 to 13 × 10^{-5} mL/sec/g for $^{54}Mn^{2+}$, ^{54}Mn citrate, and ^{54}Mn Tf, respectively.

Influx coefficients for each Mn species were compared to their corresponding estimated diffusion rates. Significant

Table 3. Toxicokinetic Parameters in Sprague Dawley Rats After Intravenous Injection of Mn^{2+} (as $MnCl_2$) or Mn Citrate[a]

Mn Species Injected	Cl_s (L/hr)	V_d (L/kg)	$t_{1/2}$ (hr)	Reference
Mn^{2+} ($n = 3$)	2.20 ± 0.10	1.10 ± 0.10	0.35 ± 0.08	Our results
Mn citrate ($n = 5$)	2.30 ± 0.30	0.83 ± 0.05	0.27 ± 0.33	Our results
Mn^{2+} ($n = 5$)	0.43 ± 0.13	1.20 ± 0.50	0.17 ± 0.03[b] 1.80 ± 0.60[c]	Zheng et al 2000

[a] Values are mean ± SD. Cl_s is systemic clearance; V_d,volume of distribution; $t_{1/2}$, half-life; n, number of rats.

[b] Initial half-life.

[c] Second half-life.

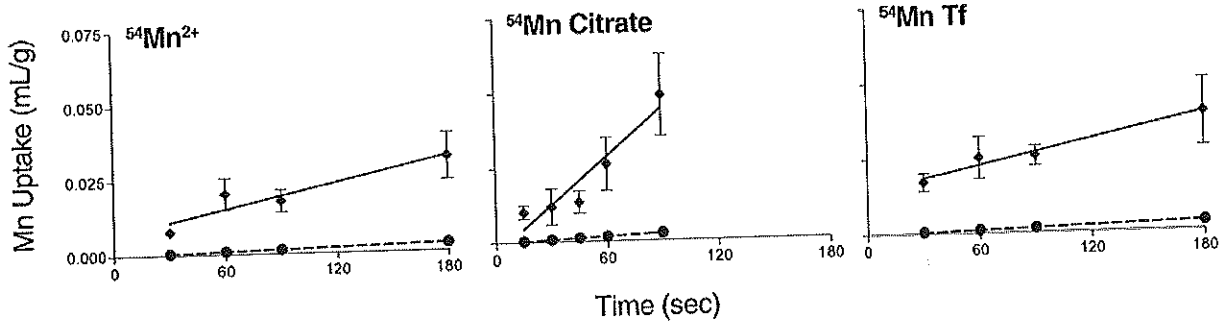

Figure 3. Determination of K_{in} for three Mn species into rat brain. Uptake space is shown for the parietal cortex (◆) and predicted uptake space for diffusion-only influx (●) for $^{54}Mn^{2+}$, ^{54}Mn citrate, and ^{54}Mn Tf. Regression analysis of individual results (——) produced the K_{in} values listed in Table 4. For comparison, predicted uptake spaces for diffusion-only influxes are shown (– – –). Values are means (± SEM) from 11, 10, 10, and 10 rats for the four increasing times, respectively, for $^{54}Mn^{2+}$; 7, 11, 7, 11, and 4 rats for the five increasing times, respectively, for ^{54}Mn citrate; and 7 rats for all four times for ^{54}Mn Tf.

differences between K_{in} values and the predicted diffusion rates were found for each tissue (Table 4). These K_{in} values were derived from the individual data rather than the mean uptake values shown in Figure 3. With each Mn species, there was at least one brain region for which the influx rate exceeded that predicted for diffusion. Generally, influx into the choroid plexus was at least 10-fold greater than influx into the brain regions for each Mn species. Within a given brain region, ^{54}Mn citrate influx rates were generally higher than $^{54}Mn^{2+}$ and ^{54}Mn Tf influx rates and were significantly different in a number of brain regions (see Table 4).

Comparison of K_{in} values obtained with brain perfusion rates of 10 and 20 mL/min did not show a significant effect of flow rate on brain Mn^{2+} uptake in any of the nine brain regions or the choroid plexus. Figure 4 shows results from two representative brain regions, the parietal cortex and caudate. Furthermore, the space occupied by ^{14}C-sucrose, which represents the vascular volume, did not differ with flow rate (Table 5).

Separation of the capillaries from the brain parenchyma revealed that most of the radioactivity in the brain after perfusion with $^{54}Mn^{2+}$, ^{54}Mn citrate, and ^{54}Mn Tf (92% ± 2%, 89% ± 2%, and 75% ± 10%; mean ± SD, respectively) was associated with the brain cells and brain extracellular fluid fraction, suggesting most of the Mn passed through the endothelial cells. The influx transfer coefficients in Table 4 have been adjusted to account for the fraction of ^{54}Mn associated with the endothelial cells.

In the presence of increasing amounts of $^{55}Mn^{2+}$, the influx rate of 7 nM $^{54}Mn^{2+}$ was reduced in the choroid plexus and in the frontal cortex, parietal cortex, hippocampus, caudate, and pons/medulla regions of the brain. The rates of Mn^{2+} influx in the parietal cortex and caudate are shown in Figure 5A. There was no concentration-dependent effect over the 10^6-fold concentration range studied. ^{55}Mn citrate significantly inhibited uptake of 7 nM ^{54}Mn citrate in the caudate and parietal cortex (Figure 5B) and in the choroid plexus at the highest concentration studied (10^7 nM).

The concentration and the velocity of brain uptake were fit to models of enzyme kinetics involving zero, one, and two Michaelis-Menten terms. Seven of eight regions treated with ^{54}Mn citrate and two of eight regions treated with $^{54}Mn^{2+}$ (caudate and thalamus/hypothalamus) were best fit by J_1 described as

$$J_1 = V_{max} \times C/[K_m + C] + K_d \times C.$$

The remaining regions were best fit by J_0, the diffusion-only model of brain Mn uptake. Very high K_m values and some negative V_{max} values were obtained. Statistically, this results from the apparent lack of concentration-dependent inhibition over the concentration range tested. For this reason, K_m and V_{max} values for most tissues are not reported. Only in the caudate region was there evidence for uptake of both Mn^{2+} and Mn citrate via a single-carrier model (J_1). The Michaelis-Menten values are shown in Table 6.

Table 4. Influx Transfer Coefficients (K_{in}) for Three Mn Species in Rat Brain[a]

Region	K_{in} (shown × 10^{-5} mL/sec/g)		
	$^{54}Mn^{2+}$	^{54}Mn Citrate	^{54}Mn Tf
Frontal cortex	11.0 ± 4.0	42.0 ± 12.0[b]	6.0 ± 4.3[d]
Parietal cortex	13.0 ± 4.0[b]	40 .0 ± 13.0[b]	12.0 ± 6.0
Occipital cortex	11.0 ± 6.0	51.0 ± 15.0[b,c]	7.9 ± 4.8[d]
Cerebellum	6.7 ± 2.3	22.0 ± 5.0[b]	1.9 ± 2.5[d]
Caudate	4.7 ± 2.3	19.0 ± 5.0[b]	1.8 ± 2.0[d]
Hippocampus	9.8 ± 3.1[b]	8.0 ± 8.9	2.7 ± 2.5
Thalamus/hypothalamus	7.4 ± 3.1	31.0 ± 9.0[b,c]	3.8 ± 3.7[d]
Midbrain/colliculus	8.8 ± 4.7	2.7 ± 17.1	13.0 ± 4.0[b]
Pons/medulla	4.9 ± 2.0	9.9 ± 10.0	1.7 ± 3.7
Choroid plexus	850 ± 468	463 ± 283	1383 ± 912

[a] The K_{in} values are the slope of the uptake spaces versus time for data shown in Figure 3. Values shown are means ± SEM.

[b] Significant differences at $P < 0.05$ (t test) for K_{in} versus diffusion permeability (shown in Table 2).

[c] Significant differences at $P < 0.05$ (t test) for ^{54}Mn citrate versus $^{54}Mn^{2+}$.

[d] Significant differences at $P < 0.05$ (t test) for ^{54}Mn citrate versus ^{54}Mn Tf.

STUDY 4: Mn BRAIN EFFLUX

The brain efflux index was determined after injection of the $^{54}Mn^{2+}$ or ^{54}Mn citrate as an indication of the rate of Mn efflux from the brain, compared to a coinjected marker substance that slowly diffuses across the BBB. Because no differences were seen in results obtained with sucrose versus dextran as the marker substance, those results were combined. An average of 98.7% of Mn remaining in the brain was in the central one third of the brain hemisphere ipsilateral to the injection site, indicating little distribution from the injection site to other brain sections. The index results are graphically shown as 100−BEI(%) versus time, an indication of the percentage of ^{54}Mn remaining in the brain after its injection (Figure 6). The results show a small increase in Mn remaining in the parietal cortex over time, compared to coinjected ^{14}C-sucrose or ^{14}C-dextran. These results suggest that Mn distributes out of the brain more slowly than sucrose or dextran. The calculated rates

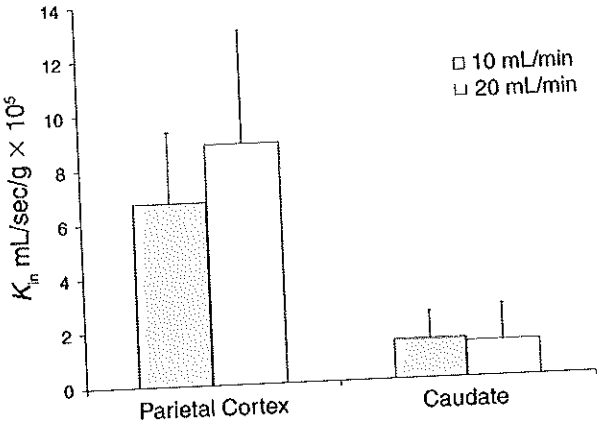

Figure 4. $^{54}Mn^{2+}$ uptake was independent of perfusion flow rate. Uptake at 10 mL/min versus 20 mL/min was studied in paired animals at 30, 60, 90, and 180 seconds, with $n = 4$ to 5 pairs per time point. Mean values ± SEM are shown in two brain regions. There were no significant differences (t test) in any of the nine brain regions or in the lateral ventricular choroid plexus.

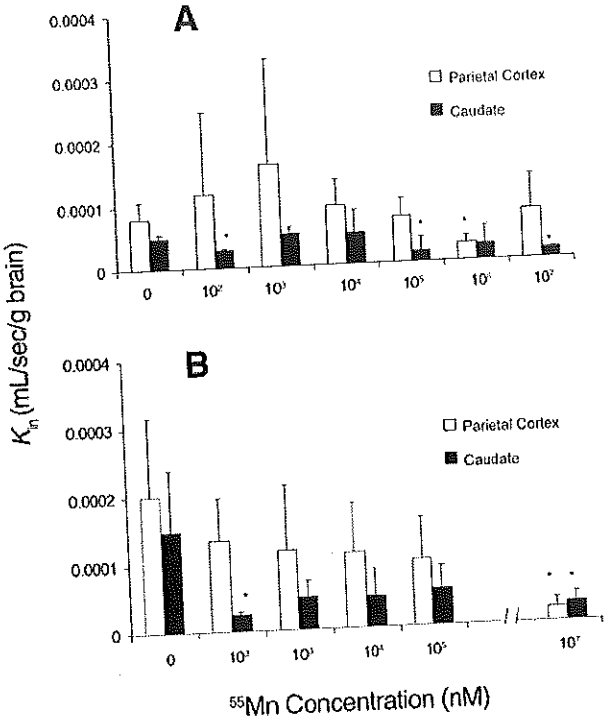

Figure 5. Effect of ^{55}Mn on uptake of $^{54}Mn^{2+}$ (*A*) and of ^{55}Mn citrate on uptake of ^{54}Mn citrate (*B*). The medium contained 7 nM ^{54}Mn plus increasing concentrations of ^{55}Mn as indicated on the x-axis. Influx transfer coefficient (K_{in}) values are means ± SEM, with $n = 3$ to 5 for each concentration. *Significant differences (one-way ANOVA) from 0 nM ^{55}Mn.

Table 5. Vascular Space of the Brain as Measured by ^{14}C-Sucrose Delivered at Different Flow Rates[a]

Region	Vascular Space (μL/g brain)	
	at 10 mL/min	at 20 mL/min
Frontal cortex	9.2 ± 0.9	10.5 ± 0.9
Parietal cortex	10.7 ± 1.1	12.8 ± 1.5
Occipital cortex	10.8 ± 0.9	13.2 ± 1.4
Cerebellum	12.3 ± 0.8	13.2 ± 1.6
Caudate	5.5 ± 0.4	6.8 ± 0.5
Hippocampus	8.4 ± 0.8	9.7 ± 1.0
Thalamus/ hypothalamus	8.0 ± 0.8	10.3 ± 1.0
Midbrain/colliculus	9.0 ± 0.8	11.0 ± 1.6
Pons/medulla	13.5 ± 1.0	15.2 ± 1.5
Choroid plexus	206 ± 38	236 ± 69

[a] Values shown are means ± SEM for 16 animals per flow rate after perfusion for 90 seconds. There are no significant differences in vascular space or in $^{54}Mn^{2+}$ uptake rates (shown in Figure 4) when these flow rates are compared for each region (t test with Bonferroni correction).

Table 6. Estimates of Michaelis-Menten Kinetic Parameters for Mn Influx[a]

Kinetic Parameter	$^{54}Mn^{2+}$	^{54}Mn Citrate
K_m (μM)	11,400 (660)	7,560 (150)[b]
V_{max} (nmol/sec/g brain)	0.311 (0.010)	0.265 (0.002)[b]

[a] Values are means (± SEM) for the average velocity at each of seven $^{54}Mn^{2+}$ or six ^{54}Mn citrate concentrations.

[b] Significantly different from $^{54}Mn^{2+}$ (t test).

of diffusion of mannitol, dextran, sucrose, and inulin across the capillaries of the BBB, as $P_{diffusion}S$, are 2.5, 4.8, 2.9, and 12×10^{-5} mL/sec/g brain tissue, respectively.

The uptake of the three Mn species into brain slices enabled calculation of V_{brain} as an indication of the volume of Mn distribution in the brain from which it could distribute to blood. No differences were seen in V_{brain} results from anesthetized rats versus those from unanesthetized rats, so the results were combined. The ^{14}C from ^{14}C-sucrose that was associated with the parietal Par2 slices increased linearly over 180 minutes. Linear regression showed a correlation between time and ^{14}C associated with brain slices of 0.955. The y-intercept, 0.15 mL/g, was taken as the extracellular space of the brain slice and subtracted from all Mn uptake values represented in Figure 7. The ^{54}Mn associated with the parietal Par2 slices increased over time to a significantly greater extent for each of the three Mn species than for ^{14}C. The V_{brain} values for the $^{54}Mn^{2+}$ at 45 versus 60 minutes, ^{54}Mn citrate at 120 versus 180 minutes, and ^{54}Mn Tf at 60 versus 75 minutes were not significantly different from each other. Therefore the means of these pairs of values, 2.7, 5.1, and 3.2 mL/g, were taken as estimates of the V_{brain} of the $^{54}Mn^{2+}$, ^{54}Mn citrate, and ^{54}Mn Tf, respectively. Addition of the aconitase inhibitors aconitine, monofluoroacetate, and oxalomalate and the electron transport chain inhibitor sodium azide did not consistently decrease ^{54}Mn citrate uptake (Figure 8).

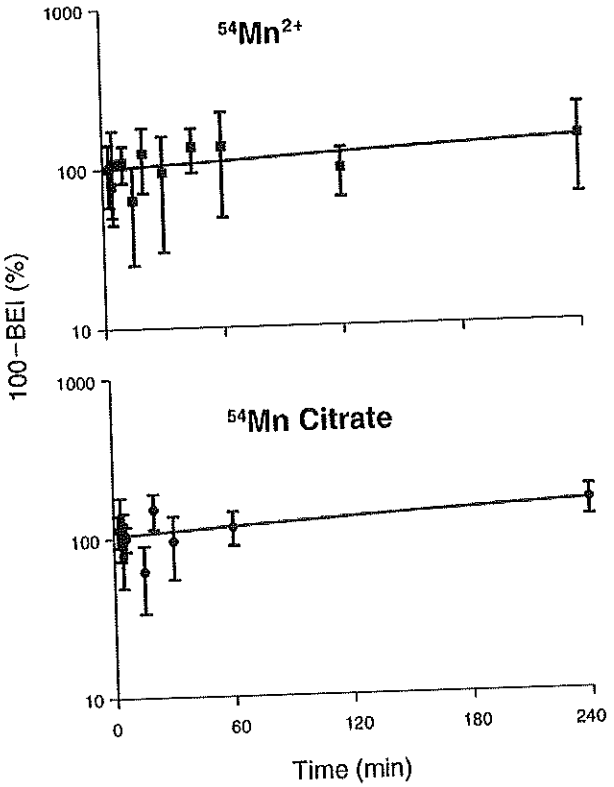

Figure 6. Percentage of Mn remaining in the brain (100−BEI[%]) versus time after coinjection of ^{54}Mn and ^{14}C-sucrose or ^{14}C-dextran. The injection was made into the parietal cortex as $^{54}Mn^{2+}$ (upper panel) or ^{54}Mn citrate (lower panel). Values are means ± SD from 5 to 23 animals. The lines represent linear regressions of the points.

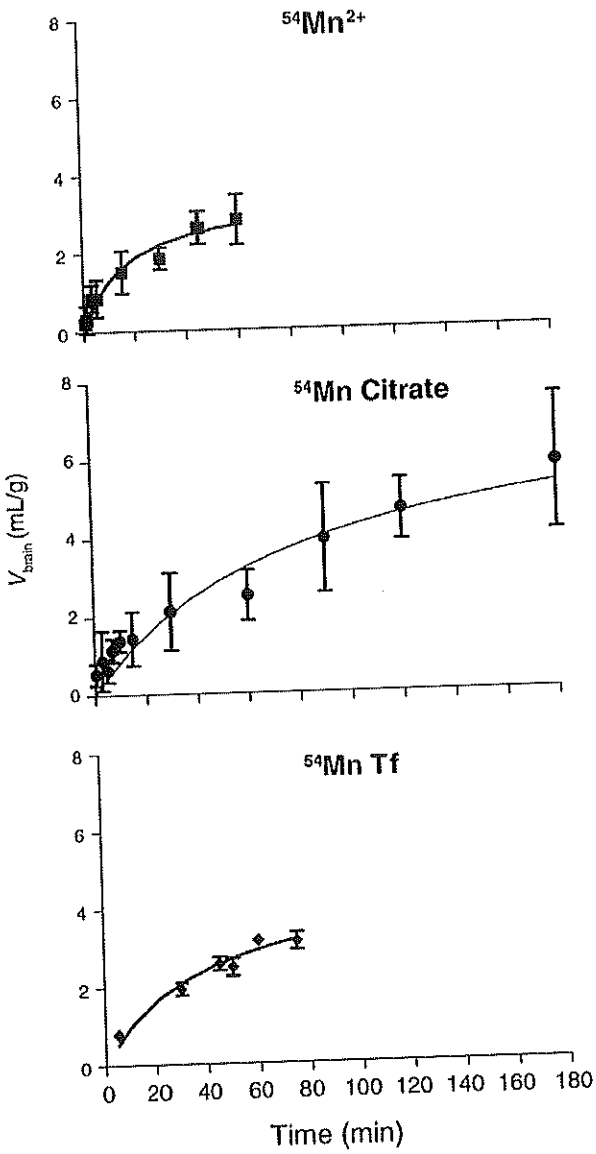

Figure 7. Volume of Mn distribution in the brain (V_{brain}) determined from uptake into rat parietal cortex slices versus time. The uptake of ^{54}Mn was determined, which had been added to the uptake solution as $^{54}Mn^{2+}$ (upper panel), ^{54}Mn citrate (center panel), or ^{54}Mn Tf (lower panel). Values are means ± SD from 4 to 13 experiments, each with triplicate observations. The SD for Mn Tf at 5 minutes is less than the symbol height.

STUDY 5: CHARACTERIZATION OF Mn TRANSPORTERS AT BBB

$^{54}Mn^{2+}$ uptake into bBMECs was initially studied for up to 120 minutes to determine whether uptake was linear over all or a portion of that time. Uptake values were converted to intracellular Mn concentrations and plotted versus time (Figure 9). Regression analysis with GraphPad Prizm allowed comparison of first-order and second-order fits. It showed that $^{54}Mn^{2+}$ uptake at pH 7.4 was better fit by a linear regression with slope 0.080 pmol/μL cell vol/min and intercept 1.022 pmol/μL cell vol. The pH 6.4 data were also better fit by the linear regression with a slope of 0.021 pmol/μL cell vol/min and intercept 0.877 pmol/μL cell volume. The 95% confidence intervals for these slopes exclude one another, and the uptake of $^{54}Mn^{2+}$ at pH 6.4 was significantly less than the uptake at pH 7.4.

Uptake was linear throughout the experiment and was not saturable up to 120 minutes. Therefore, steady state had not been achieved, and any duration was an acceptable selection for influx characterization studies. The 30-minute incubation was chosen to optimize conditions for low relative standard error, low time required for experiments, and high total counts per sample.

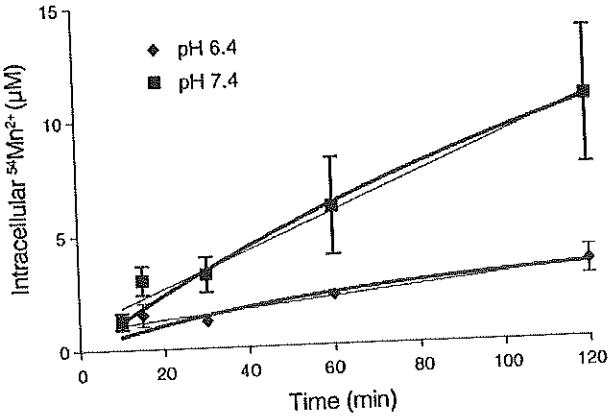

Figure 9. $^{54}Mn^{2+}$ uptake into bBMECs was linear at pH 7.4 and 6.4 up to 120 minutes. Intracellular Mn concentration in bBMECs was determined after exposure to uptake media for 10 to 120 minutes. Values are means ± SEM for 2 to 3 experiments, each with 2 to 3 replicates. Lines represent best-fit regression analysis for first-order processes (line) and second-order processes (bold line).

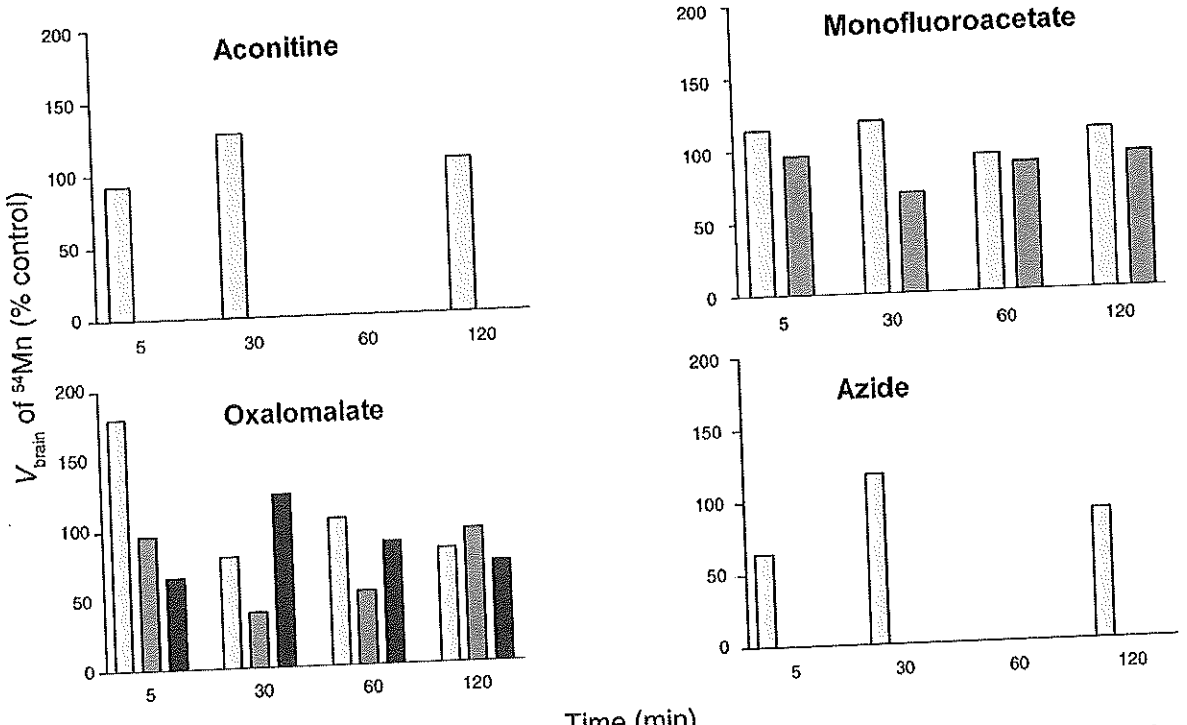

Figure 8. Effect of metabolic inhibitors on ^{54}Mn citrate uptake into rat parietal cortex slices versus time. The uptake of ^{54}Mn citrate was determined in the presence of aconitase inhibitors (1 mM aconitine; 1 and 10 mM monofluoroacetate; and 0.2, 1, and 5 mM oxalomalate) and the complex IV inhibitor azide (1 mM). Values are the means of 1 to 3 experiments, shown as separate histograms, each conducted with triplicate observations, expressed as a percentage of the within-experiment control (lack of inhibitor).

The intracellular Mn concentration in bBMECs exceeded the concentration of total Mn in the media by 10-fold. Uptake solution contained 184 nM total $^{54}Mn^{2+}$ (0.184 μM), and bBMECs contained 1 to 12 μM total $^{54}Mn^{2+}$. These results provide evidence for carrier-mediated Mn^{2+} uptake.

Mn uptake was positively correlated with pH. That is, uptake increased with decreased H^+ concentration. This was seen in the time course of $^{54}Mn^{2+}$ uptake at pH 6.4 and 7.4 (Figure 9) and in the uptake study conducted at pH 5.4, 6.4, 6.9, 7.4, and 7.9 (Figure 10). Uptake at pH 5.4 was quite low compared to that in control cells (pH 7.4). Cell toxicity, indicated by decreased conversion of MTT to formazan and increased release of lactate dehydrogenase, was high. Cells treated at pH 5.4 for 30 minutes produced only 6% of the formazan product/mg protein that was found in control cells at pH 7.4. Therefore these results were not analyzed. Uptake was significantly greater at pH 7.4 than at pH 6.4. This does not support the hypothesis that DMT-1, a proton cotransporter, mediates the uptake of Mn^{2+} at the BBB. The role of sodium in $^{54}Mn^{2+}$ uptake into bBMECs was measured by replacing 50% of the sodium with choline or all of the sodium with choline or lithium. $^{54}Mn^{2+}$ uptake was not inhibited by replacement of the sodium (Figure 11). Replacement of sodium by choline resulted in a significant increase of $^{54}Mn^{2+}$ uptake into bBMECs. Addition of energy inhibitors to the uptake medium reduced formazan production to approximately 60% of control. This inhibition was believed to be sufficient to determine whether Mn uptake was energy-dependent.

The addition of energy production inhibitors did not produce a significant effect on $^{54}Mn^{2+}$ uptake into bBMECs (Figure 12). Addition of 0.003 mM or 1 mM vanadate inhibited $^{54}Mn^{2+}$ uptake into bBMECs (Figure 13).

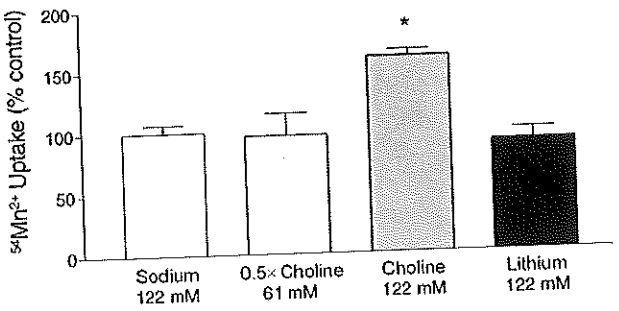

Figure 11. $^{54}Mn^{2+}$ uptake into bBMECs was sodium-independent. Values are means and relative SD for each treatment. Sodium replacement did not inhibit $^{54}Mn^{2+}$ uptake. *A Dunnett test showed that replacement of sodium with choline significantly increased $^{54}Mn^{2+}$ uptake.

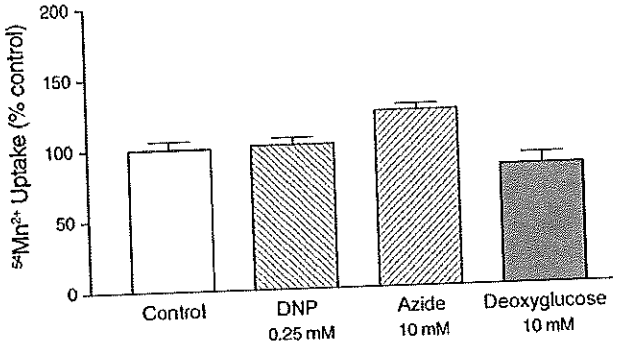

Figure 12. Energy inhibitors did not decrease $^{54}Mn^{2+}$ uptake into bBMECs. Values are means and relative SD of the uptake, compared to control, expressed as a percentage, with $n = 8, 6, 3$, and 4 for control, 2,4-dinitrophenol (DNP), sodium azide, and deoxyglucose treatments, respectively. Each experiment had duplicate or triplicate observations. None of the treatments significantly differed from control by Dunnett test.

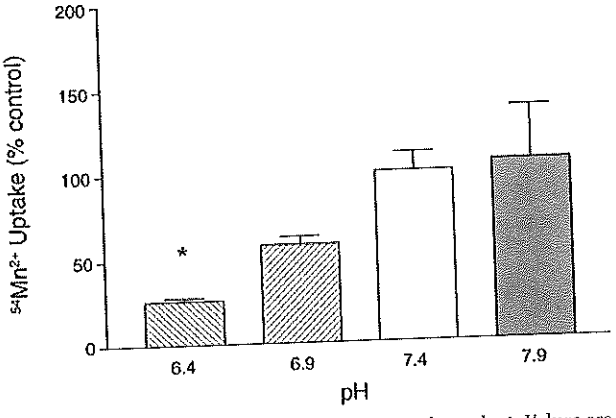

Figure 10. $^{54}Mn^{2+}$ uptake into bBMECs was pH-dependent. Values are means and relative SD of uptake relative to control (pH 7.4) uptake. *A Dunnett test revealed that uptake at pH 6.4 was significantly less than uptake at pH 7.4.

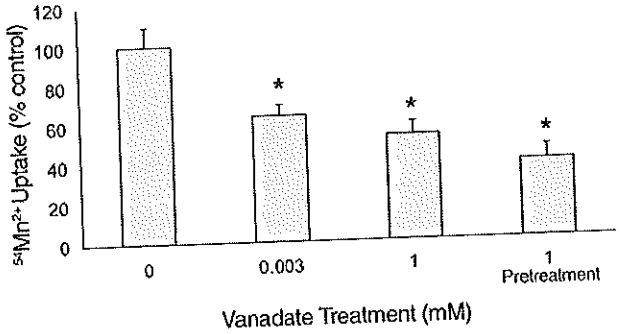

Figure 13. Vanadate inhibited $^{54}Mn^{2+}$ uptake into bBMECs. Values are means and SD of uptake relative to control (no vanadate). In the pretreatment condition, vanadate was added 30 minutes prior to the Mn uptake study to address the concern that vanadate may not enter bBMECs rapidly enough. *Each treatment resulted in significantly less $^{54}Mn^{2+}$ uptake than control by t test.

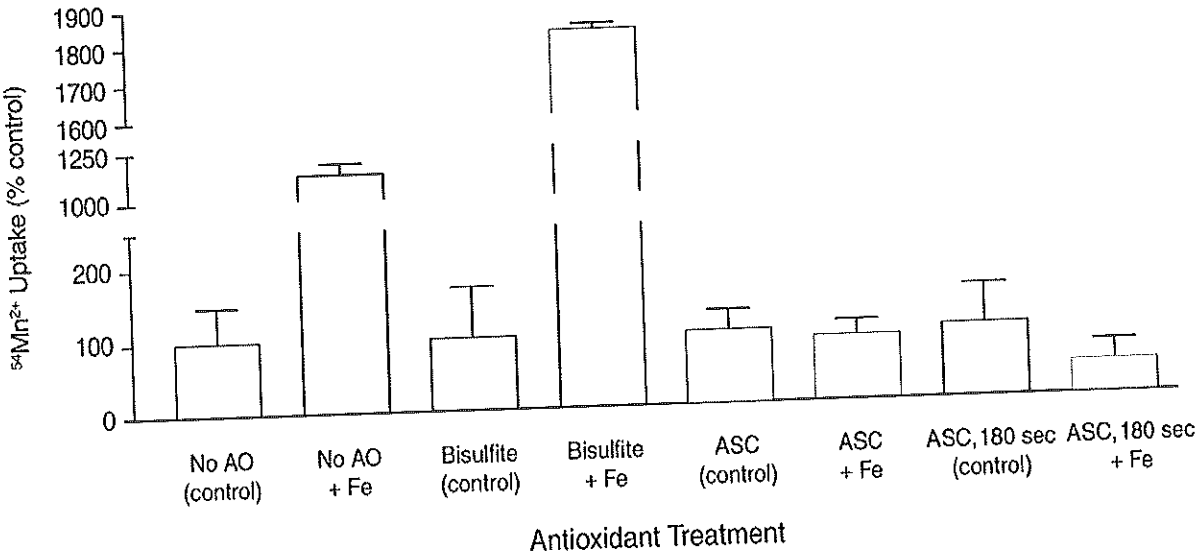

Figure 14. Iron did not inhibit uptake of $^{54}Mn^{2+}$ into the parietal cortex. Values are means ± SD. The perfusate contained 184 nM $^{54}Mn^{2+}$ and 0 or 100 μM $FeSO_4$ for 90 or 180 seconds. Experiments were completed without antioxidant (AO) present or with 0.01% (5.3 mM) sodium bisulfite or 0.1 mM ascorbic acid (Asc).

Furthermore, this effect persisted after vanadate was washed out. In cells treated 30 minutes with 1 mM vanadate, washed twice, and then incubated with vanadate-free uptake media, ^{54}Mn uptake was only 39% of control uptake. Treatment with ouabain did not inhibit $^{54}Mn^{2+}$ uptake. In the assessment by in situ brain perfusion in rats, addition of iron, in the presence or absence of antioxidants, did not significantly affect brain $^{54}Mn^{2+}$ uptake (Figure 14). Vanadate did not significantly inhibit $^{54}Mn^{2+}$ influx into any of the nine brain regions or the choroid plexus (Figure 15). The most pronounced treatment difference was in the choroid plexus, where P was 0.1047. In each tissue, the average $^{54}Mn^{2+}$ uptake was greater in the presence of vanadate treatment than control. Experiments that included 0.4 mM *p*-hydroxyhippuric acid in the brain perfusate did not show an inhibition of $^{54}Mn^{2+}$ uptake into rat brain (Figure 16). Only in the cerebellum was there a nonsignificant trend for a *p*-hydroxyhippuric acid–induced decrease of $^{54}Mn^{2+}$ uptake.

In the preliminary experiment to determine the rates of $^{54}Mn^{2+}$ brain uptake in homozygous (*b/b*) Belgrade rats, which do not express functional transporter DMT-1, and heterozygous (*+/b*) Belgrade rats, which do, there were no statistically significant increases in $^{54}Mn^{2+}$ uptake in *b/b* rats compared to *+/b* rats. The subsequent study, conducted under more controlled conditions using paired homozygous and heterozygous Belgrade rats (littermates) and control Wistar rats, tested $^{54}Mn^{2+}$ and ^{54}Mn Tf uptake and also failed to show any statistically significant differences (Figure 17). Cerebrovascular washout did not significantly affect brain Mn uptake. There were no significant differences in the percentage of Mn in the isolated brain capillaries among the *b/b*, *+/b*, and Wistar rats after $^{54}Mn^{2+}$ or ^{54}Mn Tf perfusion.

The calcium concentration in the uptake medium negatively correlated with Mn^{2+} influx into rat brain (Figure 18). This could not be attributed to uptake through voltage-gated calcium channels, as nifedipine failed to decrease Mn influx (data not shown), as did amiloride and verapamil (Figure 19), relative to controls without calcium channel blockers. La^{3+} and Ni^{2+} also failed to block Mn influx into rats (Figures 18 and 20); however, Ni^{2+} significantly blocked 80% of Mn^{2+} uptake into bBMECs (Figure 21). In

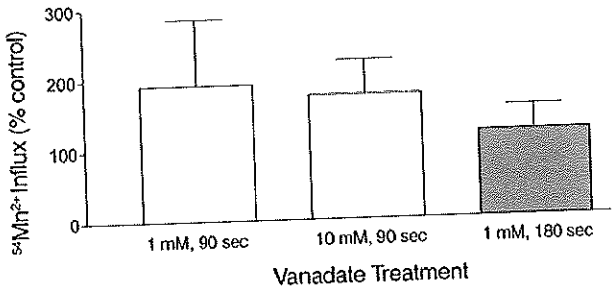

Figure 15. Vanadate did not inhibit Mn influx into brain after perfusion. Values are from the parietal cortex and are mean percentages and relative SEM of uptake, for perfusion with 1 mM vanadate for 90 seconds (n = 3), 10 mM vanadate for 90 seconds (n = 4), or 1 mM vanadate for 180 seconds (n = 5).

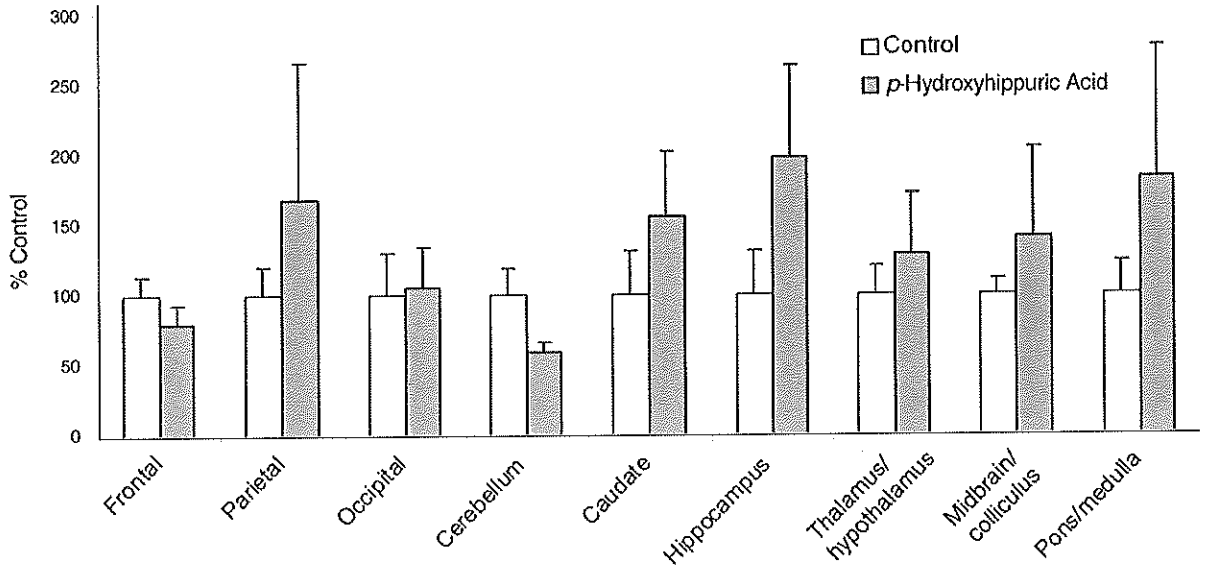

Figure 16. *p*-Hydroxyhippuric acid (100 μM) did not inhibit $^{54}Mn^{2+}$ brain influx. Values are mean percentages of control with relative standard deviation for 6 control or 7 treated animals.

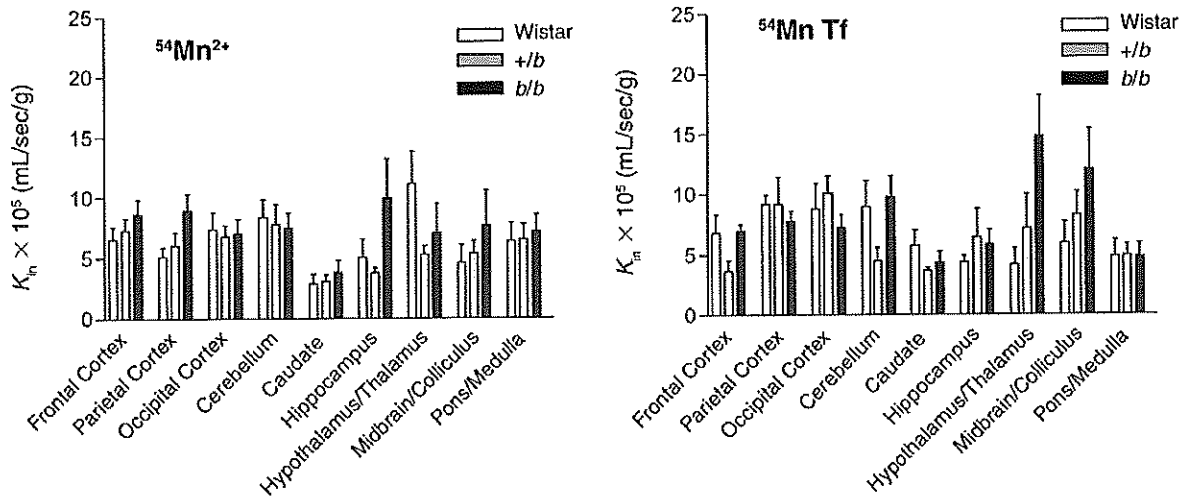

Figure 17. Brain $^{54}Mn^{2+}$ and ^{54}Mn Tf uptake in paired Wistar, Belgrade +/b, and Belgrade b/b rats. Uptake of $^{54}Mn^{2+}$ and ^{54}Mn Tf into nine brain regions was not lower in DMT1-deficient (*b/b*) rats. Left panel: $^{54}Mn^{2+}$ in the perfusate. Right panel: ^{54}Mn Tf in the perfusate. Results with $^{54}Mn^{2+}$ are means ± SEM from 7, 8, and 8 Wistar, +/*b*, and *b/b* rats, respectively. Results with ^{54}Mn Tf are means ± SEM from 6, 8, and 6 Wistar, +/*b*, and *b/b* rats, respectively. There were no statistically significant differences among rat strains for either Mn species.

bBMEC uptake studies, cyclopiazonic acid and thapsigargin significantly increased Mn^{2+} uptake (Figure 22).

Uptake of lactate into rat erythrocytes after 20, 60, and 300 seconds at 6°C averaged 0.32, 0.36, and 0.50 nmol/μL cell volume. The addition of 2 mM pyruvate decreased lactate uptake to 58%, 53%, and 90% of control after 20, 60, and 300 seconds, respectively. In contrast, lactate uptake at the same respective times averaged 128%, 102%, and 99% of control in the presence of 5 mM Mn citrate and 146%, 107%, and 100% of control in the presence of 10 mM Mn citrate. In contrast to the rapid uptake of lactate at 6°C, citrate and Mn citrate uptake achieved only 0.05 and 0.04 nmol/μL cell volume after 60 minutes at room temperature (data not shown).

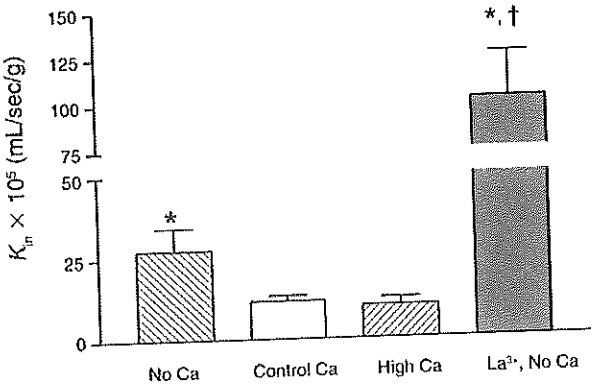

Figure 18. Calcium, but not lanthanum, inhibited Mn^{2+} uptake into rat brain. Mn^{2+} influx was determined at Ca concentrations of 0 mM (no Ca), 1.5 mM (control), and 9 mM (high Ca) and at 0 mM with 50 μM La^{3+} (La^{3+}, no Ca). Values are means of K_{in} ± SEM for nine brain regions with n = 5, 9, 4, and 4 animals for no Ca; control Ca; high Ca; and La^{3+}, no Ca, respectively. *Significant difference from control Ca. †Significant difference from no Ca. Both calculated by t test.

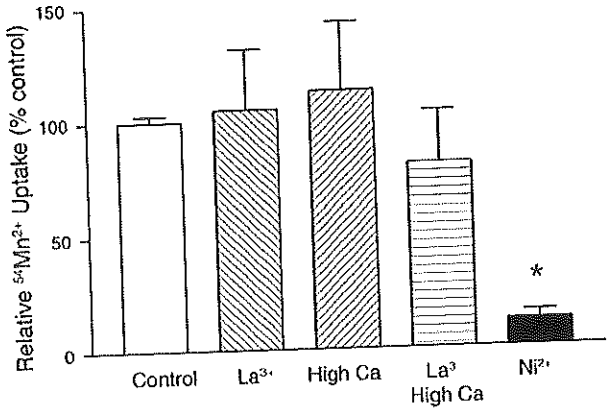

Figure 21. $^{54}Mn^{2+}$ uptake into bBMECs was inhibited by Ni^{2+} (1 mM) but not by La^{3+} (50 μm) or high Ca (9 mM). Values are mean percentages of uptake ± SEM relative to control (1.5 mM Ca). *Significant difference from control by t test.

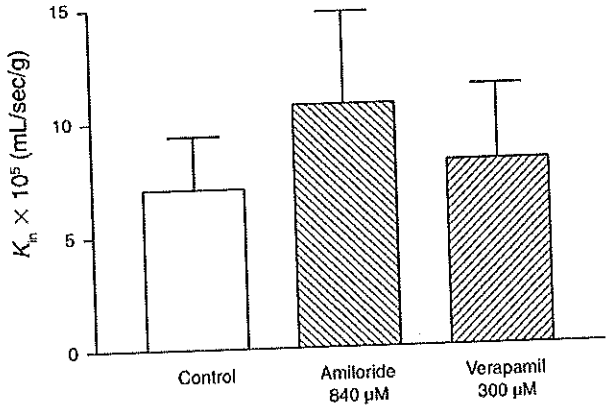

Figure 19. Calcium channel blockers did not inhibit Mn^{2+} influx. Values shown are means ± SEM of Mn^{2+} uptake averaged from nine brain regions per experiment from three to four animals per treatment.

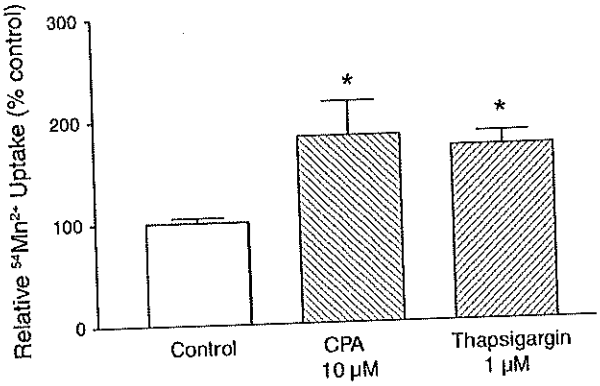

Figure 22. $^{54}Mn^{2+}$ uptake was increased in response to Ca store depletion by cyclopiazonic acid (CPA) and thapsigargin. Values shown are mean percentages of vehicle-treated control uptake ± SEM for duplicate observations in 3 or 4 experiments. *Significant difference from control by t test.

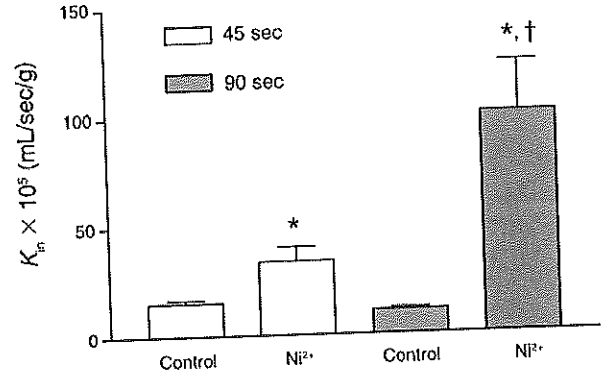

Figure 20. Ni^{2+} increased Mn^{2+} influx into rat brain. Values are means of K_{in} ± SEM for 6 (control) or 7 (1 mM Ni^{2+}) experiments at 45 seconds and 5 (control) or 4 (1 mM Ni^{2+}) experiments at 90 seconds. *Significant differences from time-matched control. †Significant difference from Ni^{2+} treatment at 45 seconds. Both calculated by t test.

The uptake of ^{14}C-citrate, Mn ^{14}C-citrate, and Al ^{14}C-citrate into b.End5 cells increased linearly over 4 hours. The uptake rate of Mn citrate was similar to that of citrate and less than that of Al ^{14}C-citrate. The uptakes of ^{14}C-citrate and Mn ^{14}C-citrate were approximately 170% and 185% greater at pH 6.9 than 7.4, whereas Al ^{14}C-citrate uptake was not pH-dependent. Mn ^{14}C-citrate uptake averaged 102% ± 16% and 109% ± 50% of ^{14}C-citrate uptake, at pH 6.9 and 7.4, respectively (data not shown).

In situ brain perfusion was conducted in five or six Sprague Dawley rats with ^{54}Mn citrate perfusate containing 2 μM quercetin or very low sodium. The results from all brain regions were combined. Quercetin significantly reduced Mn citrate uptake into brain (Figure 23), while low sodium had no significant effect on Mn citrate uptake.

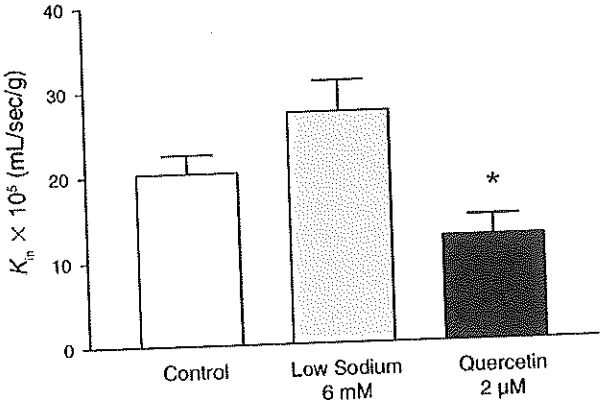

Figure 23. ^{54}Mn citrate influx at the BBB was inhibited by quercetin and did not require Na. Values are the mean uptakes of nine brain regions ± SEM for $n = 5$ (low Na) or 6 (control, quercetin) experiments.

DISCUSSION AND CONCLUSIONS

The work reported herein describes studies that address several aims: to determine whether the chemical species of Mn in the blood that are the primary candidates for distribution into the brain through the BBB enter the brain by processes other than diffusion; to determine whether Mn distributes out of the brain by processes other than diffusion; and if this is the case, to characterize, and ultimately identify, the transporters that mediate Mn distribution across the BBB. We focused on three Mn species for this work: Mn^{2+} and Mn citrate, which are important low molecular weight Mn species in blood plasma and possibly in brain extracellular fluid; and Mn Tf, a protein-bound Mn species for which evidence of carrier-mediated transport across the BBB has been reported.

FORMATION OF Mn-LIGAND COMPLEXES

We used established methods to prepare a 1:1 complex of Mn and citrate and a 1:1 complex of Mn and Tf. The near-infrared results suggest that the Mn citrate complex was formed. The studies of Mn in the presence of Tf showed most of the Mn was not able to penetrate a membrane in an equilibrium dialysis chamber, and the absorbance increased at 300 nm, suggesting we also successfully prepared Mn Tf. When the free Mn^{2+} aquo ion and a suitable ligand such as citrate or Tf are mixed, one would expect rapid formation of the Mn-ligand complex. This would be expected based on a set of calculations provided by Dr Wesley Harris (Appendix B). These calculations show that equilibrium among Mn^{2+} and Mn complexes with citrate, phosphate, histidine, albumin, cysteine, oxalate, glutamate, and Tf will occur within seconds.

This rapid equilibrium among Mn^{2+} species suggests very rapid formation of Mn citrate and Mn Tf. This also explains the comparable toxicokinetic parameters of Mn after intravenous administration of Mn^{2+} or Mn citrate (Study 2) and the comparable V_{brain} results obtained with Mn^{2+}, Mn citrate, and Mn Tf (Study 4), discussed later.

CEREBRAL CAPILLARY DIFFUSION PERMEABILITY

In Study 1, the octanol/aqueous partition coefficients of Mn^{2+}, Mn citrate, and Mn Tf were found to be less than 0.001 (Table 2). These octanol/aqueous partition coefficients were used in calculations of $P_{diffusion}S$ (product of diffusion permeability and surface area) for the three Mn species (Levin 1980). The $P_{diffusion}S$ values for sucrose and dextran were also calculated for comparison and to assist in the interpretation of the results of this work. The $P_{diffusion}S$ values for the three Mn species and for sucrose and dextran were similar and very small, suggesting that diffusion of all three Mn species through the BBB would be very slow; however, sucrose and dextran would be expected to diffuse more rapidly through the BBB than Mn citrate and Mn^{2+} if there were no carrier for these Mn species.

In the uptake studies the amount of sucrose in the brain when the animals were killed indicated the volume of the perfusate that was in the brain as well as sucrose that had diffused across the BBB into the brain. Subtraction of brain sucrose from brain Mn revealed Mn that entered the brain by carrier-mediated uptake. This result is expressed as the brain influx transfer coefficient (K_{in}). Our positive values suggest carrier-mediated uptake. Sucrose and dextran were coinjected with ^{54}Mn for determination of brain Mn efflux. If both Mn and sucrose or dextran distributed

across the BBB from brain to blood (brain efflux) by diffusion alone, their $P_{diffusion}S$ values would suggest sucrose and dextran would efflux from the brain faster than Mn. Over time, the percentage of Mn remaining in the brain [referred to as *100−BEI(%)*] would increase relative to that of the reference compound, sucrose or dextran. We found increasing 100−BEI(%) values, suggesting the lack of carrier-mediated brain Mn efflux.

Transferrin, a large protein with a molecular weight of approximately 77 kDa, would not be expected to cross an intact BBB in the absence of a carrier. TfR-mediated endocytosis is a known Tf transport mechanism at the BBB. Because the relation between octanol/aqueous partition coefficients, molecular weight, and diffusion across the BBB was defined using low molecular weight compounds, however, the relation may not directly indicate the rate of Mn Tf diffusion across the BBB.

Mn TOXICOKINETICS AFTER INTRAVENOUS INJECTION AND BRAIN–BLOOD RATIO

We determined the toxicokinetics of Mn in rats (Study 2) after an intravenous injection of $MnCl_2$ or Mn citrate at approximately 22% of the injected dose previously studied (Zheng et al 2000). Whereas those authors described clearance from two compartments, we were able to characterize only the first elimination phase because the smaller Mn dose did not enable us to quantify plasma Mn concentrations for as long after the injection as would be possible with a higher dose. The greater clearance and shorter mean residence time we found (see Table 3) probably reflect the first of two or more phases, accounting for their higher values compared to previous results (Zheng et al 2000). Because Mn very rapidly respeciates, the similar toxicokinetic results obtained after injection of $MnCl_2$ and Mn citrate probably reflect the equilibrium among all Mn species formed in vivo.

The steady-state Mn results in brain and blood extracellular fluid determined using microdialysis are consistent with greater Mn brain efflux than influx. Another interpretation is that unbound, extracellular, dialyzable Mn species in plasma are not able to enter the brain, but the rapid respeciation of Mn would not support this interpretation. Because of the rapid respeciation of Mn expected in vivo, we could not control Mn species in the rat in experiments that used microdialysis. Therefore we used in situ brain perfusion for subsequent studies of Mn distribution across the BBB. This approach did allow control of Mn species in the perfusate within the brain because we could eliminate from the perfusate the ligands that would cause respeciation of the introduced Mn species (Mn^{2+}, Mn citrate, and Mn Tf). The results from the preliminary studies using microdialysis were not supported by the results we subsequently obtained using the more rigorous in situ brain perfusion and brain efflux index methods. We concluded that the observation of greater efflux than influx with microdialysis was not valid.

Mn BRAIN INFLUX

Influx Transfer Coefficients for Three Mn Species

In situ brain perfusion (Study 3) enabled determination of the brain influx transfer coefficient (K_{in}) for Mn species. The results obtained for Mn^{2+} are similar to results reported in buffered saline from the laboratory of Dr Quentin Smith (Rabin et al 1993), suggesting that we properly used the in situ brain perfusion technique. The influx rates of Mn^{2+}, Mn citrate, and Mn Tf were approximately 4-fold, 20- to 40-fold, and 1- to 3-fold greater than their predicted rates of capillary diffusion through the BBB, respectively. This is consistent with the suggestion that Mn can enter the brain by mechanisms other than diffusion. At least two mechanisms have been described: TfR-mediated endocytosis and another mechanism mediating brain influx of Mn^{2+} (Murphy et al 1991; Aschner and Gannon 1994). This influx was independent of flow rate, showing Mn brain uptake was not rapid enough to be limited by the rate of perfusate flow through the brain.

The present work is unique in that it examined Mn brain uptake with control of its chemistry. Several studies previously estimated carrier-mediated brain uptake of Mn that was administered systemically as the ion (Aschner and Aschner 1990; Murphy et al 1991; Rabin et al 1993; Aschner and Gannon 1994), but rapid respeciation of ^{54}Mn confounded the identity of the transported Mn species. Furthermore, administration of Mn in buffered solutions allows formation of Mn complexes with HCO_3^-, SO_4^{2-}, and $H_2PO_4^-$, which have log stability constants of 0.45, 0.7, and 3.2, respectively, for their 1:1 complex formation (National Institute of Standards and Technology 1995). The present study excluded all anions except chloride in the uptake studies of $^{54}Mn^{2+}$; chloride and citrate in those of ^{54}Mn citrate; and chloride, Tf, and bicarbonate in those of ^{54}Mn Tf.

Our results agree with earlier reports suggesting carrier-mediated transport of Mn at the BBB (Murphy et al 1991; Rabin et al 1993). The predicted diffusion rates of Mn^{2+}, Mn citrate, and Mn Tf are slightly less than those of sucrose and dextran (Table 2), which are considered to very slowly distribute across the BBB. $^{54}Mn^{2+}$, ^{54}Mn citrate, and ^{54}Mn Tf entered the brain more rapidly than predicted by diffusion and more rapidly than sucrose, suggesting carrier-mediated transport. Brain influx transfer coefficients (K_{in} values), which represent brain uptake in excess of that predicted by diffusion, were all positive.

Choroid plexus influx values were more than 10-fold greater than overall brain influx values, a finding consistent with suggestions that the choroid plexus rapidly sequesters metals (Zheng et al 1991; Zheng 2001).

Previous studies suggested the rate of brain uptake of Mn ion would greatly exceed that of Mn Tf. We found more rapid uptake of Mn^{2+} than Mn Tf but not the 62-fold greater rate from an unsaturated system than a saturated, protein-bound form that was previously suggested (Murphy et al 1991). Furthermore, Mn uptake decreased 70% in the presence of Tf (Rabin et al 1993). This corresponds to a 3-fold greater Mn influx of Mn^{2+} than Mn Tf, which is also consistent with our results.

When the $^{54}Mn^{2+}$ uptake rate into the parietal cortex reported here is compared with that previously reported in other perfusates, the influx transfer coefficient in the present work is twice the value reported for ^{54}Mn in whole blood and two thirds the value reported for buffered saline (Rabin et al 1993). The influx values determined using the in situ brain perfusion technique are less than those reported for the cerebral cortex with the infusion model (Murphy et al 1991; Rabin et al 1993). To some extent, these differences may be due to rapid respeciation of Mn to Mn citrate with the infusion model, compared to the lack of respeciation expected using the in situ brain perfusion technique with cell-free and protein-free perfusate.

Mn Influx into Specific Brain Regions

The regional differences in Mn brain influx were examined in the context of function and pathology. Greater Mn influx into specific brain regions may correlate with greater expression of a carrier or a greater requirement for Mn. The astrocyte-specific enzyme glutamine synthetase accounts for approximately 80% of the total brain Mn (Wedler and Denman 1984). Areas of high astrocyte density include the hypothalamus and hippocampus, with low astrocyte density in the cerebral cortex, neostriatum, midbrain, medulla oblongata, and cerebellum (Savchenko et al 2000). The relatively high influx rates for Mn^{2+} (hippocampus) and Mn citrate (thalamus/hypothalamus) support a correlation, but the high influx despite low astrocyte density in cortical regions for Mn^{2+}, Mn citrate, and Mn Tf and in the cerebellum for Mn citrate decreases the strength of the putative correlation. In manganism, the caudate and basal ganglia accumulate more Mn than other brain regions. In our results, the influx transfer coefficients for Mn^{2+}, Mn citrate, and Mn Tf were lower in these regions than in most other regions. A lower Mn influx rate in these susceptible regions may indicate a neuroprotective mechanism.

Results of the capillary enrichment method suggested 92%, 90%, and 75% of the ^{54}Mn taken up by endothelial cells had passed through brain endothelial cells into brain parenchyma. The distribution of Mn species into brain endothelial cells and the brain parenchyma from perfusate in blood as a result of diffusion and equilibrium between the two brain compartments would result in 0.1% of Mn in the brain endothelial cells because they represent approximately 0.1% of brain volume (Pardridge 2003). Total Mn concentration in the brain endothelial cell and brain parenchymal compartments represents Mn in bulk brain, as collected after in situ brain perfusion with Mn^{2+}, Mn citrate, or Mn Tf. To model this system, the Mn concentration found in bulk brain was set to 100% after perfusion with each of the three Mn species. The mass transfer of Mn into bulk brain followed the same scheme as results for comparison of influx transfer coefficients versus diffusion rates (eg, Mn citrate > Mn^{2+} > Mn Tf). The ratio of Mn in the brain endothelial cell to that in brain parenchyma was based on the results of our capillary enrichment studies.

The similar ratios of brain endothelial cell Mn concentration to brain parenchymal Mn concentration for Mn^{2+} and Mn citrate suggest a similar rate of Mn distribution from the brain endothelial cells to the brain parenchyma. This would be expected because Mn released into brain endothelial cell cytoplasm from the carrier that imports it into these cells would be expected to very rapidly respeciate (association rate, approximately 10^6/sec) within the cytoplasm to the same mix of Mn species. Mn species effluxing from the brain endothelial cells to the brain parenchyma would be the same irrespective of the Mn species taken up into the cells. Therefore the more rapid uptake of Mn citrate into the brain can be attributed to more rapid uptake of this Mn species into the endothelial cell. The greater percentage of Mn in brain endothelial cells after uptake of Mn Tf can be attributed to the longer time required to form the endosome around the Mn Tf–TfR complex, decrease the pH within the endosome to free Mn ion, and transport it out of the endosome into the cytoplasm. We interpreted these results to suggest that Mn^{2+} and Mn citrate enter the brain by different carriers, or by the same carrier at different rates.

Mn Tf Brain Uptake

The influx of ^{54}Mn Tf exceeded its predicted rate of brain entry by diffusion into only one brain region, the pons/medulla. However, we did not conclude that Mn Tf enters the brain via diffusion. Mn Tf can enter the brain via TfR-mediated endocytosis (Aschner and Gannon 1994; Aschner et al 1999). In our study Mn Tf uptake was not significantly greater than the uptake rate predicted for a diffusion-mediated process into most brain regions (shown in Table 4). This may reflect two practical limitations of these

experiments: (1) the linear relation between lipophilicity and molecular weight versus BBB permeability (Levin 1980) may not apply to molecules as large as Mn Tf; and (2) endocytosis is a slow process relative to movement via ion channels and nutrient carriers. The higher fraction (25%) of ^{54}Mn Tf associated with the endothelial cells, relative to Mn^{2+} and Mn citrate, may reflect the slow rate of TfR-mediated endocytosis, determined for iron to be 2.5 molecules/min for each receptor (Cole and Glass 1983; Bradbury 1997). Brain regions found to have higher Mn Tf influx rates generally have moderate to high TfR density (Hill et al 1985). The Tf-dependent route of Mn brain entry appears to play a limited role in total Mn uptake (Takeda et al 2000; Malecki 2001).

Mn^{2+} and Mn Citrate Brain Uptake

We found that Mn citrate transfer coefficients at the BBB were greater than those predicted for Mn citrate diffusion. Our data are the first evidence that transport of Mn citrate at the BBB is facilitated by some mechanism. Furthermore, the transfer coefficients for Mn citrate are generally higher than those for Mn^{2+} determined in the present study (Table 4) and previous experiments (Murphy et al 1991; Rabin et al 1993). Our infusion experiments found brain Mn^{2+} influx from blood to be faster than that reported from saline or blood using in situ brain perfusion (Murphy et al 1991; Rabin et al 1993). From the onset of infusion to initial sampling, the ^{54}Mn had sufficient time (20 minutes) to enter blood cells or change chemical species by binding to plasma proteins or low molecular weight ligands, including citrate. The total uptake of all ^{54}Mn species was greater than the uptake of $^{54}Mn^{2+}$ (Rabin et al 1993). This and the present work suggest that Mn bound to low molecular weight ligands in plasma can enter the brain more rapidly than the hydrated Mn ion. By excluding the low molecular weight ligands, we could examine and differentiate the influx rates of hydrated Mn ion from Mn citrate. Even with the considerable variability of Mn citrate data and the correction for multiple comparisons, we detected two regions (occipital cortex and thalamus/hypothalamus) with faster uptake of Mn citrate than Mn^{2+}. These different rates may be due to different affinities for the same carrier system, or they may result from different carriers mediating Mn^{2+} and Mn citrate brain uptake.

Differences between Mn^{2+} uptake and Mn citrate uptake were suggested in experiments using $^{55}Mn^{2+}$, which inhibited the influx of $^{54}Mn^{2+}$ even though the results did not show a concentration-dependent inhibition across the 10^6-fold concentration range studied. In four brain regions the influx was not inhibited by any tested concentration of $^{55}Mn^{2+}$. The highest tested concentration exceeded normal serum Mn concentrations by 500,000-fold (Keen et al 2000). Similar studies of Mn citrate showed inhibition in three of nine brain regions tested, with significant inhibition at the highest concentration of Mn citrate. We did not extend the study beyond these ^{55}Mn concentrations because 10^8 nM Mn would significantly affect the osmolarity of the perfusate. These results agree with the description of a nonsaturable component of Mn^{2+} uptake from blood (Murphy et al 1991).

Mn Brain Influx Modeling

All of the brain regions tested in the in situ brain perfusion studies were fit best, for at least one Mn species, by an equation with one Michaelis-Menten (facilitated transport) term and a nonsaturable (diffusion) term. The K_m values generated were at the upper end of the concentrations tested, however, and must be regarded in a qualitative manner only. The caudate region of the brain, which is relevant in the pathology of manganism, produced K_m values near or below the highest Mn concentration tested for both Mn species. Although the K_m values were significantly different for Mn^{2+} and Mn citrate (see Table 6), the magnitudes of these values ($> 10^6$ nM) are so great that they are not physiologically relevant. In the caudate, the V_{max} values of Mn citrate and Mn^{2+} were significantly different. This is evidence that, in at least one brain region, Mn^{2+} and Mn citrate have different influx carriers or different affinities for the same carrier.

That Mn citrate plays an important role in brain Mn influx becomes more apparent when one considers Mn speciation in blood relative to Mn^{2+} and Mn citrate influx rates. Thermodynamic modeling suggests that 40% of Mn available to cross the BBB is in the form of the hydrated ion, while about 15% is Mn citrate. With about one third the concentration and with an uptake rate three times faster (40 versus 13×10^{-5} mL/sec/g in the parietal cortex), Mn citrate total influx (J) is comparable to Mn^{2+} influx. It appears that Mn citrate is a major species of Mn that enters the brain.

Mn BRAIN EFFLUX

The brain efflux study (Study 4) attempted to quantify the rate of Mn efflux across the BBB from brain to blood using established methods (Kakee et al 1996). The rate of brain efflux (K_{out}) is calculated from the volume of distribution of Mn species in the brain(V_{brain}) and the rate of disappearance of the test substance from the brain after its discrete microinjection (K_{el}), which is determined from the brain efflux index. However, 100−BEI(%) increased over time after microinjection of Mn^{2+} and Mn citrate, preventing calculation of K_{el}, and therefore K_{out}. The results

of the V_{brain} determinations and brain efflux index studies are individually discussed.

The extracellular space of the brain slice can be estimated from the ^{14}C-sucrose results of the V_{brain} determinations extrapolated to time zero. This was found to be 0.15 mL/g, comparable to the 0.13 mL/g reported with ^{14}C-inulin (Hosoya et al 2000). The V_{brain} for sucrose in our studies was 0.057 mL/g. This is reasonable when compared to the vascular volume of the brain, which is about 3%, and brain extracellular fluid volume, which is about 10%. Sucrose would be expected to rapidly diffuse into blood vessels and the extracellular space but not to rapidly achieve equilibrium in these compartments.

Uptake of Mn^{2+}, Mn citrate, and Mn Tf into parietal cortical brain slices was concentrative for all three Mn species. The volume of distribution was greater than the whole-rat total volume of distribution (Zheng et al 2000), consistent with a report that Mn accumulates in the brain from blood (Gianutsos et al 1985). Previous studies of uptake into brain slices revealed a plateau (steady state) for 3-*O*-methyl-D-glucose of 0.78 mL/g (Kakee et al 1996) and for *p*-aminohippurate at approximately 60 minutes of 0.8 mL/g (Kakee et al 1997). Concentrative uptake into brain slices was seen with estrone-3-sulfate, L-aspartate, estrone, dehydroepiandrosterone, and GABA, which reached steady-state V_{brain} values of 1.1, 2.5, 3.3, 4.7, and 26 mL/g at approximately 30, 10, 30, 60, and 60 minutes, respectively (Hosoya et al 1999, 2000; Asaba et al 2000; Kakee et al 2001). L-Glutamate appeared to be reaching a steady state of 13 mL/g at 120 minutes (Hosoya et al 1999). However, D-aspartate brain slice uptake was linear for 120 minutes, reaching a V_{brain} of 59 mL/g, but not a steady state (Hosoya et al 1999). The uptake of Mn^{2+}, Mn citrate, and Mn Tf was intermediate to these results, approaching a steady state of approximately 3 to 5 mL/g after 45 to 120 minutes. The uptake of Mn citrate does not appear to be driven by its use as a source of citrate for the citric acid cycle or to be ATP-dependent, as it was not affected by the aconitase inhibitors aconitine, monofluoroacetate, and oxalomalate or the respiratory inhibitor sodium azide. The accumulation of Mn in the brain slice may be due to its association with enzymes such as glutamine synthetase in astrocytes.

After coinjection of ^{54}Mn or ^{54}Mn citrate and sucrose or dextran into the brain for the brain efflux index determinations, the Mn-sucrose or Mn-dextran ratio increased over time, indicating that Mn was distributing out of the brain more slowly than the reference compound. Sucrose and dextran distribute very slowly out of the brain across the BBB by diffusion. Our calculations suggest sucrose and dextran diffuse out of the brain more rapidly than Mn. The slightly increasing 100−BEI(%) Mn values over time are consistent with the slightly slower diffusion efflux of Mn from the brain than sucrose or dextran. These results suggest brain Mn efflux is mediated by diffusion. This novel observation is consistent with brain Mn accumulation during repeated or continuous exposure.

Although there are no previous reports of an increase of 100−BEI(%) over time, it has been concluded that there was no brain efflux of L-glucose after 20 minutes, octreotide after 60 minutes, or D-aspartate after 20 minutes (Kakee et al 1996; Kitazawa et al 1998; Hosoya et al 1999). The results for octreotide were not shown. A best fit of the 100−BEI(%) results obtained with L-glucose up to 20 minutes after its coinjection into the brain with inulin would probably result in a positive slope (Kakee et al 1996). L-Glucose would be expected to diffuse from brain to blood slightly more slowly than inulin ($P_{diffusion}S$ = 9.4 and 12 × 10^{-5}, respectively), which should produce a positive slope for 100−BEI(%). D-Aspartate would also be expected to diffuse across the BBB more slowly than inulin ($P_{diffusion}S$ was calculated to be 0.4 × 10^{-5}, based on a log $D_{o/a}$ = −6.5) (Advanced Chemistry Development 2002).

The 100−BEI(%) values after the injection of Mn^{2+} and Mn citrate into the brain were similar. After injection into the brain, it is expected that Mn^{2+} and Mn citrate would rapidly equilibrate to the same species. Dr Wesley Harris used the composition and concentration of ligands in cerebrospinal fluid to calculate these species: Mn^{2+} aquo ion represented 56% of total Mn; Mn(citrate) and Mn(H_{-1} citrate) together represented 20%; and Mn phosphate represented 15%, with the balance as other species.

Although TfRs have been found at both the luminal and abluminal surfaces of brain endothelial capillaries (Huwyler and Pardridge 1998), their role in the efflux of metals from the brain has not been well studied. Brain efflux of Tf was recently demonstrated, after its injection into the brain, using the brain efflux index method (Zhang and Pardridge 2001). However, the mammalian brain extracellular fluid concentration of Tf is very low (< 0.25 μM), which is less than 1% of its concentration in blood plasma. Furthermore, it has been suggested that the Tf in brain extracellular fluid may be saturated with iron, leaving no available binding sites for Mn (Bradbury 1997). The lack of Mn binding sites on Tf in brain extracellular fluid suggests TfR-mediated endocytosis may not contribute to brain-to-blood Mn transfer. As Tf is believed to play only a minor role in brain Mn influx from blood to brain, it would not be expected to play an important role in brain Mn efflux to blood. For these reasons, the brain efflux index of Mn after Mn Tf injection into the brain was not determined.

CHARACTERIZATION OF Mn TRANSPORTERS AT BBB

Prior to Study 5, some potential carriers for Mn^{2+} and Mn citrate had been predicted from the knowledge of transporter systems at the BBB. A review of the carriers at the BBB (Table 1) suggested that the most likely candidates for mediating transport of Mn^{2+} across mammalian membranes were DMT-1 and one or more members of the ATP-binding cassette (ABC) superfamily. DMT-1 serves as a high-affinity non-Tf-bound Fe membrane transporter (Garrick et al 1999) with nonselective affinity for Mn^{2+}, Co^{2+}, Fe^{2+}, Ni^{2+}, Cu^{2+}, Zn^{2+}, and Cd^{2+} (Knöpfel et al 2000; Picard et al 2000). Based on the known carriers at the BBB, candidates for transport of Mn citrate across mammalian membranes were more difficult to predict. At the dilute Mn and citrate concentrations and pH (7.4) of the in situ brain perfusion studies, they would be expected to remain as a 1:1 Mn citrate complex (Glusker and Carrell 1973; Amico and Daniele 1979), as shown in Appendix A. Each citrate ion forms a tridentate complex with Mn involving the hydroxyl group and two terminal carboxylates, leaving a noncoordinated central carboxylate (Glusker and Carrell 1973; Amico and Daniele 1979; Gregor and Powell 1986) that may serve as the recognition moiety of Mn citrate for an organic anion transporter or a monocarboxylate transporter. Candidates for transport of Mn citrate were thought to include monocarboxylate transporters or members of the organic anion transporter polypeptide (Oatp) or ABC superfamilies.

Mn^{2+} uptake into bBMECs was linear from 10 to 120 minutes. Uptake was also concentrative, providing evidence of a carrier-mediated process of brain Mn uptake. The increased Mn^{2+} uptake in the presence of reduced hydrogen ion concentration is not consistent with DMT-1 being the sole mediator of brain Mn uptake. The brain uptake of Mn^{2+} was sodium-independent, suggesting the uptake carriers do not utilize a sodium gradient as a driving force. Replacing sodium with choline increased brain Mn^{2+} uptake. There is no other published report of a choline effect on Mn uptake. One study suggested that Mn inhibits choline uptake at the BBB (Lockman et al 2001). The authors suggested that the choline transporter may be involved in brain Mn uptake. Choline uptake has been described to be sodium-independent (Allen and Smith 2001). We did not find reduction of Mn uptake in the presence of reduced sodium in the uptake medium. In fact, reduction of sodium in studies reported by Lockman and colleagues (2001) and in our studies increased choline and Mn uptake, an interesting commonality for which we do not have a good explanation. We found that choline increased Mn uptake, which would not be expected if they were competing for an uptake process. Although the basis of any interaction between Mn and choline is unclear, it is clear that Mn^{2+} uptake at the BBB is sodium-independent. Further work will be necessary to test the hypothesis forwarded by Lockman and coworkers (2001) that the choline transporter mediates Mn uptake.

Despite indications in cell culture work, results of addition of vanadate to the in situ brain perfusate did not support a role of ATPases in Mn^{2+} uptake at the BBB. Although vanadate, an inhibitor of ATPases, inhibited Mn^{2+} influx into bBMECs, it did not inhibit brain Mn^{2+} uptake. Nor was brain Mn uptake inhibited by ouabain, showing Mn^{2+} uptake to be independent of Na^+/K^+-ATPase. *p*-Hydroxyhippuric acid, a relatively selective Ca^{2+}-ATPase inhibitor, did not inhibit Mn^{2+} uptake into brain, providing further evidence of lack of a role for Ca^{2+}-ATPase.

Rats that do not express a functional form of DMT-1 (*b/b* Belgrade rats) were included in this research to assess the role of DMT-1 in brain Mn uptake. Brain Mn uptake was not lower in the *b/b* Belgrade rats than in their *+/b* littermate or control (Wistar) rats. The lack of significant differences in Mn^{2+} or Mn Tf uptake among the three groups in the absence versus presence of cerebrovascular washout and in Mn associated with the brain endothelial cells shows that the absence of DMT-1 function did not affect brain Mn uptake. These results suggest that the DMT-1 is not essential for brain Mn uptake. These results were not expected. The lack of difference between *b/b* Belgrade rats and *+/b* littermates in brain Mn uptake suggests the lack of an essential role of this DMT-1-mediated process in the endosome. Mn uptake into a human erythroleukemia cell line (K562 cells) was inhibited in pH 7.4 media in the presence of a DMT-1-blocking antibody (Conrad et al 2000). This suggests DMT-1 may mediate Mn transport at blood pH into this transformed cell line. However, DMT-1 does not appear to play a major role in Mn uptake into the brain.

Fe^{2+} did not significantly inhibit uptake of Mn^{2+} into the brain of Sprague Dawley rats, using the in situ brain perfusion technique. To the contrary, the nonsignificant trend was that Fe increased, rather than decreased, Mn uptake. The conclusion that DMT-1 is not essential for brain Mn uptake is consistent with the lack of inhibition of Mn^{2+} uptake by Fe. These results do not provide evidence that brain Mn^{2+} uptake is mediated by a carrier that transports both Fe and Mn into the brain, such as DMT-1, unless the V_{max} of the uptake transporter is much larger than the concentrations of Fe and Mn tested.

The results with calcium uptake modulators suggest a possible role for store-operated calcium channels in Mn uptake. This is consistent with the proposed uptake of Mn from the gastrointestinal tract by processes that mediate calcium uptake (Leblondel and Allain 1999). The concentration-dependent effect of calcium on Mn uptake (Figure 18)

suggests calcium plays an active role in Mn uptake, either as a competitive inhibitor at the transporter site or as a noncompetitive inhibitor at any number of sites. Cyclopiazonic acid and thapsigargin, which cause release and depletion of calcium stores and thereby activate store-operated calcium channels, also increased Mn^{2+} uptake by 1.8-fold and 1.7-fold, respectively, over vehicle-treated control uptake. In the same cell type, lead uptake was increased by 1.7-fold or 2.1-fold over vehicle control after treatment with cyclopiazonic acid or thapsigargin, respectively (Kerper and Hinkle 1997a). Nickel inhibits calcium flux through plasma membrane channels and is not specific to the store-operated channel. Treatment with nickel also inhibited Mn uptake into bBMECs, consistent with a role for calcium channels in Mn uptake. The effect was significant, with 80% less uptake than in the absence of nickel. However, studies in the whole animal had the opposite result. Nickel significantly increased Mn uptake into brain after perfusions of 45 and 90 seconds. The effect at 90 seconds was greater than the influx at 45 seconds, which implies an early activation of Mn transport. This activation must be short-lived to produce the net decrease in Mn uptake after a 30-minute incubation in bBMECs.

The results with the calcium channel blocker lanthanum (La^{3+}) do not suggest a role of store-operated calcium channels in Mn uptake. The cell culture studies failed to show any effect on Mn uptake due to La^{3+}. In animals, La^{3+} significantly increased Mn uptake more than 3.7-fold compared to control. We were unable to find other reports of La^{3+} activation of a transporter or carrier. A slight, nonsignificant increase in Mn uptake with La^{3+} treatment is consistent with the hypothesis that calcium channel blockers cause a fast but transient activation of a Mn transporter that is not inhibited by La^{3+}. An alternative explanation is that the inhibitors were not effective in blocking calcium pathways, which we did not directly measure. To examine the relation of Ca and Mn at the BBB, we are currently conducting experiments to follow influx of both ^{45}Ca and ^{54}Mn in the presence of calcium channel inhibitors and activators. If ^{45}Ca is unaffected by the inhibitors or activators, then the early activation is a specific response of Mn transporters to the presence of the inhibitors or activators. If the calcium influx is affected as predicted (decreased by inhibitors, increased by activators), then the early increase in Mn influx may occur as a homeostatic mechanism to restore calcium or divalent charges within the cell. If calcium influx increases in response to inhibitors, then the increase in Mn influx parallels the increase in calcium influx and the two ions may be utilizing the same carrier. These experiments are vital to understand the nature of the interaction of Ca and Mn uptake at the BBB.

Mn citrate did not serve as a substrate for the MCT1 or band 3 (anion exchange) transporters. Mn citrate did not inhibit lactate uptake into erythrocytes under conditions in which pyruvate, a monocarboxylate transporter substrate and therefore an inhibitor of lactate uptake, inhibited uptake by approximately 50%. These results suggest the lack of ability of Mn citrate to serve as a substrate for the monocarboxylate transporter at low millimolar concentrations. Mn citrate uptake by rat erythrocytes was not significant after 60 minutes at room temperature. These results suggest that Mn citrate does not serve as an effective substrate for either the MCT1 or anion exchange transporter.

One shortcoming of the use of pharmacologic agents, as in the present work, is their lack of specificity. However, studies in cell lines and primary cultures were usually completed in conjunction with animal studies. In other cases, two or more agents modulating the same carrier system were used to increase confidence in the conclusion that the effect, or lack of effect, could be attributed to the carrier being studied. Conclusions were drawn from more than a single probe or technique. The use of broad-spectrum inhibitors can be advantageous. For instance, quercetin inhibition of Mn citrate uptake demonstrated that the uptake was carrier mediated. However, because of the multiple actions of quercetin, the results do not reveal the carrier.

An inherent limiting factor in the characterization of the carriers mediating transport of substances across the BBB is that only about 50% of the functional BBB transporters have been discovered, according to one recent estimate (Pardridge 2003). The specific carriers mediating Mn transport across the BBB may be among those that have not yet been identified.

IMPLICATIONS OF FINDINGS

The results show evidence of carriers that mediate the influx of Mn^{2+}, Mn citrate, and Mn Tf into the brain. Each of these three Mn species is present in blood plasma. These carriers would increase the rate of brain Mn entry over that provided by diffusion. This might provide benefit if the brain required further Mn, an essential element (eg, when blood Mn levels are low). However, these carriers might mediate excessive brain Mn in the presence of elevated blood Mn, as might result from increased Mn exposure to environmental or other sources.

The results suggest that diffusion mediates brain Mn efflux. In light of carrier-mediated brain influx, but not efflux, repeated excessive Mn exposure would be anticipated to result in brain Mn accumulation over time. Observations in animals and humans confirm that Mn persists in

the brain for some time. If this persistence is paired with repeated or continuous Mn exposure, one would expect to see increasing brain Mn concentrations over time. This has been observed in animals (Gianutsos et al 1985). Similarly, human brain Mn concentration rose from 0.15 μg/g wet brain weight in human infants to 0.26 μg/g wet brain weight in adults. The highest concentrations were in the basal ganglia, the site of Mn-induced neurotoxicity (Markesbery et al 1984).

The results indicate that brain Mn^{2+} uptake is not mediated by MCT1 or the anion exchange transporter. It negatively correlated with proton availability, suggesting a role for another ion in the brain Mn uptake process. Mn^{2+} brain uptake is not directly dependent on a source of ATP and is not inhibited by Fe or ATPase inhibitors. Brain Mn uptake appears to be mediated by an electromotive force. The transporters responsible for this uptake have not yet been identified. Further work must be conducted to identify the carriers responsible for Mn influx.

ACKNOWLEDGMENTS

We thank Dr Bonny L Bukaveckas for conducting Study 1 and initiating Study 4. We thank Dr Robert Lodder for conducting the near-infrared studies of Mn citrate we prepared. We thank Susan Rhineheimer for her technical assistance with many aspects of this work and students Surjya Bhattacharyya, Karl Deibel, Adrienne Ellis, and Li Li, who conducted research rotations in our lab and contributed to this work. We thank Dr Michael Jay for assistance with the radiochemistry of this study; Dr Wesley Harris, University of Missouri–St Louis, for the discussion related to Mn reaction rates and calculation of brain extracellular fluid Mn species; and Dr David Allen, Texas Tech Health Science Center–Amarillo, for training us in the use of the in situ brain perfusion technique and many suggestions for the use of this method and the capillary depletion method. Further support was provided by the University of Kentucky Graduate School (JSC) and National Institute of Environmental Health Sciences, US National Institutes of Health, grant T32 ES7266 (JSC and BLB). The University of Kentucky College of Pharmacy Pharmaceutical Sciences Division contributed salary support for the summer research of Karl Deibel.

REFERENCES

Ackley DC, Yokel RA. 1997. Aluminum citrate is transported from brain into blood via the monocarboxylic acid transporter located at the blood-brain barrier. Toxicology 120:89–97.

Ackley DC, Yokel RA. 1998. Aluminum transport out of brain extracellular fluid is proton dependent and inhibited by mersalyl acid, suggesting mediation by the monocarboxylate transporter (MCT1). Toxicology 127:59–67.

Advanced Chemistry Development. 2002. ACD/pKa v5.0. ACD/I-Lab, Toronto ON, Canada. *http://ilab.acdlabs.com.*

Agency for Toxic Substances and Disease Registry. 2000. Toxicological Profile for Manganese. ATSDR, Atlanta GA.

Aisen P, Aasa R, Redfield AG. 1969. The chromium, manganese, and cobalt complexes of transferrin. J Biol Chem 244:4628–4633.

Akeson MA, Munns DN. 1989. Lipid bilayer permeation by neutral aluminum citrate and by three alpha-hydroxy carboxylic acids. Biochim Biophys Acta 984:200–206.

Allen DD, Orvig C, Yokel RA. 1995. Evidence for energy-dependent transport of aluminum out of brain extracellular fluid. Toxicology 98:31–39.

Allen DD, Smith QR. 2001. Characterization of the blood-brain barrier choline transporter using the in situ rat brain perfusion technique. J Neurochem 76:1032–1041.

Ambrosi G, Virgintino D, Benagiano V, Maiorano E, Bertossi M, Roncali L. 1995. Glial cells and blood-brain barrier in the human cerebral cortex. Ital J Anat Embryol 100:177–184.

Amico P, Daniele PG. 1979. Equilibrium study of iron(II) and manganese(II) complexes with citrate ion in aqueous solution: Relevance to coordination of citrate to the active site of aconitase and to gastrointestinal absorption of some essential metal ions. Inorg Chim Acta 36:1–7.

Asaba H, Hosoya K, Takanaga H, Ohtsuki S, Tamura E, Takizawa T, Terasaki T. 2000. Blood-brain barrier is involved in the efflux transport of a neuroactive steroid, dehydroepiandrosterone sulfate, via organic anion transporting polypeptide 2. J Neurochem 75:1907–1916.

Aschner M, Aschner JL. 1990. Manganese transport across the blood-brain barrier: Relationship to iron homeostasis. Brain Res Bull 24:857–860.

Aschner M, Gannon M, Kimelberg HK. 1992. Manganese uptake and efflux in cultured rat astrocytes. J Neurochem 58:730–735.

Aschner M, Gannon M. 1994. Manganese (Mn) transport across the rat blood-brain barrier: Saturable and transferrin-dependent transport mechanisms. Brain Res Bull 33:345–349.

Aschner M, Vrana KE, Zheng W. 1999. Manganese uptake and distribution in the central nervous system (CNS). Neurotoxicology 20:173–180.

Audus KL, Ng L, Wang W, Borchardt RT. 1996. Brain microvessel endothelial cell culture systems. Pharm Biotechnol 8:239–258.

Bonate PL. 1995. Animal models for studying transport across the blood-brain barrier. J Neurosci Methods 56:1–15.

Borges N, Shi F, Azevedo I, Audus KL. 1994. Changes in brain microvessel endothelial cell monolayer permeability induced by adrenergic drugs. Eur J Pharmacol 269:243–248.

Bowman PD, Ennis SR, Rarey KE, Betz AL, Goldstein GW. 1983. Brain microvessel endothelial cells in tissue culture: A model for study of blood-brain barrier permeability. Ann Neurol 14:396–402.

Bradbury MW, Deane R. 1993. Permeability of the blood-brain barrier to lead. Neurotoxicology 14:131–136.

Bradbury MWB. 1997. Transport of iron in the blood-brain-cerebrospinal fluid system. J Neurochem 69:443–454.

Breitbart H, Rubinstein S, Nass-Arden L. 1985. The role of calcium and Ca^{2+}-ATPase in maintaining motility in ram spermatozoa. J Biol Chem 260:11548–11553.

Burdo JR, Menzies SL, Simpson IA, Garrick LM, Garrick MD, Dolan KG, Haile DJ, Beard JL, Connor JR. 2001. Distribution of divalent metal transporter 1 and metal transport protein 1 in the normal and Belgrade rat. J Neurosci Res 66:1198–1207.

Carafoli E, Brini M. 2000. Calcium pumps: Structural basis for and mechanism of calcium transmembrane transport. Curr Opin Chem Biol 4:152–161.

Cheng AM, Morrison SW, Yang DX, Hagen SJ. 2001. Energy dependence of restitution in the gastric mucosa. Am J Physiol Cell Physiol 281:C430–C438.

Cole ES, Glass J. 1983. Transferrin binding and iron uptake in mouse hepatocytes. Biochim Biophys Acta 762:102–110.

Conrad ME, Umbreit JN, Moore EG, Hainsworth LN, Porubcin M, Simovich MJ, Nakada MT, Dolan K, Garrick MD. 2000. Separate pathways for cellular uptake of ferric and ferrous iron. Am J Physiol Gastrointest Liver Physiol 279:G767–G774.

Cornford EM, Diep CP, Pardridge WM. 1985. Blood-brain barrier transport of valproic acid. J Neurochem 44:1541–1550.

Cotton FA, Wilkinson G. 1980. Advanced Inorganic Chemistry: A Comprehensive Text, 4th edition, pp 741–743. John Wiley & Sons, New York NY.

Couper J. 1837. On the effects of black oxide of manganese when inhaled into the lungs. Br Ann Med Pharmacy, Vital Stat Gen Sci 1:41–42.

Critchfield JW, Keen CL. 1992. Manganese^{+2} exhibits dynamic binding to multiple ligands in human plasma. Metabolism 41:1087–1092.

Crone C. 1963. The permeability of capillaries in various organs as determined by use of the indicator diffusion method. Acta Physiol Scand 58:292–305.

Dastur DK, Manghani DK, Raghavendran KV, Jeejeebhoy KN. 1969. Distribution and fate of Mn^{54} in the rat, with special reference to the CNS. Q J Exp Physiol Cogn Med Sci 54:322–331.

Dastur DK, Manghani DK, Raghavendran KV. 1971. Distribution and fate of ^{54}Mn in the monkey: Studies of different parts of the central nervous system and other organs. J Clin Invest 50:9–20.

Davidsson L, Cederblad A, Lonnerdal B, Sandstrom B. 1989. Manganese retention in man: A method for estimating manganese absorption in man. Am J Clin Nutr 49:170–179.

Deane R, Bradbury MW. 1990. Transport of lead-203 at the blood-brain barrier during short cerebrovascular perfusion with saline in the rat. J Neurochem 54:905–914.

Deguchi Y, Morimoto K. 2001. Application of an in vivo brain microdialysis technique to studies of drug transport across the blood-brain barrier. Curr Drug Metab 2:411–423.

Deguchi Y, Naito T, Yuge T, Furukawa A, Yamada S, Pardridge WM, Kimura R. 2000. Blood-brain barrier transport of ^{125}I-labeled basic fibroblast growth factor. Pharm Res 17:63–69.

District of Columbia Circuit Court. 1995. Ethyl Corporation versus EPA. Federal Court Decision 94-1505. In: United States Court of Appeals for the District of Columbia, pp 94–151. Fed Regist, June 27, 1994.

Drown DB, Oberg SG, Sharma RP. 1986. Pulmonary clearance of soluble and insoluble forms of manganese. J Toxicol Environ Health 17:201–212.

Edlund GL, Halestrap AP. 1988. The kinetics of transport of lactate and pyruvate into rat hepatocytes. Evidence for the presence of a specific carrier similar to that in erythrocytes. Biochem J 249:117–126.

Ejima A, Imamura T, Nakamura S, Saito H, Matsumoto K, Momono S. 1992. Manganese intoxication during total parenteral nutrition. Lancet 339:426.

Fasolato C, Hoth M, Matthews G, Penner R. 1993a. Ca^{2+} and Mn^{2+} influx through receptor-mediated activation of nonspecific cation channels in mast cells. Proc Natl Acad Sci U S A 90:3068–3072.

Fasolato C, Hoth M, Penner R. 1993b. Multiple mechanisms of manganese-induced quenching of fura-2 fluorescence in rat mast cells. Pflugers Arch 423:225–231.

Fell JM, Reynolds AP, Meadows N, Khan K, Long SG, Quaghebeur G, Taylor WJ, Milla PJ. 1996. Manganese toxicity in children receiving long-term parenteral nutrition. Lancet 347:1218–1221.

Festa M, Colonna A, Pietropaolo C, Ruffo A. 2000. Oxalomalate, a competitive inhibitor of aconitase, modulates the RNA-binding activity of iron-regulatory proteins. Biochem J 348:315–320.

Finley JW. 1998. Manganese uptake and release by cultured human hepato-carcinoma (Hep-G2) cells. Biol Trace Elem Res 64:101–118.

Fitzgerald K, Mikalunas V, Rubin H, McCarthey R, Vanagunas A, Craig RM. 1999. Hypermanganesemia in patients receiving total parenteral nutrition. JPEN J Parenter Enteral Nutr 23:333–336.

Fox JL, Lamson ML. 1989. RSTRIP: Pharmacokinetic data stripping/least squares parameter optimization. MicroMath, Salt Lake City UT.

Furchner JE, Richmond CR, Drake GA. 1966. Comparative metabolism of radionuclides in mammals. 3. Retention of manganese-54 in the mouse, rat, monkey and dog. Health Phys 12:1415–1423.

Garcia CK, Goldstein JL, Pathak RK, Anderson RG, Brown MS. 1994. Molecular characterization of a membrane transporter for lactate, pyruvate, and other monocarboxylates: Implications for the Cori cycle. Cell 76:865–873.

Garrick LM, Dolan KG, Romano MA, Garrick MD. 1999. Non-transferrin-bound iron uptake in Belgrade and normal rat erythroid cells. J Cell Physiol 178:349–358.

Gianutsos G, Seltzer MD, Saymeh R, Wu ML, Michel RG. 1985. Brain manganese accumulation following systemic administration of different forms. Arch Toxicol 57:272–275.

Glusker JP, Carrell HL. 1973. X-ray crystal analysis of the substrates of aconitase: XI. Manganous citrate decahydrate. J Mol Struct 15:151–159.

Gregor JE, Powell HKJ. 1986. Aluminium(III)-citrate complexes: A potentiometric and ^{13}C NMR study. Aust J Chem 39:1851–1864.

Gunshin H, Mackenzie B, Berger UV, Gunshin Y, Romero MF, Boron WF, Nussberger S, Gollan JL, Hediger MA. 1997. Cloning and characterization of a mammalian proton-coupled metal-ion transporter. Nature 388:482–488.

Gunter KK, Miller LM, Aschner M, Eliseev R, Depuis D, Gavin CE, Gunte TE. 2002. XANES spectroscopy: A promising tool for toxicology: A tutorial. Neurotoxicology 23:127–146.

Harris WR. 1998. Binding and transport of nonferrous metal ions by serum transferrin. Structure and Bonding 92:121–162.

Harris WR, Chen Y. 1994. Electron paramagnetic resonance and difference ultraviolet studies of Mn^{2+} binding to serum transferrin. J Inorg Biochem 54:1–19.

Health Effects Institute. 1998. Attachment A: Summary of a workshop on metal-based fuel additives and new engine technologies. In: Request for Applications. Fall 1998 Research Agenda, pp 7–12. Health Effects Institute, Cambridge MA.

Hill JM, Ruff MR, Weber RJ, Pert CB. 1985. Transferrin receptors in rat brain: Neuropeptide-like pattern and relationship to iron distribution. Proc Natl Acad Sci U S A 82:4553–4557.

Hosoya K, Asaba H, Terasaki T. 2000. Brain-to-blood efflux transport of estrone-3-sulfate at the blood-brain barrier in rats. Life Sci 67:2699–2711.

Hosoya K, Sugawara M, Asaba H, Terasaki T. 1999. Blood-brain barrier produces significant efflux of L-aspartic acid but not D-aspartic acid: In vivo evidence using the brain efflux index method. J Neurochem 73:1206–1211.

Hsiu SL, Hou YC, Wang YH, Tsao CW, Su SF, Chao PD. 2002. Quercetin significantly decreased cyclosporin oral bioavailability in pigs and rats. Life Sci 72:227–235.

Huang JD. 1990. Comparative drug exsorption in perfused rat intestine. J Pharm Pharmacol 42:167-170.

Hudnell HK. 1999. Effects from environmental Mn exposures: A review of the evidence from non-occupational exposure studies. Neurotoxicology 20:379–397.

Huwyler J, Pardridge WM. 1998. Examination of blood-brain barrier transferrin receptor by confocal fluorescent microscopy of unfixed isolated rat brain capillaries. J Neurochem 70:883–886.

Iregren A. 1999. Manganese neurotoxicity in industrial exposures: Proof of effects, critical exposure level, and sensitive tests. Neurotoxicology 20:315–323.

Jankowski J, Tepel M, Stephan N, van der Giet M, Breden V, Zidek W, Schluter H. 2001. Characterization of p-hydroxy-hippuric acid as an inhibitor of Ca^{2+}-ATPase in end-stage renal failure. Kidney Int Suppl 78:S84–S88.

Johnson MD, Anderson BD. 1996. Localization of purine metabolizing enzymes in bovine brain microvessel endothelial cells: An enzymatic blood-brain barrier for dideoxynucleosides? Pharm Res 13:1881–1886.

Johnson MD, Anderson BD. 2000. Use of cultured cerebral capillary endothelial cells in modeling the central nervous system availability of 2′,3′-dideoxyinosine. J Pharm Sci 89:322–335.

Johnson PE, Lykken GI, Korynta ED. 1991. Absorption and biological half-life in humans of intrinsic and extrinsic ^{54}Mn tracers from foods of plant origin. J Nutr 121:711–717.

Kabata H, Matsuda A, Yokoi K, Kimura M, Itokawa Y. 1989. The effect of the dosage and route of manganese administration on manganese concentration in rat brain [in Japanese]. Nippon Eiseigaku Zasshi 44:667–672.

Kakee A, Takanaga H, Terasaki T, Naito M, Tsuruo T, Sugiyama Y. 2001. Efflux of a suppressive neurotransmitter, GABA, across the blood-brain barrier. J Neurochem 79:110–118.

Kakee A, Terasaki T, Sugiyama Y. 1996. Brain efflux index as a novel method of analyzing efflux transport at the blood-brain barrier. J Pharmacol Exp Ther 277:1550–1559.

Kakee A, Terasaki T, Sugiyama Y. 1997. Selective brain to blood efflux transport of *para*-aminohippuric acid across the blood-brain barrier: *In vivo* evidence by use of the brain efflux index method. J Pharmacol Exp Ther 283:1018–1025.

Keen CL, Ensunsa JL, Clegg MS. 2000. Manganese metabolism in animals and humans including the toxicity of manganese. In: Manganese and Its Role in Biological Processes (Segal A, Sigel H, eds), pp 89–121. Marcel Dekker, New York NY.

Keen CL, Lönnerdal B. 1995. Manganese. In: Handbook of Metal-Ligand Interactions in Biological Fluids, Vol 2 (Berthon G, ed), pp 683–688. Marcel Dekker, New York NY.

Keep RF, Ulanski LJ Jr, Xiang J, Ennis SR, Lorris Betz A. 1999. Blood-brain barrier mechanisms involved in brain calcium and potassium homeostasis. Brain Res 815:200–205.

Kerper LE, Hinkle PM. 1997a. Cellular uptake of lead is activated by depletion of intracellular calcium stores. J Biol Chem 272:8346–8352.

Kerper LE, Hinkle PM. 1997b. Lead uptake in brain capillary endothelial cells: Activation by calcium store depletion. Toxicol Appl Pharmacol 146:127–133.

Ketchum KA. 1999. Genome based comparisons of transporters. In: Second AAPS Frontier Symposium: Membrane Transporters and Drug Therapy. National Institutes of Health, Bethesda MD.

Kitazawa T, Terasaki T, Suzuki H, Kakee A, Sugiyama Y. 1998. Efflux of taurocholic acid across the blood-brain barrier: Interaction with cyclic peptides. J Pharmacol Exp Ther 286:890–895.

Klaassen CD. 1974. Biliary excretion of manganese in rats, rabbits, and dogs. Toxicol Appl Pharmacol 29:458–468.

Knöpfel M, Schulthess G, Funk F, Hauser H. 2000. Characterization of an integral protein of the brush border membrane mediating the transport of divalent metal ions. Biophys J 79:874–884.

Kusuhara H, Suzuki H, Terasaki T, Kakee A, Lemaire M, Sugiyama Y. 1997. P-Glycoprotein mediates the efflux of quinidine across the blood-brain barrier. J Pharmacol Exp Ther 283:574–580.

Laterra J, Keep R, Betz A, Goldstein G. 1999. Blood-brain-cerebrospinal fluid barriers. In: Basic Neurochemistry: Molecular, Cellular and Medical Aspects, 6th edition (Siegel GJ, Albers RW, Agranoff BW, Fisher SK, Uhler MD, eds), pp 671–689. Lippincott-Raven Publishers, Philadelphia PA.

Leblondel G, Allain P. 1999. Manganese transport by Caco-2 cells. Biol Trace Elem Res 67:13–28.

Lee DY, Johnson PE. 1988. Factors affecting absorption and excretion of ^{54}Mn in rats. J Nutr 118:1509–1516.

Lee DY, Johnson PE. 1989. ^{54}Mn absorption and excretion in rats fed soy protein and casein diets. Proc Soc Exp Biol Med 190:211–216.

Leininger B, Ghersi-Egea JF, Siest G, Minn A. 1991. In vivo study of the elimination from rat brain of an intracerebrally formed xenobiotic metabolite, 1-naphthyl-beta-D-glucuronide. J Neurochem 56:1163–1168.

Leslie EM, Mao Q, Oleschuk CJ, Deeley RG, Cole SPC. 2001. Modulation of multidrug resistance protein 1 (MRP1/ABCC1) transport and ATPase activities by interaction with dietary flavonoids. Mol Pharmacol 59:1171–1180.

Levin VA. 1980. Relationship of octanol/water partition coefficient and molecular weight to rat brain capillary permeability. J Med Chem 23:682–684.

Lockman PR, Roder KE, Allen DD. 2001. Inhibition of the rat blood-brain barrier choline transporter by manganese chloride. J Neurochem 79:588–594.

Lucaciu CM, Dragu C, Copaescu L, Morariu VV. 1997. Manganese transport through human erythrocyte membranes. An EPR study. Biochim Biophys Acta 1328:90–98.

Lucchini R, Apostoli P, Perrone C, Placidi D, Albini E, Migliorati P, Mergler D, Sassine MP, Palmi S, Alessio L. 1999. Long-term exposure to "low levels" of manganese oxides and neurofunctional changes in ferroalloy workers. Neurotoxicology 20:287–297.

Lucchini R, Selis L, Folli D, Apostoli P, Mutti A, Vanoni O, Iregren A, Alessio L. 1995. Neurobehavioral effects of manganese in workers from a ferroalloy plant after temporary cessation of exposure. Scand J Work Environ Health 21:143–149.

Lynam DR, Roos JW, Pfeifer GD, Fort BF, Pullin TG. 1999. Environmental effects and exposures to manganese from use of methylcyclopentadienyl manganese tricarbonyl (MMT) in gasoline. Neurotoxicology 20:145–150.

Lynch CJ, Deth RC. 1984. Release of a common source of intracellular Ca^{2+} by alpha-adrenergic agonists and dinitrophenol in rat liver slices. Pharmacology 28:74–85.

Mahoney JP, Small WJ. 1968. Studies on manganese. III. The biological half-life of radiomanganese in man and factors which affect this half-life. J Clin Invest 47:643–653.

Malecki EA, Devenyi AG, Beard JL, Connor JR. 1999. Existing and emerging mechanisms for transport of iron and manganese to the brain. J Neurosci Res 56:113–122.

Malecki EA. 2001. Limited role of transferrin in manganese transport to the brain. J Nutr 131:1584–1585.

Manghani DK, Dastur DK, Jeejeebhoy KN, Raghavendran KV. 1970. Effect of stable manganese on the fate of radiomanganese in the rat with special reference to the CNS. Indian J Med Res 58:209–215.

Manoonkitiwongsa PS, Whitter EF, Wareesangtip W, McMillan PJ, Nava PB, Schultz RL. 2000. Calcium-dependent ATPase unlike ecto-ATPase is located primarily on the luminal surface of brain endothelial cells. Histochem J 32:313–324.

Markesbery WR, Ehmann WD, Hossain TI, Alauddin M. 1984. Brain manganese concentrations in human aging and Alzheimer's disease. Neurotoxicology 5:49–57.

Martell AE, Smith RM. 1974–1982. Critical Stability Constants. Plenum Press, New York NY.

Mason MJ, Mayer B, Hymel LJ. 1993. Inhibition of Ca^{2+} transport pathways in thymic lymphocytes by econazole, miconazole, and SKF 96365. Am J Physiol Cell Physiol 264:C654–C662.

Masumoto K, Suita S, Taguchi T, Yamanouchi T, Nagano M, Ogita K, Nakamura M, Mihara F. 2001. Manganese intoxication during intermittent parenteral nutrition: Report of two cases. JPEN J Parenter Enteral Nutr 25:95–99.

Maynard E, Schultz RL, Pease DC. 1957. Electron microscopy of the vascular bed of rat cerebral cortex. Am J Anat 100:409–434.

Mena I, Horiuchi K, Burke K, Cotzias GC. 1969. Chronic manganese poisoning. Individual susceptibility and absorption of iron. Neurology 19:1000–1006.

Mena I, Marin O, Fuenzalida S, Cotzias GC. 1967. Chronic manganese poisoning. Clinical picture and manganese turnover. Neurology 17:128–136.

Mergler D, Baldwin M, Bélanger S, Larribe F, Beuter A, Bowler R, Panisset M, Edwards R, de Geoffroy A, Sassine M-P, Hudnell K. 1999. Manganese neurotoxicity, a continuum of dysfunction: Results from a community based study. Neurotoxicology 20:327–342.

Mergler D, Huel G, Bowler R, Iregren A, Bélanger S, Baldwin M, Tardif R, Smargiassi A, Martin L. 1994. Nervous system dysfunction among workers with long-term exposure to manganese. Environ Res 64:151–180.

Moore JW, Pearson RG. 1981. Kinetics and Mechanism, 3rd edition, p 304. Wiley & Sons, New York NY.

Mossmann T. 1983. Rapid colorimetric assay for cellular growth and survival: application to proliferation and cytotoxicity assays. J Immunol Methods 65:55–63.

Murakami H, Takanaga H, Matsuo H, Ohtani H, Sawada Y. 2000. Comparison of blood-brain barrier permeability in mice and rats using in situ brain perfusion technique. Am J Physiol Heart Circ Physiol 279:H1022–H1028.

Murphy VA, Wadhwani KC, Smith QR, Rapoport SI. 1991. Saturable transport of manganese(II) across the rat blood-brain barrier. J Neurochem 57:948–954.

Nagatomo S, Umehara F, Hanada K, Nobuhara Y, Takenaga S, Arimura K, Osame M. 1999. Manganese intoxication during total parenteral nutrition: Report of two cases and review of the literature. J Neurol Sci 162:102–105.

National Institute of Standards and Technology (US). 1995. NIST Critically Selected Stability Constants of Metal Complexes: Version 2.0 (database software). NIST, Gaithersburg MD.

National Research Council (US). 1996. Guide for the Care and Use of Laboratory Animals. National Academy Press, Washington DC.

Newland MC, Ceckler TL, Kordower JH, Weiss B. 1989. Visualizing manganese in the primate basal ganglia with magnetic resonance imaging. Exp Neurol 106:251–258.

Newman GC, Hospod FE, Patlak CS. 1990. Kinetic model of 2-deoxyglucose metabolism using brain slices. J Cereb Blood Flow Metab 10:510–526.

Ohno K, Pettigrew KD, Rapoport SI. 1978. Lower limits of cerebrovascular permeability to nonelectrolytes in the conscious rat. Am J Physiol Heart Circ Physiol 235:H299–H307.

Oldendorf WH, Pardridge WM, Braun LD, Crane PD. 1982. Measurement of cerebral glucose utilization using washout after carotid injection in the rat. J Neurochem 38:1413–1418.

Ono J, Harada K, Kodaka R, Sakurai K, Tajiri H, Takagi Y, Nagai T, Harada T, Nihei A, Okada A, Okada S. 1995. Manganese deposition in the brain during long-term total parenteral nutrition. JPEN J Parenter Enteral Nutr 19:310–312.

Pardridge WM. 1998. CNS drug design based on principles of blood-brain barrier transport. J Neurochem 70:1781–1792.

Pardridge WM. 2003. Blood-brain barrier drug targeting: The future of brain drug development. Mol Interv 3:90–105.

Patel N, Khayat ZA, Ruderman NB, Klip A. 2001. Dissociation of 5′ AMP-activated protein kinase activation and glucose uptake stimulation by mitochondrial uncoupling and hyperosmolar stress: differential sensitivities to intracellular Ca^{2+} and protein kinase C inhibition. Biochem Biophys Res Commun 285:1066–1070.

Pavlinova AV, Shnarevich AI. 1960. The composition and the stability of the citrate compound of manganese. Zhur Neorg Khim 5:2759–2763.

Paxinos G, Watson C. 1986. The Rat Brain in Stereotaxic Coordinates, 2nd edition. Academic Press, Orlando FL.

Petti L, Powell KJ. 1997. IUPAC Stability Constant Database [database on CD-ROM]. Academic Software, Yorks, United Kingdom. Information available from *www.acadsoft.co.uk/scdbase/scdbase.htm#acsoft*.

Picard V, Govoni G, Jabado N, Gros P. 2000. Nramp 2 (DCT1/DMT1) expressed at the plasma membrane transports iron and other divalent cations into a calcein-accessible cytoplasmic pool. J Biol Chem 275:35738–35745.

Poole RC, Halestrap AP, Price SJ, Levi AJ. 1989. The kinetics of transport of lactate and pyruvate into isolated cardiac myocytes from guinea pig. Kinetic evidence for the presence of a carrier distinct from that in erythrocytes and hepatocytes. Biochem J 264:409–418.

Poole RC, Halestrap AP. 1993. Transport of lactate and other monocarboxylates across mammalian plasma membranes. Am J Physiol Cell Physiol 264:C761–C782.

Price NT, Jackson VN, Halestrap AP. 1998. Cloning and sequencing of four new mammalian monocarboxylate transporter (MCT) homologues confirms the existence of a transporter family with an ancient past. Biochem J 329:321–328.

Rabin O, Hegedus L, Bourre J-M, Smith QR. 1993. Rapid brain uptake of manganese(II) across the blood-brain barrier. J Neurochem 61:509–517.

Roels H, Lauwerys R, Buchet JP, Genet P, Sarhan MJ, Hanotiau I, de Fays M, Bernard A, Stanescu D. 1987. Epidemiological survey among workers exposed to manganese: effects on lung, central nervous system, and some biological indices. Am J Ind Med 11:307–327.

Roels HA, Ghyselen P, Buchet JP, Ceulemans E, Lauwerys RR. 1992. Assessment of the permissible exposure level to

manganese in workers exposed to manganese dioxide dust. Br J Ind Med 49:25–34.

Roos JTH, Williams DR. 1977. Formation constants for citrate-, folic acid-, gluconate-, and succinate-proton, -manganese(II), and -zinc(II) systems: Relevance to absorption of dietary manganese, zinc and iron. J Inorg Nucl Chem 39:367–369.

Rosenberg SO, Fadil T, Schuster VL. 1993. A basolateral lactate/H^+ co-transporter in Madin-Darby Canine Kidney (MDCK) cells. Biochem J 289:263–268.

Rowland M, Tozer TN. 1995. Clinical Pharmacokinetics: Concepts and Applications, 3rd edition. Williams & Wilkins Co, Baltimore MD.

Sandström B, Davidsson L, Cederblad A, Eriksson R, Lonnerdal B. 1986. Manganese absorption and metabolism in man. Acta Pharmacol Toxicol 59(Suppl 7):60–62.

Savchenko VL, McKanna JA, Nikonenko IR, Skibo GG. 2000. Microglia and astrocytes in the adult rat brain: Comparative immunocytochemical analysis demonstrates the efficacy of lipocortin 1 immunoreactivity. Neuroscience 96:195–203.

Scheuhammer AM, Cherian MG. 1985. Binding of manganese in human and rat plasma. Biochim Biophys Acta 840:163–169.

Schnarevich AI. 1963. Structure of manganese(II) citrate. Zhur Neorg Khim 8:2074–2079.

Schramm VL, Brandt M. 1986. The manganese(II) economy of rat hepatocytes. Fed Proc 45:2817–2820.

Schuler P, Oyanguren H, Maturana V, Valenzuela A, Cruz E, Plaza V, Schmidt E, Haddad R. 1957. Manganese poisoning: Environmental and medical study at a Chilean mine. Ind Med Surg 26:167–173.

Shinoda K, Mitsumori K, Uneyama C, Uchara M. 2000. Induction and inhibition of testicular germ cell apoptosis by fluoroacetate in rats. Arch Toxicol 74:33–39.

Simpson RJ, Peters TJ. 1985. Fe^{2+} uptake by intestinal brush-border membrane vesicles from normal and hypoxic mice. Biochim Biophys Acta 814:381–388.

Sjögren B, Gustavsson P, Hogstedt C. 1990. Neuropsychiatric symptoms among welders exposed to neurotoxic metals. Br J Ind Med 47:704–707.

Sjögren B, Iregren A, Frech W, Hagman M, Johansson L, Tesarz M, Wennberg A. 1996. Effects on the nervous system among welders exposed to aluminium and manganese. Occup Environ Med 53:32–40.

Smith QR. 1989. Quantitation of blood-brain barrier permeation. In: Implications of the Blood-Brain Barrier and its Manipulation (Neuwelt EA, ed), pp 85–118. Plenum Medical Book Co, New York NY.

Smith QR. 1990. Regulation of metal uptake and distribution within the brain. In: Nutrition and the Brain. Vol 8, Choline Metabolism and Brain Function (Wurtman RJ, Wurtman JJ, eds), pp 25–74. Raven Press, New York NY.

Smith QR. 1996. Brain perfusion systems for studies of drug uptake and metabolism in the central nervous system. Pharm Biotechnol 8:285–307.

Song J, Kwon O, Chen S, Daruwala R, Eck P, Park JB, Levine M. 2002. Flavonoid inhibition of sodium-dependent vitamin C transporter 1 (SVCT1) and glucose transporter isoform 2 (GLUT2), intestinal transporters for vitamin C and glucose. J Biol Chem 277:15252–15260.

Sugawara N, Li D, Sugawara C. 1994. Biliary excretion of exogenous cadmium and manganese in Long-Evans Cinnamon (LEC) rats characterized by an inherently gross amount of copper-metallothionein in the liver. Arch Toxicol 68:520–523.

Takasato Y, Rapoport SI, Smith QR. 1984. An in situ brain perfusion technique to study cerebrovascular transport in the rat. Am J Physiol Heart Circ Physiol 247:H484–H493.

Takasawa K, Terasaki T, Suzuki H, Sugiyama Y. 1997. *In vivo* evidence for carrier-mediated efflux transport of 3′-azido-3′-deoxythymidine and 2′,3′-dideoxyinosine across the blood-brain barrier *via* a probenecid-sensitive transport system. J Pharmacol Exp Ther 281:369–375.

Takeda A, Ishiwatari S, Okada S. 2000. Influence of transferrin on manganese uptake in rat brain. J Neurosci Res 59:542–552.

Takeda A, Sawashita J, Okada S. 1995. Biological half-lives of zinc and manganese in rat brain. Brain Res 695:53–58.

Takeda A. 2003. Manganese action in brain function. Brain Res Brain Res Rev 41:79–87.

Tiffert T, Lew VL. 2001. Kinetics of inhibition of the plasma membrane calcium pump by vanadate in intact human red cells. Cell Calcium 30:337–342.

Trapp GA. 1983. Plasma aluminum is bound to transferrin. Life Sci 33:311–316.

Triguero D, Buciak J, Pardridge WM. 1990. Capillary depletion method for quantification of blood-brain barrier transport of circulating peptides and plasma proteins. J Neurochem 54:1882–1888.

Verity MA. 1999. Manganese neurotoxicity: A mechanistic hypothesis. Neurotoxicology 20:489–497.

Virgintino D, Monaghan P, Robertson D, Errede M, Bertossi M, Ambrosi G, Roncali L. 1997. An immunohistochemical and morphometric study on astrocytes and microvasculature in the human cerebral cortex. Histochem J 29:655–660.

Vitarella D, Wong BA, Moss OR, Dorman DC. 2000. Pharmacokinetics of inhaled manganese phosphate in male Sprague-Dawley rats following subacute (14-day) exposure. Toxicol Appl Pharmacol 163:279–285.

Wadhwani KC, Murphy VA, Smith QR, Rapoport SI. 1992. Saturable transport of manganese(II) across blood-nerve barrier of rat peripheral nerve. Am J Physiol Regul Integr Comp Physiol 262:R284–R288.

Weber SJ, Abbruscato TJ, Brownson EA, Lipkowski AW, Polt R, Misicka A, Haaseth RC, Bartosz H, Hruby VJ, Davis TP. 1993. Assessment of an in vitro blood-brain barrier model using several [Met5]enkephalin opioid analogs. J Pharmacol Exp Ther 266:1649–1655.

Wedler FC, Denman RB. 1984. Glutamine synthetase: The major Mn(II) enzyme in mammalian brain. Curr Top Cell Regul 24:153–169.

Wedler FC, Ley BW, Grippo AA. 1989. Manganese(II) dynamics and distribution in glial cells cultured from chick cerebral cortex. Neurochem Res 14:1129–1135.

Wolff J. 1963. Contributions to the ultrastructure of the capillaries in the normal cerebral cortex. Z Zellforsch 60:409–431.

Wong J, Deutsch SE, Colemnares CA, Reynolds JG, Roos JW, Smith IL, Fort BF. 1997. Manganese particulates from vehicles using MMT fuel. Abstract presented at the 15th International Neurotoxicology Conference, Little Rock AR, October 26–29, 1997.

Yamakami J, Sakurai E, Sakurada T, Maeda K, Hikichi N. 1998. Stereoselective blood-brain barrier transport of histidine in rats. Brain Res 812:105–112.

Yokel R, Wilson M, Harris W, Halestrap A. 2002. Aluminum citrate uptake by immortalized brain endothelial cells: Implications for its blood-brain barrier transport. Brain Res 930:101–110.

Yokel RA, Kostenbauder HB. 1987. Assessment of potential aluminum chelators in an octanol/aqueous system and in the aluminum-loaded rabbit. Toxicol Appl Pharmacol 91:281–294.

Yokel RA. 2001. Aluminum toxicokinetics at the blood-brain barrier. In: Aluminium and Alzheimer's Disease: The Science That Describes the Link (Exley C, ed), pp 233–260. Elsevier Science Publishing Co, New York NY.

Zayed J, Vyskocil A, Kennedy G. 1999. Environmental contamination and human exposure to manganese – Contribution of methylcyclopentadienyl manganese tricarbonyl in unleaded gasoline. Int Arch Occup Environ Health 72:7–13.

Zhang Y, Liu GQ, Liu XD, Xiao XQ. 1999. Efflux transport of [^{3}H]GABA across blood-brain barrier after cerebral ischemia-reperfusion in rats. Zhongguo Yao Li Xue Bao 20:223–226.

Zhang Y, Pardridge WM. 2001. Rapid transferrin efflux from brain to blood across the blood-brain barrier. J Neurochem 76:1597–1600.

Zheng W, Kim H, Zhao Q. 2000. Comparative toxicokinetics of manganese chloride and methylcyclopentadienyl manganese tricarbonyl (MMT) in Sprague-Dawley rats. Toxicol Sci 54:295–301.

Zheng W, Perry DF, Nelson DL, Aposhian HV. 1991. Choroid plexus protects cerebrospinal fluid against toxic metals. FASEB J 5:2188–2193.

Zheng W. 2001. Toxicology of choroid plexus: Special reference to metal-induced neurotoxicities. Microsc Res Tech 52:89–103.

APPENDIX A. TECHNICAL PROCEDURES

PREPARATION AND MEASUREMENT OF Mn

Mn Citrate

We prepared Mn citrate by conditions reported to produce a 1:1 complex of Mn citrate: that is, incubation of $^{54}MnCl_2$ or $^{55}MnCl_2$ with a 10% molar excess of Na_3 citrate for 1 hour at 37°C (Pavlinova and Shnarevich 1960; Schnarevich 1963). The citrate ion rapidly complexes with Mn. Near-infrared spectra of citric acid and Mn citrate we produced were compared by Dr Robert Lodder of the College of Pharmacy, University of Kentucky. Using sophisticated modeling he calculated the wavelengths of the near-infrared signal for the three OH groups of citric acid that are

predicted to interact with Mn to form Mn citrate (Figure A.1). Those OH groups are the central hydroxyl group and components of the two terminal carboxylates. He then analyzed the difference spectrum for citric acid versus Mn citrate. The attenuation at 1950, 2075, and 2300 nm suggested that Mn citrate preparation differed from the citrate at these positions (Figure A.1). These results imply interaction between Mn and citrate at those three positions.

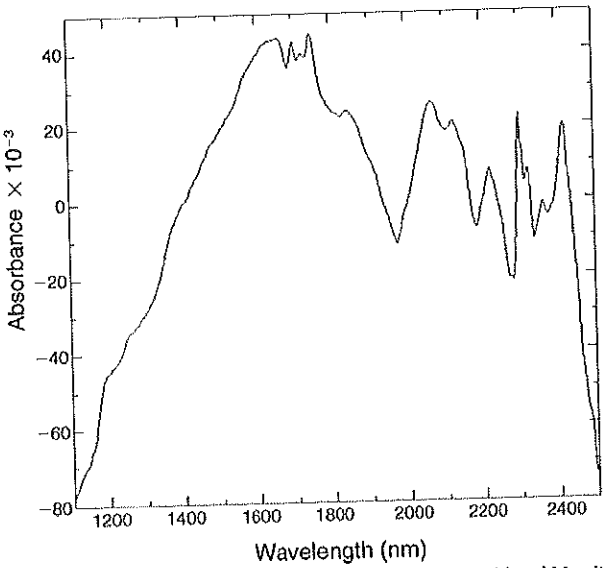

Figure A.1. Difference of near-infrared spectra of citric acid and Mn citrate, produced in an oxygen-containing environment. The spectral difference indicates the changes in functional groups of citrate due to its binding with Mn.

Mn Tf

Tf has two Mn binding sites. To maximize Mn binding to Tf, $^{54}MnCl_2$ or $^{55}MnCl_2$ and apo-Tf, in a ratio of Mn to metal-binding sites of 3:4, were incubated in 15 mM HCO_3^- for 1 hour at 37°C. Carbonate was introduced as $NaHCO_3$ because it was shown to be necessary to form the Tf metal complex (Trapp 1983). Evidence of Mn Tf complex formation included (1) increased UV absorbance at 300 nm after incubation and (2) reduction of the ability of Mn to pass through a membrane with a 10-kDa molecular weight cutoff, as follows.

Demonstration of Mn Tf Formation Carbonate has been shown to be necessary for the formation of Tf metal complexes in vitro. The UV absorbance increase of a Tf solution has been shown to indicate that Tf is binding the metal (Trapp 1983). Therefore an increase in the UV absorbance of Tf in the presence of Mn would be expected to confirm preparation of the Mn Tf complex. Two questions were addressed: (1) Is Mn Tf formed? and (2) What is the effect of increasing the HCO_3^- concentration above 15 mM? To demonstrate production of Mn Tf, combinations of 37.5 μM Mn, 25 μM Tf, and 15, 30, or 60 mM $NaHCO_3$ were introduced into a microcentrifuge tube at pH ~8.0 and incubated at 37°C for 1 hour (Table A.1). UV absorbance of these solutions was measured over the range of 240 to 400 nm. A characteristic Tf peak, in the absence of Mn, occurred at approximately 290 nm. In the presence of Tf and Mn and 15 mM HCO_3^-, UV absorbance increased with a peak at 300 nm (Figure A.2). Increasing the HCO_3^- concentration above 15 mM did not further increase absorbance (data not shown).

Table A.1. Conditions Tested to Confirm Mn Tf Complex Formation[a]

Trial	Mn	Tf	HCO_3^- (mM)
1	−	−	−
2	+	−	−
3	−	+	−
4	−	−	15
5	+	−	15
6	−	+	15
7	−	+	30
8	+	+	15
9	+	+	30
10	+	+	60

[a] Minus (−) denotes not included; plus (+), included. Mn included at 37.5 μM Mn^{2+} as $MnCl_2$; Tf included at 25 μM as human apotransferrin; and HCO_3^- = $NaHCO_3$.

Demonstration and Quantification of Mn Tf Formation The ability of Mn to pass through a filter was initially assessed using Amicon Centrifree devices that have membranes with a 30-kDa molecular weight cutoff. These devices enable quantification of the fractions of Mn that are bound to Tf (which will not pass through the membrane) and the unbound Mn (which appears in the ultrafiltrate). Three sets of duplicate devices were loaded with Tf in 15 mM HCO_3^-, Mn^{2+} as $MnCl_2$, or Mn Tf in 15 mM HCO_3^-. A sample of each loading solution was retained. The devices were centrifuged at 3000g for 5 minutes to generate the ultrafiltrate (liquid that had passed through the membrane). The ultrafiltrate and the loading solutions were analyzed to quantitate Mn. However, we did not find the devices to be satisfactory as we could not obtain mass balance of Mn. Evidently a significant fraction was adsorbing to the device.

To quantitate the fraction of Mn bound to Tf and determine the cause of Mn loss in the Centrifree devices, we utilized equilibrium dialysis. Equilibrium dialysis experiments were performed in a two-chambered Plexiglas apparatus.

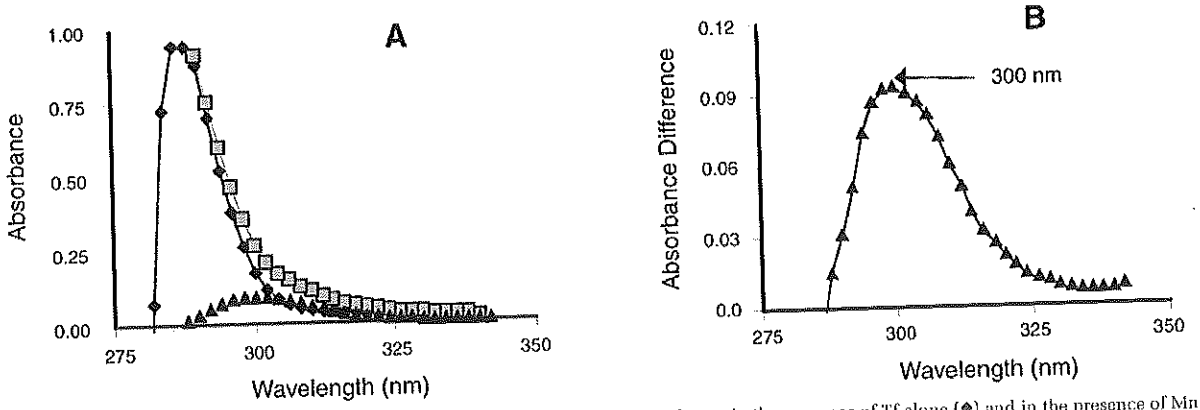

Figure A.2. Mn binding to Tf increased absorbance, with a peak at 300 nm. (A) Absorbance in the presence of Tf alone (◆) and in the presence of Mn, Tf, and 15 mM HCO_3^- (▨). The difference between the presence of both Mn and Tf versus Tf alone is shown as (▲) and in panel B. (B) The difference spectrum. Note a change in the y-axis scale compared to panel A.

The capacity of each chamber was 0.5 mL. A presoaked Spectrapore cellulose membrane, with a 10-kDa molecular weight cutoff, separated the two cells. Both chambers contained 0.3 mL of a buffer solution (4.5 mM K^+ as KCl, 145 mM Na^+ as NaCl, 15 mM HCO_3^-, at pH 7.4). In one chamber the solution also contained ^{55}Mn Tf solution, prepared as 37.5 µM Mn^{2+} (from $MnCl_2$) and 25 µM Tf, or Mn^{2+} alone. The solutions were incubated at 37°C. Mn concentration was determined in both compartments by ETAAS. The results indicated that 81% of the total ^{55}Mn was associated with Tf and 19% was not.

Mn Determination by ETAAS

The atomic absorption system consisted of an electrothermal atomic absorption spectrophotometer (Perkin Elmer 4100 AL) coupled to an AS-70 autosampler. Samples were diluted in a modifier containing 2.4 mM Pd, 6.2 mM Mg, and 0.2% HNO_3 prior to analysis at 279.5 nm.

IN SITU BRAIN PERFUSION TECHNIQUE

The unidirectional influx transfer coefficient (K_{in}) of Mn^{2+}, Mn citrate, and Mn Tf was determined using the in situ brain perfusion technique (Takasato et al 1984). To acquire this technique, the principal investigator visited the laboratories of Drs Smith and Allen and subsequently trained other personnel in his own laboratory.

Preparation of Perfusate for in Situ Studies

To minimize the formation of unwanted Mn complexes in the brain perfusate, an isotonic perfusion solution was prepared to contain the minimum number of anions. Chloride salts of the physiologically relevant cations (153 mM Na^+, 4.2 mM K^+, 1.5 mM Ca^{2+}, 0.9 mM Mg^{2+}) were used in the preparation of the fluid for in situ brain perfusion studies. The perfusate did not contain phosphate or carbonate, to avoid formation of Mn carbonates or phosphates, thereby maintaining Mn^{2+} as the free ion when introduced as $MnCl_2$. Mn citrate was produced by incubation of Mn with trisodium citrate in 10% molar excess. Mn Tf was introduced into the perfusion solution with the addition of 15 mM $NaHCO_3$, to ensure maintenance of the Mn Tf complex. $MnCl_2$, Mn citrate, and Mn Tf were administered as carrier-free ^{54}Mn, 5 µCi/mL (5 to 12 nM ^{54}Mn, with 8 to 4400 nM ^{55}Mn, depending on specific activity of each ^{54}Mn stock).

Perfusates also contained 1 µCi/mL ^{14}C-sucrose (0.2 µM) as a marker of the intravascular volume of the brain sampled and diffusion through the BBB. Sucrose does not appreciably diffuse from the cerebral vasculature across the intact BBB into the brain during the course of these studies (Takasato et al 1984). A significant increase of sucrose in brain samples indicated damage to the BBB. Results in such cases were not included in data analysis. This perfusate is not well buffered and is therefore very sensitive to pH changes. It was indicated that the BBB withstands variation in isosmotic perfusate composition as long as the pH remains between 7.0 and 7.5 (Smith 1996). Great care was taken to ensure the final pH was within this pH range prior to its use. Each solution was prepared by mixing salts, glucose, water, and radioisotopes (with citrate or Tf, as indicated). The solution was incubated at 37°C for at least 1 hour before bubbling 2 minutes with 5% CO_2 in air. The pH was adjusted to 7.4 ± 0.1, and the solution was returned to the 37°C water bath until being loaded into the syringe just before its use. Perfusates were prepared on the day of the experiment.

For the studies using in situ brain perfusion to further pursue the results of the bBMEC studies, the perfusate salt concentrations were changed to more closely model the

uptake media from the bBMEC studies. A buffer was used to maintain the solution pH. The perfusate contained the following components (concentration in mM): Na^+ (122), K^+ (4.2), Ca^{2+} (1.5), Mg^{2+} (0.9), Cl^- (131), HEPES (10), and glucose (10). $^{54}Mn^{2+}$ was present at approximately 1 μCi/mL (5 to 12 nM ^{54}Mn with a ^{55}Mn concentration of 360 nM).

RADIOACTIVITY ASSAYS

Tissue Preparation

The brain sections were weighed and γ radiation was counted for ^{54}Mn. We found that ScintiGest could not be used to solubilize the brain samples for ^{14}C determination because the volume required was prohibitively large. Therefore we used 10% piperidine and a biodegradable scintillation fluid (BioSafe II; Research Products International, Mount Prospect IL). A quench curve for ^{54}Mn was produced including the ratio of piperidine to scintillant that was used for the brain tissue. A quench curve for ^{14}C did not reveal any effect of piperidine on ^{14}C counts per minute (cpm). The brain tissue was dissolved in 10% piperidine at 55°C overnight. The samples were then diluted to approximately 1:10 v/v with biodegradable scintillation fluid and counted for ^{14}C determination in borosilicate glass vials. An aliquot of the injected solution was similarly analyzed.

^{54}Mn Determination

^{54}Mn was determined in brain tissue and perfusates using a γ counter (Packard model A5550:Minaxi Auto with a counting efficiency of 16.8% or Packard Cobra II model with a counting efficiency of 17.8%). Samples were counted for 2 minutes at 750 to 1090 keV. The peak energy for ^{54}Mn occurs at 838 keV.

^{14}C Determination

A quench curve to define the effects of 1% piperidine on ^{54}Mn counting in the window of 6 to 156 keV was determined in the LSC (Packard Tri-carb 2200 CA). Piperidine (10%) was used as the brain digestion medium, and a 1:10 dilution of the digestion medium was made with scintillation fluid. After LSC energy window optimization and quench curve construction, calculations that included factors for nuclide counting efficiencies indicated that a $^{54}Mn/^{14}C$ ratio of no more than 2:1 could be used to ensure that less than 10% of the counts within 6 to 156 keV in the LSC would be due to ^{54}Mn. This $^{54}Mn/^{14}C$ ratio is lower than those in published reports. It is unclear to us how other authors overcame this problem.

Optimization of Radioactivity Counting

In the LSC the ^{54}Mn produces a peak that overlaps with that of ^{14}C. To optimize counting conditions for ^{54}Mn and ^{14}C, we began with conditions in published reports. Unfortunately, these produced unacceptable ^{54}Mn interference to the LSC counting of ^{14}C. To minimize LSC interference, we constructed an optimization graph with increasing energy window size (Figure A.3). ^{54}Mn produced a signal in the β window from 0 to 12 keV, which overlapped the normal measurement of the ^{14}C signal (0 to 156 keV). The counting window of 6 to 156 keV was selected to minimize both the contribution of ^{54}Mn to the β counts (a contribution of 4.7% of the ^{54}Mn dpm to the ^{14}C dpm) and the reduction of ^{14}C activity due to the narrower β counting window (a loss of 13.2% of the total ^{14}C cpm). Therefore 6 to 156 keV was used for all LSC determinations of ^{14}C.

Brain tissue weighing up to 600 mg did not have a quenching effect on 50 nCi ^{54}Mn activity. Digested brain weighing 0 to 600 mg was found to quench linearly the ^{14}C signal, with 0.0524% cpm loss/mg brain. Efficiency of the LSC for the 0 to 156 keV ^{14}C window was 96.1% for the unquenched standards. Taken together, these produced a correction equation as follows:

$$^{14}C\ dpm = [(^{14}C\ cpm - 0.047 \times {}^{54}Mn\ dpm) \times (1 + 0.524 \times \text{brain wt [g]})] / [(1 - 0.132) \times (0.961)].$$

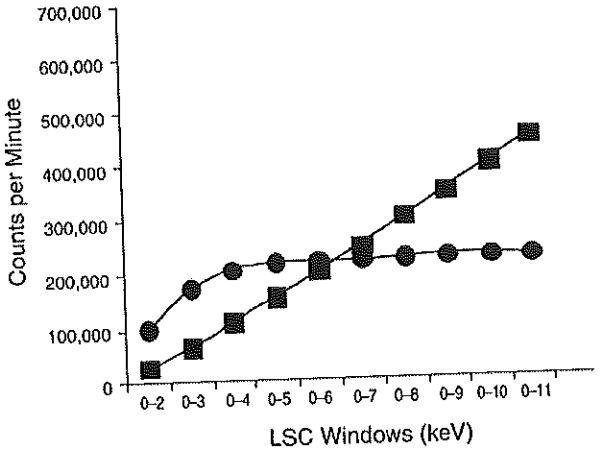

Figure A.3. Window energy optimization for liquid scintillation counter (LSC). ^{54}Mn produces Cerenkov radiation that overlaps with the LSC energy window for ^{14}C. Two replicates of ^{54}Mn (●) and ^{14}C-sucrose (■) were repeatedly counted at energies of 0–2 keV to 0–11 keV. Results are expressed in counts per minute.

This equation was used for all tissue samples. Perfusate sample results were analyzed using a similar equation without the correction for brain quenching.

CAPILLARY DEPLETION

In this technique, the brain is not dissected, but homogenized after in situ brain perfusion. We had to modify the published procedure to obtain a homogenized sample that would separate into the proper fractions during centrifugation. With the help of Dr David Allen, this technique was mastered. Briefly, the key technical points we employed are as follows:

1. Mince the brain, after removing the choroid plexus and meninges, into small cubes (about 1 mm) on a marble tile on ice.
2. Weigh the brain in the ice-cold homogenizer and add 3.5 mL of ice-cold buffer. Homogenize with 8 to 10 strokes in a 15-mL Tenbroeck tissue grinder (Wheaton Scientific, Milville NJ). The buffer contains the following (concentration in mM): NaCl (141), KCl (4), $CaCl_2$ (2.8), NaH_2PO_4 (1), $MgSO_4$ (1), glucose (10), and HEPES (10) at pH 7.4.
3. Do not push the pestle to the bottom of the homogenizer to directly mash the tissue. Rather, let the "shearing forces" pull the tissue up the sides of the homogenizer. The tissue is properly mashed as it passes between the pestle and the walls of the homogenizer.
4. Add dextran (70,000 g/mol) to a final concentration of 18% w/v and homogenize the solution with five additional strokes. This was found, by visual examination, to be the most effective method to separate the capillary cells.
5. Using the swinging bucket rotor (HS-4) in a Sorvall RC 28S at approximately 4°C, centrifuge the suspension for 15 minutes at 5400*g*.

After centrifugation, a thin dusting of cells and cell fragments migrates to the bottom of the tube in a layer approximately the thickness of a sheet of paper. The remaining liquid appears transparent, with a small layer of lipid-like material at the top.

Under microscopic examination, the pelleted cell fraction contains tubular cells and cell fragments that exist in straight or branching patterns. In discussion with Dr David Allen, we agreed that these are endothelial cells or cell fragments. This fraction also contains unidentified cellular debris not seen in the liquid fraction. This separation technique produced a 3-fold enrichment of alkaline phosphatase (EC 3.1.3.1) activity, a capillary-specific enzyme, in the capillary-enriched fraction (25 U/mg protein) using enzyme activity kit 104-L from Sigma (St Louis MO).

VALIDATION OF CEREBRAL MICROINJECTION TECHNIQUE FOR BRAIN EFFLUX INDEX STUDY

Cerebral microinjection of a visual marker into the targeted brain region, followed by rapid removal of the brain, was used for the brain efflux index study. To demonstrate our ability to perform this technique, Berlin blue dye was prepared in 0.9% saline and injected over 1 second into the left brain ($n = 2$) or right brain ($n = 2$) of rats that had been anesthetized with 75 mg/kg ketamine and 5 mg/kg xylazine. The solution was injected into the parietal lobe 0.2 mm anterior and 5.5 mm lateral from bregma and 4.5 mm below the skull surface. The 0.2 µL of injected solution was delivered from a 0.5-µL syringe (Hamilton series 7000, catalog no. 86257). The syringe was removed over 30 seconds, starting 1 minute after the injection. The rat was decapitated, and the brain removed, frozen and sectioned to visualize dye placement. The dye was in the target location in all 4 rats.

We also demonstrated our ability to reproducibly perform the intracerebral microinjection by injection of radionuclides into the brain. ^{54}Mn and ^{14}C-sucrose were dissolved at isosmotic concentration. An intracerebral microinjection of 0.2 µL was made into two anesthetized, male Sprague Dawley rats (250 to 300 g) at each of two times prior to termination on four different days. Brain samples were counted to quantitate ^{54}Mn and ^{14}C. Upon replication, the values were within 10% of each other. Data from these animals were not used in brain efflux index calculations.

PROCEDURES FOR USING bBMECs FROM BOVINE BRAINS

Validation of Isolation and Culture of bBMECs

To verify that the cells we isolated and grew were bBMECs, several measures were obtained, as follows.

Enzyme Activity The activities of selective enzymes (markers) of endothelial and glial cells were determined at two steps in the isolation procedure and in the cultured cells 8 to 10 days after plating. During isolation, aliquots were taken before and after the first enzymatic step. The enzyme activity results are shown in Table A.2. Alkaline phosphatase and γ-glutamyltransferase are positive markers for microvascular endothelial cells. 5'-Nucleotidase is a positive marker for glial cells. Determination of endothelial cell marker activity showed increasing activity during the subsequent steps of the bBMEC isolation. However, the

Table A.2. Enzyme Activity of Brain Homogenate, Partially Purified Homogenate, Freshly Isolated bBMECs, and 8- to 10-Day Cultures of Cell Isolates of Two Endothelial Cell Markers[a]

Cells	Total Protein (μg/mL)	γ-Glutamyltransferase (U/mg protein)	Alkaline Phosphatase (U/mg protein)
Brain homogenate	550–586	3–15	15–26
Partially purified homogenate	223–243	11–42	50–63
Freshly isolated bBMECs	—	35±4	460±90
Cultured cells	329–333	13–32	84–95

[a] Results are the range of two or three observations from one brain homogenate. For comparison, the means ± SEM of these enzymes, activities in freshly isolated cells, as previously reported (Johnson and Anderson 1996), are shown. 5′-Nucleotidase, a glial cell marker, was not detected in the partially purified or cultured cells and not determined in the other preparations.

activity in cultured cells was well below that found in fresh isolates (Johnson and Anderson 1996). This was probably due to the decrease in protein expression and activity that occur with the cell growth decreases after plating as cells approach confluence. The positive endothelial cell markers were still active in the cultures, and the negative marker could not be detected. These results suggest the cell cultures were probably endothelial cells.

Transmission Electron Microscopy TEM was completed at the University of Kentucky Medical Center Imaging Facility, under the direction of technicians Mary Gail Engle and Mary Jennes. The Medical Center Imaging Facility's protocol for fixing and staining cells was used. bBMECs from two dishes of 60% to 80% confluent cells were implanted into five beam capsules for TEM imaging. Twenty-four images were recorded from four of the capsules. Figure A.4 shows two images of the cultured cells. To interpret the images, we consulted with Dr Bruce Maley, director of the Medical Center Imaging Facility, who has experience with TEM images of neurons, astrocytes, and other glial cells. Although he rarely views images of endothelial cell cultures, he viewed all 24 images and concluded that perhaps only one cell was neuronal (Figure A.4, right

Figure A.4. Transmission electron micrographs of putative bBMECs in culture. Left panel: Confluent cells have close membranes and few spaces between them. In more highly magnified images, dense areas between cell membranes that could be tight junctions can be seen. Right panel: The one cell that may be neuronal noted in the 24 images examined.

panel). When viewed with TEM, neurons are large and round. They have very little cytoplasm and condensed nuclear material. Because neuronal cultures are notoriously difficult to establish, Dr Maley suggested that the much greater problem would be contamination of the cultures with glial cells, primarily astrocytes. Dr Maley found no evidence of glial cells, which have very dark cytoplasm and many ribosomes.

L-Histidine Uptake Assay An uptake assay of [^{3}H]L-histidine was conducted using confluent bBMECs. The results (Table A.3) were compared to published results of L-histidine uptake at concentrations of 10 and 100 µm (Yamakami et al 1998). Because we used radiolabeled L-histidine, we were able to study both a lower and a comparable concentration (0.1 and 250 µm) in the uptake media. Because the media concentrations were so different from those of Yamakami, all values were converted from a "volume-cleared" term to a "mass-cleared" term. Two uptake trials were completed. Previous results suggest at least two carrier systems (system N and system L) are involved in L-histidine transport. The difference between the values we obtained from the reported values may be due to the difference in affinity of these two systems at low L-histidine concentrations and differences between rat and bovine bBMECs.

Table A.3. L-Histidine Uptake into Confluent bBMECs[a]

	L-Histidine Concentration (µM)			
Trial (temp)	0.1	10	100	250
1 (29.5°C)	256 ± 0.5			
2 (30°C)	1185 ± 95			
3 (23°C)				569 ± 324
Published[b] (37°C)		1.25	8.3	

[a] Values are expressed in pmol L-histidine uptake/sec/mg cell protein. Values are the means ± SD of three observations.

[b] Yamakami et al 1998.

Procedures for Uptake Studies with bBMECs

1. Prepare uptake and wash media. Bring them to the temperature of the uptake study.
2. Wash cells three times with Mn-free uptake buffer at the study temperature. Leaving the third wash on the cells, maintain the cells at the study temperature for at least 10 minutes.
3. To initiate the uptake study, remove the wash medium. Wick the remaining solution away with absorbent paper brought in contact with the side of the cell culture dish, but not cells. Add the uptake medium containing the radiolabeled uptake test substances and MMT. Return dish to the correct temperature.
4. To terminate uptake, pour the uptake solution into a waste container and rinse the cells five times with ice-cold buffer without Mn. Remove the remaining liquid by capillary action using absorbent paper between each rinse.
5. After the final rinse and removal of remaining liquid, allow the cells to dry at room temperature. Subsequently add 0.75 mL sodium hydroxide (1 M) to each dish. After 15 minutes at room temperature, add equimolar HCl (0.75 mL) to each dish. Collect the cell lysate in a γ-counting tube for γ and LSC quantification of the uptake test substrates.
6. Determine formazan production. When formazan production is below 80% of control production, the cells are not considered to be viable and the results are not used. The study of metabolic inhibitors was an exception, however, as the objective was to induce metabolic inhibition.

GENOTYPING BELGRADE RATS

The homozygous (*b/b*, Belgrade) rats were distinguished from their heterozygous (*+/b*) littermates by their visual appearance. The *b/b* rats' eyes, ears, and tails were less pink. All visual impressions of genotype were supported by the differences in spleen weight relative to whole-body weight and by hematology values (Table A.4).

MATERIALS

$^{54}MnCl_2$ (specific activity, 28 to 7600 nCi/ng) in 0.1 to 0.5 M HCl was purchased from Perkin-Elmer/NEN (Boston MA) and Isotope Products Laboratories (Burbank CA). ^{14}C-Sucrose was purchased dry from NEN (3.6 nCi/nmol) and in 2% ethanol from Moravek (Brea CA; 495 nCi/nmol); [carboxyl-^{14}C]dextran and [^{3}H]L-histidine were purchased from Moravek. All other chemicals were purchased from Sigma unless otherwise noted.

APPENDIX B. CALCULATION OF Mn-LIGAND COMPLEX FORMATION RATE

The rate of water exchange for Mn^{2+} is approximately 10^7/sec; other ligands bind metals at rates within a factor of 10 of the water exchange rate (Cotton and Wilkinson 1980). Therefore the association rate for a new ligand binding to the Mn aquo ion, such as citrate, to form a metal chelate (Mn citrate), should be about 10^6/sec^{-1}. One can estimate the rate that Mn might exchange citrate for

Table A.4. Ratio of Spleen Weight to Body Weight and Hematology Values from Homozygous (*b/b*; Belgrade) Rats, Their Heterozygous (+/*b*) Littermates, and Wistar Control[a]

Rats	Spleen Wt/ Body Wt	RBC (10^6/mm^3)	HGB (g/dL)	HCT (%)	MCV (μm^3)
Homozygous ($n = 38$)	0.0056 ± 0.0003	2.07 ± 0.06	6.9 ± 0.3	8.5 ± 0.2	40.8 ± 0.4
Heterozygous ($n = 41$)	0.0022 ± 0.0001	6.76 ± 0.08	14.6 ± 0.1	38.8 ± 0.5	57.4 ± 0.4
Wistar controls ($n = 38$)	0.0024 ± 0.0001	6.48 ± 0.08	14.6 ± 0.1	39.3 ± 0.4	60.7 ± 0.4

[a] Values are presented as means ± SEM. RBC is red blood cells; HGB, hemoglobin; HCT, hematocrit; MCV, mean cell (corpuscular) volume. There is no overlap between the homozygous and heterozygous littermates for any variable except the spleen weight–body weight ratio of two heterozygous rats (0.0027 and 0.0046), which overlapped that of the homozygous rats.

another ligand as follows. The equilibrium constant (K_{eq}, log K) for a metal chelate is equal to the ratio of the metal association (binding) rate constant (K_{on}) to the metal dissociation rate constant (K_{off}).

$$K_{eq} = K_{on} / K_{off}$$

K_{on} is approximately 10^6/sec. One reported equilibrium constant for citrate is ~4 (Petti and Powell 1997). Therefore a dissociation rate (K_{off}) for Mn citrate can be calculated as

$$K_{eq} = 10^4 = 10^6 \text{ sec}^{-1} / K_{off}$$

or

$$K_{off} = 10^6 \text{ sec}^{-1} / 10^4 = 100 \text{ sec}^{-1}.$$

If one now considers a ligand exchange reaction,

$$Mn^{2+} L_1 + L_2 \underset{k_r}{\overset{k_f}{\rightleftarrows}} Mn^{2+} L_2 + L_1$$

assuming both ligands (L_1 and L_2) form complexes with comparable K_{eq} values (~10^4), then the equilibrium constant for this exchange reaction will be approximately 1, with $k_f = k_r = 100$/sec. The K_{eq} values for ligands present in blood plasma that have the strongest association with Mn (citrate, phosphate, histidine, albumin, cysteine, oxalate, and glutamate) are all approximately 10^3 to 10^4. The approach to equilibrium will be a first-order process with a rate constant equal to $k_f + k_r$ (Moore and Pearson 1981). For these Mn-ligand complexes, this is approximately 200/sec. This corresponds to a half-life of 3 msec. The complete reaction would occur in about 5 to 6 half-lives, or about 20 msec. Therefore equilibrium among the Mn^{2+} and Mn complexes with citrate, phosphate, histidine, albumin, cysteine, oxalate, glutamate, and Tf will occur within seconds.

APPENDIX AVAILABLE ON REQUEST

The following appendix is available from the Health Effects Institute. In your request, please provide the author name, full title and number of the report, and the title of the appendix you request.

Appendix C. Isolation of Bovine Brain Microvascular Endothelial Cells (bBMECs)

ABOUT THE AUTHORS

Robert A Yokel received his BS in pharmacy from the University of Wisconsin–Madison and his PhD in pharmacology from the University of Minnesota–Minneapolis. He completed postdoctoral study at Concordia University in Montreal. He was affiliated with the University of Cincinnati before joining the College of Pharmacy at the University of Kentucky in 1979, where he has advanced from assistant to associate to full professor. He has had a joint appointment in the Graduate Center for Toxicology at the University of Kentucky since joining the University of Kentucky. The major emphasis of his research at the University of Kentucky has been the toxicity and toxicokinetics of neurotoxic metals, particularly aluminum. A focus for over a decade has been distribution across the BBB.

Janelle S Crossgrove received her BA in chemistry from Hiram College and conducted much of this work as a doctoral candidate in toxicology. She completed her PhD in toxicology in 2003 and is currently a postdoctoral research associate at Purdue University. Her interests include formation of metal-ligand complexes and targeted movement of toxic complexes throughout an organism.

OTHER PUBLICATIONS RESULTING FROM THIS RESEARCH

Crossgrove JS, Allen DD, Bukaveckas BL, Rhineheimer SS, Yokel RA. 2003. Manganese distribution across the blood-brain barrier: I. Evidence for carrier-mediated influx of managanese citrate as well as manganese and manganese transferrin. Neurotoxicology 24:3–13.

Yokel RA, Crossgrove JS, Bukaveckas BL. 2003. Manganese distribution across the blood-brain barrier: II. Manganese efflux from the brain does not appear to be carrier mediated. Neurotoxicology 24:15–22.

Yokel RA. 2002. Brain uptake, retention and efflux of aluminum and manganese. Environ Health Perspect 110(Suppl 5):699–704.

Crossgrove JS, Yokel RA. Manganese distribution across the blood–brain barrier III. The divalent metal transporter-1 is not the major mechanism mediating brain manganese uptake. Neurotoxicology. In press (2004).

ABBREVIATIONS AND OTHER TERMS

ABC	ATP-binding cassette
ACGIH	American Conference of Governmental Industrial Hygienists
ANOVA	analysis of variance
ATP	adenosine triphosphate
ATPase	adenosine triphosphatase
ATSDR	Agency for Toxic Substances and Disease Registry (US)
BBB	blood–brain barrier
bBMEC	bovine brain microvascular endothelial cell
BEI	brain efflux index
Cl_s	clearance
cpm	counts per minute
DCT	divalent cation transporter
DMT	divalent metal transporter
dpm	disintegrations per minute
$D_{o/a}$	octanol/aqueous partitioning coefficient
EPA	Environmental Protection Agency (US)
ETAAS	electrothermal atomic absorption spectrometry
GABA	γ-aminobutyric acid
GLUT	glucose transporter
HCl	hydrochloric acid
HCO_3^-	bicarbonate
HEPES	4-(2-hydroxyethyl)-piperazine-1-ethane-sulfonic acid
IOM	Institute of Medicine (US)
K_{el}	apparent elimination rate constant
K_{eq}	equilibrium constant
K_{in}	influx transfer coefficient
K_m	Michaelis-Menten constant of saturable uptake
K_{off}	dissociation rate constant
K_{on}	association rate constant
K_{out}	efflux rate
LSC	liquid scintillation counter
MCT1	monocarboxylate transporter 1
MMT	methylcyclopentadienyl manganese tricarbonyl
$MnCl_2$	manganese chloride
MnO_2	manganese dioxide
MRP	multidrug-resistance-associated protein
MTT	methylthiazoletetrazolium
$NaHCO_3$	sodium bicarbonate
NIOSH	National Institute of Occupational Safety and Health (US)
Nramp	natural-resistance-associated macrophage protein
Oatp	organic anion transporter polypeptide
OSHA	Occupational Safety and Health Administration (US)
P	brain capillary permeability
$P_{diffusion}$	brain capillary diffusion permeability
Q	distribution volume (uptake space)
S	surface area
$t_{1/2}$	half-life
TEM	transmission electron microscopy
Tf	transferrin
TfR	transferrin receptor
V_{brain}	volume of distribution in brain
V_d	volume of distribution
V_{max}	maximum velocity
WHO	World Health Organization

COMMENTARY
Health Review Committee

HEI

INTRODUCTION

Metals comprise a large group of elements that can exist in several valence states and combine with other elements or compounds to form organic and inorganic compounds. Many metals are critical for living systems because they participate in essential biological functions. For example, iron is part of the hemoglobin molecule that binds oxygen; and copper, manganese, and zinc are part of several enzymes that catalyze chemical reactions in the body. Deficiencies of these essential metals result in adverse symptoms, such as anemia; however, at doses above what the body needs, the same metals can be toxic (eg, US Agency for Toxic Substances and Disease Registry [ATSDR*] 1994; 2000; 2002). Toxic effects vary among metals and may range from damage to the nervous system, heart, kidney, immune system, reproductive system, and fetus to gene damage and cancer.

Metal accumulation in the environment raises concern because metals are not biodegradable. Transition metals (eg, iron, nickel) associated with particulate matter have been implicated as possible active components in the adverse health effects associated with particulate matter exposure (Carter et al 1997; Dreher et al 1997). In addition, exposure to metals has been shown to cause neurologic damage—for instance, in children exposed to low levels of lead via ingestion (see Needleman 1993), and in workers exposed to moderate to high levels of manganese via inhalation (see Levy and Nassetta 2003). Currently, metals are used in a variety of ways in motor vehicles. Some of those uses (for example, in catalytic converters, brake pads, and fuel additives to reduce certain emissions and improve engine performance) can result in vehicle emissions containing metals as particles or particle components.

In February 1998 HEI held a workshop to define priorities for research to address the possible health effects of these metals emitted from motor vehicles and fuels. Much of the workshop focused on fuel additives containing cerium, iron, and manganese. Manganese is part of methylcyclopentadienyl manganese tricarbonyl (MMT), an antiknock agent that also reduces emissions of nitrogen oxides. MMT is currently used in Canada and parts of the United States. Following an earlier ban, MMT was approved for use in the United States by the US Environmental Protection Agency (EPA) in 1995, but further decisions about regulation are pending completion in 2004 of a series of emissions and toxicity tests. The Preface provides detailed information on the regulatory status of MMT in the United States.

After the 1998 workshop, HEI issued a Request for Preliminary Applications, RFPA 98-4, *Research on Metals Emitted by Motor Vehicles*. The goal of the RFPA was a broad-based investigation of metals that may be found in motor vehicle emissions, which ranged from characterizing emissions to investigating their health effects.

In response to RFPA 98-4, Dr Robert Yokel at the University of Kentucky submitted an application entitled "Manganese Toxicokinetics at the Blood–Brain Barrier." Yokel proposed to study the mechanisms by which manganese enters and leaves the brain across the blood–brain barrier. This barrier consists of the walls of small blood vessels in the brain and shields the brain from possible harmful molecules (see sidebar 1). Certain molecules may cross the blood–brain barrier via simple diffusion or carrier-mediated transport, which moves molecules at a faster rate than simple diffusion. Carrier-mediated transport includes facilitated diffusion, a process that requires no energy, and active transport, an energy-dependent process that can move molecules against a concentration gradient. Yokel proposed to study the rates of influx and efflux of three forms of manganese (manganese chloride [$MnCl_2$], Mn citrate, and Mn transferrin) using in vitro methods as well as in situ brain perfusion in rats. Yokel hypothesized that transporters (see sidebar 1) are involved in both influx and efflux of manganese. He proposed additional work to characterize and identify the putative carriers.

The HEI Research Committee thought Yokel's proposed study would provide valuable information on the mechanisms of transport of manganese across the blood–brain barrier. It would be the first study to specifically investigate manganese efflux from intact rat brain. Evidence for carrier-mediated transport of manganese out of the brain would be of particular interest because it would demonstrate a mechanism for preventing manganese accumulation and thus the potential for limiting the extent of neurotoxic damage during chronic exposure to Mn. The Committee also thought that the study would provide valuable information on the properties of manganese transporters.†

* A list of abbreviations and other terms appears at the end of the Investigators' Report.

This document has not been reviewed by public or private party institutions, including those that support the Health Effects Institute; therefore, it may not reflect the views of these parties, and no endorsements by them should be inferred.

† Dr Yokel's 3-year study, "Manganese Toxicokinetics at the Blood–Brain Barrier," began in August 1999. Total expenditures were $380,000. The draft Investigators' Report from Drs Yokel and Crossgrove was received for review in December 2002. A revised report, received in May 2003, was accepted for publication in June 2003. During the review process, the HEI Health Review Committee and the investigators had the opportunity to exchange comments and to clarify issues in the Investigators' Report and in the Review Committee's Commentary.

SIDEBAR 1. MOVEMENT ACROSS THE BLOOD–BRAIN BARRIER

The blood–brain barrier functionally separates the brain from the rest of the body, protecting the brain from potentially harmful substances that circulate in the blood. The barrier is formed by the walls of small blood vessels (capillaries) that deliver oxygen and glucose to the brain. The wall of capillaries in the brain consists of endothelial cells that differ from endothelial cells elsewhere in the body. For instance, brain capillary endothelial cells fuse together to form tight junctions that prevent molecules from passing between them. They also have many mitochondria, which provide energy for transport across the barrier of substances needed by the brain, such as glucose or metals.

The brain endothelial cells are surrounded by a basement membrane to which brain cells are attached. Specifically, the capillaries are covered by so-called foot processes from astrocytes, a type of brain cell that is not involved in relaying information but has a supportive role. Astrocytes, the most abundant type of brain cell, have many processes that connect to other brain cells. They are thought to be involved in guiding endothelial cells to form the blood–brain barrier during development. Other cells that are closely associated with the endothelial cells are pericytes, which also originate in the brain (similar to astrocytes) and have a clean-up function similar to that of macrophages.

Small lipophilic molecules may enter the brain by diffusion, which is a slow process. These molecules first pass through the luminal (blood side) wall of the endothelial cell, travel through the cytoplasm, and then pass through the abluminal (brain side) wall to enter the brain. Molecules that enter the brain at higher rates than by diffusion are transported through the action of large proteins spanning the membrane to form specific channels and transporters, also called carriers (see figure). For instance, D-glucose is effectively transported via a stereospecific glucose transporter that excludes the stereoisomer L-glucose.

Ion channels and transporters are complex proteins that stretch across both sides of a cell membrane. Ion channels usually have closed and open states. They are prompted to open their channel by an electrical, chemical, or mechanical stimulus. Channels provide passive transport in the form of facilitated diffusion, which does not require energy but is faster than simple diffusion. Among the several ion channels are the sodium and calcium channels, which selectively allow passage of Na^+ and Ca^{2+}, respectively.

Carriers transport molecules across a membrane either by facilitated diffusion or by active transport. Transporters are complex proteins that open only on one side of the membrane at a time and can transport molecules against their electrochemical potential gradient, which requires energy. Specific carriers have been identified for metals such as iron, an essential trace element.

Most areas of the brain are protected by the blood–brain barrier. Some leaky areas exist in the posterior pituitary and circumventricular organs. In the choroid plexus, which generates the cerebrospinal fluid that flows through the brain ventricles, the so-called blood–cerebrospinal fluid barrier provides the same protection as the blood–brain barrier in other parts of the brain.

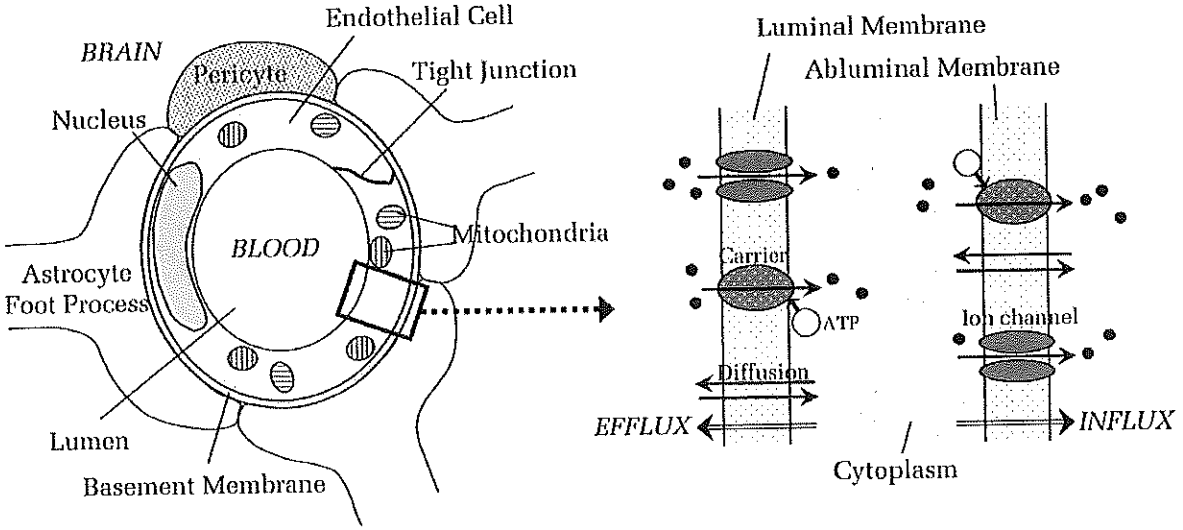

Blood vessels that form the blood–brain barrier. *Left panel:* This cross section shows the endothelial cells of the vessel wall bordered by a basement membrane, pericytes, and astrocyte foot processes. (Left panel adapted from Kandel et al 1991.) *Right panel:* Close-up of the barrier vessel wall, consisting of the inner (luminal) and outer (abluminal) endothelial cell membranes. Examples of ion channels and carriers are shown. Small black dots represent molecules that may be transported across the barrier by diffusion, facilitated diffusion, or active transport, which requires energy in the form of ATP. Although only carrier-mediated influx is shown, carriers may mediate both influx and efflux.

BACKGROUND

MANGANESE EXPOSURE

Manganese occurs naturally in the environment as a metal ore that is mined for production of steel, dry-cell batteries, matches, fireworks, and fertilizer. As an essential trace element, manganese is involved in numerous biological functions, including mammalian development and maintenance of the nervous system. It is part of several enzymes, such as glutamine synthetase, which is specific to the brain, and it is a cofactor for a number of other important enzymes (see Roth and Garrick 2003).

To maintain an optimal level of manganese in the body, the US Institute of Medicine (IOM) has identified Adequate Intake Levels of 1.8 and 2.3 mg/day for adult women and men, respectively, 1.2 to 1.9 mg/day for children, and 0.6 mg/day for infants (IOM 2003). In addition, the IOM has also established Tolerable Upper Intake Levels (UL), the highest levels at which no adverse effects have been observed. The UL for adults is 11 mg/day and for children 2-6 mg/day (IOM 2003). Ingesting consistently lower levels than recommended for daily intake causes manganese deficiency, which may result in failure of muscular coordination, impaired growth and skeletal abnormalities, impaired reproductive performance, and birth defects (ATSDR 2000; Roth and Garrick 2003).

Every day humans ingest manganese via food and drinking water. The amounts of manganese that humans ingest from drinking water are negligible. Mean levels of manganese in drinking water in the US and elsewhere have been found to range from 4 to 32 µg/L (US National Research Council 1980; World Health Organization [WHO] 1981; EPA 1984), although higher levels are occasionally present in well water.

In addition to dietary intake, humans may inhale particles that contain manganese. Exposure of the general population to low manganese concentrations in ambient air results from crustal material, industrial emissions, and combustion of fossil fuels. In urban and rural areas of the developed world that do not have significant pollution sources, annual average concentrations of manganese in the air are 0.01 to 0.07 µg/m^3 (WHO 2000). The daily intake of manganese from the air by the general population has been estimated to be less than 2 µg/day in areas without pollution sources; this level may increase to 10 µg/day in areas near pollution sources such as factories that process manganese (WHO 1981).

Although low levels of manganese are necessary for proper biological functioning, high levels may be harmful, as is evident from studies of miners and workers exposed to up to 450 mg/m^3 of inhaled manganese (EPA 1984). Since 1837, such workers have been known to develop severe neurotoxic symptoms similar to those of Parkinson disease (see Levy and Nassetta 2003). Because a much larger percentage of inhaled manganese is taken up into the body (compared with ingested manganese) and accumulates in the brain more readily, exposure via inhalation raises concern.

Use of the fuel additive MMT is likely to add small amounts of manganese to the ambient particulate matter mixture, mostly in the form of manganese oxides (MnO_2, Mn_3O_4), sulfate, and phosphate. Whether the presence of MMT in gasoline would increase the risk of manganese exposure to the general population is subject to considerable debate (Kaiser 2003). Several groups have suggested that this may be the case. Between 1981 and 1994 the manganese emission rate from autos was estimated to have increased 10% in Canada (Loranger and Zayed 1994), where use of MMT continues to date. Others have estimated that if MMT were used in all gasoline in the United States, the level of manganese in urban air would increase by about 0.05 µg/m^3 above the current level of 0.01 to 0.07 µg/m^3 (Ter Haar et al 1975). The EPA has predicted that a substantial percentage of the population could be exposed to manganese particulate levels above 0.1 µg/m^3 if all gasoline contained MMT (EPA 1994).

To establish whether MMT use increased manganese concentrations in ambient air in areas of Canada where it was added to the gasoline supply, several studies were conducted. One study in Montreal reported higher manganese levels in dust (up to 0.05 µg/m^3) at sites of high traffic density compared with sites of lower traffic density (Loranger and Zayed 1994). Similarly, Pellizzari and colleagues (1999, 2001) found that the mean outdoor manganese concentration of $PM_{2.5}$ was slightly higher in Toronto (0.0097 µg/m^3), where MMT was being used, than in Indianapolis (0.0035 µg/m^3), where MMT was not being used. Although background levels of naturally occurring manganese could not be determined in Toronto, the concentration of manganese in particulate matter showed a gradient that decreased from areas with high traffic volume to areas with low traffic volume and further to indoor air. These data suggest that car emissions increased the level of manganese in ambient air initially, but that the effect was diminished by subsequent dilution. In addition, personal exposure levels to manganese in particulate matter for the general population in Toronto did not exceed 0.05 µg/m^3 (Clayton et al 1999). A separate analysis of the Toronto data suggested that other sources (such as tobacco smoke, crustal particles, and industrial sources) contributed to the personal exposure levels (Crump 2000). A risk assessment

conducted by Health Canada (Wood and Egyed 1994) concluded that addition of MMT to the Canadian gasoline supply had not substantially increased manganese levels in ambient air above previous levels resulting from industrial sources and motor vehicle sources other than tailpipe emissions (for example, brake wear). However, the EPA concluded that "to support an improved health risk characterization for MMT, further investigation is needed in the areas of health effects, emission characterization, and exposure analysis" (Davis 1998).

MANGANESE NEUROTOXICITY

Evidence that exposure to high levels of manganese led to neurotoxicity (manganism) was described as early as 1837 (Couper 1837). Most cases of manganism have been described in workers exposed to high levels (1–450 mg/m^3) of manganese via inhalation, although neurotoxic symptoms have also been observed in individuals exposed to high levels of manganese in drinking water (US Agency for Toxic Substances and Disease Registry 2000). Manganese neurotoxicity progresses from early reversible symptoms to an irreversible debilitating disease. The first stage is characterized by general weakness, lethargy, and emotional instability. Upon continued exposure, victims progress to the second stage, characterized by impaired memory and judgment, anxiety, and sometimes hallucinations, leading to what is sometimes called *manganese madness*. The final stage is characterized by muscular impairment with tremor, difficulty walking, and rigid facial expressions (Pal et al 1999; Levy and Nassetta 2003). Symptoms are progressive and may increase even after exposure ceases. The later stages of manganism have symptoms similar to those of Parkinson disease. Both diseases involve loss of function in the extrapyramidal motor system, particularly in the basal ganglia of the midbrain. However, Parkinson disease is caused by loss of dopaminergic function in the striatum, whereas manganism is thought to be associated with loss of function of the neighboring globus pallidus, which is rich in neurons containing the neurotransmitter γ-aminobutyric acid (Lucchini et al 2000). Evidence from manganese-exposed workers points to a cumulative mechanism of action. Several studies have found associations between indices of cumulative manganese exposure and neurobehavioral outcomes (Roels et al 1987, 1992; Lucchini et al 1995, 1999).

Evidence from occupational studies that have associated neurotoxic symptoms with manganese exposure has been used as a basis to determine guidelines for safe levels of ingested and inhaled manganese (summarized in the Commentary Table). The guidelines for inhaled manganese were based on studies that showed subtle neurologic effects—less than those associated with the first stage of manganism—in workers exposed to manganese at levels lower than the occupational guidelines (Roels et al 1987, 1992; Lucchini et al 1999). Further support was provided by studies of communities exposed to increased levels of manganese in ambient air from nearby factories: small but significant declines in the ability to perform certain tasks requiring motor coordination were observed in the general population (Hudnell 1999; Mergler et al 1999).

To avoid the adverse health effects of chronic exposure, ATSDR (2000) and EPA (2003) have recommended maximum levels for adults of 0.07 and 0.14 mg/kg/day for ingestion, and 0.04 and 0.05 $\mu g/m^3$ for inhalation, respectively. The WHO-recommended guideline for air quality in Europe is 0.15 $\mu g/m^3$ (WHO 2000). (These inhalation values translate into approximately 0.01 to 0.04 μg/kg/day for a 70-kg adult inhaling air at a ventilation rate of 20 m^3/day.) As is evident from these estimates, ingested and inhaled manganese pose substantially different risks for adverse symptoms.

MANGANESE UPTAKE AND METABOLISM

Manganese that enters the body via ingestion is absorbed through the small intestine; the majority is then eliminated on its first pass through the liver and excreted in bile. About 114 μg/day (3%) of the average 3.8 mg/day dietary manganese ingested by adults is actually absorbed (EPA 1984), and only a small fraction of ingested manganese enters the systemic circulation (Andersen et al 1999). The uptake process depends on the dose: higher uptake rates occur when levels of manganese available in the diet are low, and lower uptake rates when they are high. Levels of iron in the diet also play an important role in manganese uptake. Increased uptake of manganese has been observed in individuals with iron deficiency (Mena et al 1969), whereas uptake is decreased when iron is abundant in the diet (Diez-Ewald et al 1968). Iron deficiency is common in many developing countries and should be taken into account when assessing the risk of manganese exposure in those populations. Patients with impaired liver function are also at risk from increased manganese uptake (Krieger et al 1995).

When manganese is inhaled, it enters the circulation directly without first-pass elimination by the liver. Therefore, blood levels are substantially higher after inhalation of manganese than after ingesting similar doses (Andersen 1999). In addition, inhaled manganese can enter the brain directly via the olfactory bulb. The solubility of manganese also influences its uptake into the circulation: uptake rates are faster for highly water soluble forms, such as $MnCl_2$, than for less soluble forms, such as MnO_2 (Roels et al 1997). Serum levels in people who ingest normal levels of

Commentary Table. Daily Requirements and Exposure Guidelines Applicable to Manganese[a]

Agency/Description	Guideline	Source	Equivalent Dose[b]
Dietary Requirements			
IOM			
Adequate intake level	2.3 mg/day	IOM 2003	33 µg/kg/day
Tolerable upper intake level	11 mg/day	IOM 2003	157 µg/kg/day
Chronic Exposure			
EPA			
Reference concentration for chronic inhalation exposure[c]	0.05 µg/m^3	EPA 2003	0.014 µg/kg/day
Reference dose for chronic ingestion exposure[c]	0.14 mg/kg/day	EPA 2003	140 µg/kg/day
ATSDR			
Minimal risk level for chronic inhalation exposure	0.04 µg/m^3	ATSDR 2000	0.011 µg/kg/day
Provisional guidance value for chronic ingestion exposure	0.07 mg/kg/day	ATSDR 2000	70 µg/kg/day
WHO			
Air Quality Guideline for Europe, annual average	0.15 µg/m^3	WHO 2000	0.043 µg/kg/day
Occupational Exposure			
ACGIH			
Threshold limits (8-hr workday, time-weighted average[d])			
Manganese dust and compounds, as Mn	5 mg/m^3	ACGIH 2003	857 µg/kg/workday
MMT, as Mn	0.2 mg/m^3	ACGIH 2003	34 µg/kg/workday
Short-term exposure limit[e]			
Manganese fume	3 mg/m^3	ACGIH 2003	NA[f]
NIOSH			
Recommended exposure limit, time-weighted average[d]			
Manganese fume and compounds	1 mg/m^3	NIOSH 2003	171 µg/kg/workday
Short-term exposure limit			
Manganese fume and compounds	3 mg/m^3	NIOSH 2003	NA[f]
OSHA			
Permissible exposure limit (8-hr workday, ceiling values[e])			
Manganese fume and compounds, as Mn	5 mg/m^3	OSHA 1998	NA[f]
WHO			
Recommended exposure limit in workplace air[g]			
Respirable Mn particles (< 0.5 µm)	0.3 mg/m^3	WHO 1986	51 µg/kg/workday

[a] These guidelines are for chronic exposure of the general population via inhalation of ambient air or via ingestion of food and drinking water and for occupational exposure via inhalation. Several government agencies and the WHO have established guidelines according to the duration of exposure and the form of manganese to which workers may be exposed. The values established by OSHA are enforceable regulations; the other values are recommendations. Guidelines for chronic exposure are based on lifetime exposure (70 years); occupational guidelines are established for an 8-hour workday. Additional guidelines exist for levels of manganese in drinking water as well as guidelines issued by individual states (not shown).

[b] Approximate dose, corrected for body weight, which an adult would encounter when exposed to manganese at the guideline exposure levels for 24 hours or during an 8-hour workday. Calculations for chronic exposure are based on a body weight of 70 kg and on ventilation rates during sleeping (0.45 m^3/hour), sitting (0.54 m^3/hour), and light activity (1.5 m^3/hour), each for 8 hours/day, resulting in total ventilation of 20 m^3 air in 24 hours. For occupational exposures, a ventilation rate of 1.5 m^3/hour was used, resulting in total ventilation of 12 m^3 air during an 8-hour workday.

[c] Estimates of daily inhalation or ingestion exposures to the general population (including sensitive subgroups) that are likely to be without an appreciable risk of harmful effects during a lifetime.

[d] Recommended maximum concentration to which most workers can be exposed without adverse effect, based on an exposure concentration averaged over an 8-hour workday.

[e] Maximum concentration to which workers can be exposed for up to 15 minutes continually. No more than four such exposures are allowed per day, and there must be at least 60 minutes between periods.

[f] Not applicable.

manganese from the diet, but are not exposed otherwise, range from 0.6 to 1.0 µg/L (Greger et al 1990). Because of the variable background levels of manganese in the blood from dietary intake, attempts to establish biomarkers for exposure to inhaled manganese have been largely unsuccessful (Greger 1999; Apostoli et al 2000).

After manganese enters the blood, it is distributed to several tissues and organs. This process may take up to several days after it enters the body. Toxicokinetic studies in rats exposed to manganese via intratracheal instillation showed that maximum blood levels were reached after 30 minutes for $MnCl_2$ and after 168 hours for MnO_2 (Roels et al 1997). Systemic distribution occurs predominantly as manganese bound to transferrin (Davidsson et al 1989). Elimination of manganese varies by tissue. For example, the half-lives in brain and bone are longer than 50 days, compared with 10 to 15 days in other tissues, as determined in several animal species (Furchner et al 1966). In monkeys that inhaled radioactive manganese, levels in the head peaked after 40 to 50 days and elimination occurred slowly, with a half-life of 600 days (Newland et al 1987). In humans, whole-body retention half-lives were 13 to 37 days (ATSDR 2000). In chronically exposed workers, urinary manganese levels were reported to be higher than those in unexposed individuals (Roels et al 1987, 1992).

Studies in rats showed that intranasally instilled manganese accumulated in the olfactory bulb, and significant uptake by other brain regions peaked after 7 days (Tjälve et al 1996). A study in which $MnCl_2$ or MnO_2 was administered to rats intratracheally also found higher levels in the same brain areas (Roels et al 1997). Observations in humans (for example those with liver dysfunction) indicate that manganese preferentially accumulates in the basal ganglia, specifically in the globus pallidus and the substantia nigra (Hauser et al 1996; Lucchini et al 2000). The basal ganglia are a complex of brain nuclei that form the extrapyramidal motor system. They consist of the striatum (also called *caudate-putamen*), nucleus accumbens, globus pallidus, and substantia nigra, among other areas. The mechanism by which manganese causes neuronal damage is only partly understood, although some studies reported loss of striatal dopamine and cell death in the globus pallidus (Pal et al 1999). Manganese is known to be taken up by mitochondria, the energy suppliers of cells (Liccione and Maines 1988). Excess levels of manganese in the brain may trigger neuronal death by interfering with the function of mitochondria (Gunter et al 2004; Malecki 2001).

On the basis of these observations, several studies have investigated the mechanism by which manganese enters the brain. Two general pathways have been identified in rats. One is a direct pathway in which inhaled manganese travels via the nose into the olfactory bulb and farther into the brain, bypassing the protective mechanism of the blood–brain barrier (Tjälve et al 1996; Roels et al 1997; Vitarella et al 2000; Dorman et al 2002). The other pathway involves carrier-mediated transport across the blood–brain barrier via specific carrier molecules. Prior to the current study, carrier-mediated transport of manganese into the rat brain had been demonstrated, but specific carriers had not yet been identified and the forms of manganese transported had not been firmly established (Aschner et al 1999; Malecki et al 1999). In addition, evidence that manganese accumulates in the brain prompted a need to investigate mechanisms of its elimination from the brain. The current study by Yokel and Crossgrove addressed these issues by evaluating both brain influx and brain efflux of manganese and by attempting to identify putative transporters.

TECHNICAL EVALUATION

AIMS AND OBJECTIVES

This study aimed at investigating whether transport of manganese across the blood–brain barrier (see sidebar 1) occurs via diffusion or via a transport mechanism using specific carriers. The first objective was to investigate transport of manganese into the brain (influx) to determine whether mechanisms other than simple diffusion deliver this essential trace element to the brain. The second objective was to investigate transport of manganese out of the brain (efflux) to determine whether similar mechanisms exist to remove it from the brain. Further studies were aimed at characterizing and possibly identifying the carriers involved in manganese transport across the blood–brain barrier.

STUDY DESIGN

The investigators evaluated the transport of three chemical forms (species) of manganese: (1) divalent manganese ion (Mn^{2+}) in the form of $MnCl_2$, representing all the soluble forms of manganese such as manganese phosphate and manganese sulfate that release the Mn ion on dissolution; (2) Mn citrate, a small complex molecule containing divalent manganese; and (3) Mn transferrin, a complex of divalent or trivalent (Mn^{3+}) manganese bound to a large protein found in the circulation. These three species are common forms of manganese present in the body and are readily formed from other forms of manganese (eg, phosphate, sulfate) that may be present in inhaled particles. Because of their differences in size and chemical structure,

different transport mechanisms are thought to exist for these species. These mechanisms may operate in parallel.

Preliminary Studies

Several preliminary studies were conducted to assess the lipid solubility of these three manganese species in order to calculate the rate of diffusion across the blood–brain barrier. Lipid solubility was assessed by the partitioning of manganese between octanol and water. The investigators subsequently determined the toxicokinetics of manganese in rat blood after intravenously injecting $MnCl_2$ and Mn citrate. They measured the concentration of manganese in blood over time after injection. Further, the investigators used microdialysis in rats (see sidebar 2) to assess unbound manganese (ie, Mn^{2+}) in brain extracellular fluid and blood as evidence for transport of manganese across the blood–brain barrier after intravenous injection of $MnCl_2$ and Mn citrate.

Assessing Manganese Influx

The investigators used in situ brain perfusion (see sidebar 2) to assess influx of the three manganese species into the brain. In these experiments, they used the radioisotope ^{54}Mn, which allowed them to differentiate between the administered manganese and the naturally occurring isotope ^{55}Mn present in the body. In situ brain perfusion allowed use of lower manganese concentrations and faster sampling than the microdialysis technique, resulting in better control over the manganese species. (During the 20-minute microdialysis sampling period, manganese would be able to respeciate into different forms.) ^{14}C-labeled sucrose was used as a control substance because it crosses the blood–brain barrier poorly. If the measured transport rate of a manganese species was higher than its estimated diffusion rate, this would provide evidence for carrier-mediated influx into the brain. Because the brain tissue collected after the in situ brain perfusion also contained cells from the blood capillaries forming the blood–brain barrier, capillary tissue was removed before estimating the concentration of manganese in brain tissue. Assays to measure ^{54}Mn content were conducted in nine specific brain areas—frontal cortex, parietal cortex, occipital cortex, cerebellum, caudate, hippocampus, thalamus/hypothalamus, midbrain/colliculus, and pons/medulla—and in the choroid plexus.

Assessing Manganese Efflux

The investigators microinjected $^{54}Mn^{2+}$ and ^{54}Mn citrate into the brain of anesthetized rats. Radiolabeled sucrose or dextran was coinjected as a control. Rats were decapitated at several time points (up to 240 minutes) after microinjection, and the brains were dissected and analyzed for ^{54}Mn content. The investigators calculated the brain efflux index (BEI) as the percentage of injected manganese that had crossed the blood–brain barrier into the blood. The amount of manganese injected was then compared with the amount remaining in the brain (ie, 100−BEI[%]), relative to the amount of ^{14}C-sucrose injected and the amount of sucrose remaining in the brain.

Characterizing Putative Manganese Transporters

The investigators used three types of cells to investigate characteristics such as pH and calcium dependence of the putative manganese transporters. Because Mn^{2+} is similar in size and charge to calcium (Ca^{2+}) and ferrous iron (Fe^{2+}), the investigators hypothesized that existing transporters for calcium and iron might also be involved in transporting manganese. They focused on investigating several known transporters and subsequently expanded their findings by using the in situ perfusion method in Sprague Dawley, Wistar, and Belgrade rats. Homozygous Belgrade *b/b* rats lack the functional divalent metal transporter 1 (DMT-1); their heterozygous *b*/+ littermates do express DMT-1.

General Aspects of Manganese Uptake The investigators used primary cultures of bovine brain microvascular

SIDEBAR 2: BRAIN SAMPLING IN RATS

Several techniques are available to investigate transport across the blood–brain barrier in vivo. The technique of *microdialysis* uses a small probe that is inserted into a specific brain area. The probe is a double-walled metal tube with a semipermeable membrane at the tip, which is implanted into the brain of an anesthetized animal. Fluid (called *dialysate*) circulates through the probe. The dialysate is an isotonic solution resembling the extracellular fluid surrounding brain cells. Molecules are exchanged at the probe tip via diffusion across the membrane. The dialysate, together with any molecules that diffused from the brain tissue into the probe, is then collected in vials for chemical analysis. The sample collection period is usually 20 minutes but may be shorter (5 or 10 minutes), depending on the type of study and the concentration of the substance of interest. Microdialysis can thus be used to measure concentrations of a substance in the brain over a period of several hours. Substances of interest may be endogenous to the brain (eg, neurotransmitters) or may have been introduced to the body (eg, drugs, nutrients, or in this study, manganese). The technique can also be used to sample substances in a blood vessel and in many other tissues and fluids.

In situ brain perfusion uses a small catheter (plastic tube) that is placed into an artery close to the brain, such as the carotid artery. The catheter is inserted while the animal is under anesthesia, and an isotonic fluid resembling blood plasma (called *perfusate*), together with the substance of interest, is administered into the artery using a syringe. The animal's chest cavity is exposed and the heart ventricles are cut open to allow excess blood to drain out of the animal. After completion of the perfusion (between 30 and 180 seconds), the animal is decapitated and the brain is removed. Sections of the brain may then be analyzed for the substance of interest, providing evidence that the substance moved across the blood–brain barrier. This technique is less precise than microdialysis in terms of the location of the brain that is sampled but allows much shorter sampling times.

endothelial cells (bBMECs), a model of the blood–brain barrier, to assess the time course of $^{54}Mn^{2+}$ uptake and the proton or sodium and energy dependence of the carrier. bBMECs are purified from cow brains and grown on a collagen matrix until the cells are confluent. These cultures are relatively pure, consisting of endothelial cells without the pericytes and astrocytes that are associated with the blood–brain barrier (see sidebar 1). They have several characteristics of the blood–brain barrier in vivo; for instance, similar to cells forming the blood–brain barrier, the cells line up on the matrix to provide polarity and unidirectional transport. However, bBMECs do not form tight junctions as well as the cells of the blood–brain barrier do.

Cell cultures were bathed for 10 to 120 minutes in medium containing $^{54}Mn^{2+}$ as well as ^{55}Mn and ^{14}C-sucrose. Cells were then lysed, and the ^{54}Mn and ^{14}C content was determined. Cell viability was also assessed. The investigators first determined the time course of Mn uptake and chose 30 minutes as the incubation period for subsequent experiments. To test whether the putative manganese carrier was proton (H^+) dependent, they determined the effect of pH on manganese uptake, using buffered sulfonic acids with pH values of 6.4 to 7.9. To test whether the carrier was sodium dependent, they replaced sodium in the medium with choline or lithium. Subsequently, they tested whether the manganese carrier was energy dependent. Energy for active transport of manganese across the blood–brain barrier may be provided by adenosine triphosphate (ATP) hydrolysis or movement of electrons. The investigators used several inhibitors of these energy pathways, such as 2,4-dinitrophenol, azide, and 2-deoxyglucose.

Uptake of Manganese Citrate The investigators first used rat erythrocytes, which express two transporters, a monocarboxylate transporter and an anion exchanger. The investigators hypothesized that these transporters would transport Mn citrate, because they are known to transport lactate and pyruvate across the cell surface into the cell. Manganese uptake into the erythrocytes was determined by bathing the cells in ^{14}C-citrate or ^{14}C-Mn citrate.

Subsequently the investigators used b.End5 cells, an immortalized cell line established from murine brain endothelial cells. They determined the time course and pH dependence of Mn citrate uptake into these cells. The cells were bathed for 15 to 240 minutes in ^{14}C-citrate, ^{14}C-Mn citrate, or ^{14}C-Al citrate in media at pH 6.9 or 7.4.

Involvement of Different Transporters *Iron* The investigators hypothesized that manganese may be transported by the same carrier as ferrous iron (Fe^{2+}), a metal ion with similar charge and size. To test whether iron could compete for manganese at the transporter, perfusate containing $^{54}Mn^{2+}$ and ferrous sulfate ($FeSO_4$) was administered via in situ perfusion to the brain of Sprague Dawley rats.

Divalent Metals To test the involvement of DMT-1 in manganese transport into the brain, the investigators used Belgrade b/b rats, which do not express a functional form of the DMT-1 transporter. They measured manganese uptake in b/b versus b/+ Belgrade rats as well as control Wistar rats. ^{54}Mn was administered to the brain as Mn^{2+} or Mn transferrin using in situ perfusion for a duration of 90 seconds; ^{14}C-sucrose was added as a control.

Calcium Because Mn^{2+} has the same charge and relative size as calcium (Ca^{2+}), the investigators hypothesized that calcium transporters may also be involved in manganese transport. They investigated Ca^{2+}-ATPase, a plasma membrane calcium pump. They used several pharmacologic approaches involving inhibitors of the calcium pump and of calcium influx as well as agents that deplete intracellular calcium stores. Complementing these in vitro experiments, the investigators tested the involvement of Ca^{2+}-ATPase in Sprague Dawley rats via in situ perfusion by adding the same inhibitors to the perfusate.

SUMMARY OF RESULTS

Diffusion Versus Carrier-Mediated Transport

The investigators determined that the calculated diffusion rates of the three manganese species, Mn^{2+}, Mn citrate, and Mn transferrin, were between 1.5 and 2.8×10^{-5} mL/sec/g brain tissue. These values were compared to values determined in subsequent in vitro and in vivo experiments. In experiments to assess manganese uptake via microdialysis, the investigators found that manganese entered the brain rapidly, having reached equilibrium by the time the first dialysate sample was collected after 20 minutes.

Manganese Influx

The investigators found that the rate of manganese influx as determined by in situ perfusion was higher than that observed for diffusion in at least one brain area for each manganese species. Uptake of Mn^{2+} was significantly higher in the parietal cortex and hippocampus and ranged from 5 to 13×10^{-5} mL/sec/g brain tissue for all nine brain regions examined. Uptake of Mn transferrin was significantly higher in the midbrain/colliculus and ranged from 2 to 13×10^{-5} mL/sec/g brain tissue. Uptake of Mn citrate was increased in the frontal cortex, parietal cortex, occipital cortex, cerebellum, caudate, and thalamus/hypothalamus. Uptake rates for Mn citrate ranged from 3 to 51×10^{-5} mL/sec/g brain

and were significantly higher than rates for Mn^{2+} and Mn transferrin in all brain regions except the hippocampus and midbrain. The investigators found that manganese uptake was associated mostly with the brain tissue and fluid rather than the brain capillaries. They interpreted these results to indicate that transport of manganese is carrier mediated and that of the three species tested, Mn citrate is most rapidly taken up by the brain.

Most evidence in these studies supported the hypothesis that uptake is carrier mediated, by either facilitated diffusion or active transport. The investigators found that adding Mn^{2+} to the perfusate reduced Mn^{2+} uptake; similarly, adding Mn citrate reduced Mn citrate uptake. These data support the involvement of carrier mechanisms although the effects did not depend on concentration and perfusate flow rates did not affect uptake. When the investigators modeled the uptake over time using Michaelis-Menten kinetics, they determined that a facilitated transport diffusion plus simple diffusion model provided the best fit for most brain areas. In some areas, a simple diffusion model provided the best fit. The caudate region was the only region where both Mn^{2+} and Mn citrate uptake were modeled best by the single carrier (facilitated diffusion) model. Together, these results provide evidence for carrier-mediated uptake of manganese in several brain regions.

Manganese Efflux

Experiments determining Mn^{2+} and Mn citrate efflux from the brain revealed a slight accumulation of manganese in the parietal cortex over time compared to sucrose or dextran. The investigators reported that the rate of manganese transport out of the brain was slower than that of sucrose or dextran (ie, less than 5×10^{-5} mL/sec/g brain tissue), suggesting that this process occurred via simple diffusion rather than via transporters.

Putative Manganese Transporters

The remainder of the project was devoted to characterization of and attempts to identify the manganese transporters. First, intracellular concentrations of manganese in bBMECs were found to be 10-fold higher than manganese concentrations in the solution, providing further evidence for carrier-mediated uptake. In general, Mn^{2+} uptake in bBMECs was found to be pH dependent, but not sodium or energy dependent.

The investigators reported that the metal transporters they investigated were unlikely to be involved in Mn^{2+} transport into the brain. They found that iron did not compete with Mn^{2+} for uptake, and that Mn^{2+} uptake in *b/b* Belgrade rats lacking a functional DMT-1 transporter was not different from that in *b/+* Belgrade or control Wistar rats in any of the nine brain regions examined. Results from experiments assessing transport of Mn citrate were mixed. On the one hand, the investigators found that citrate did not inhibit lactate uptake by erythrocytes, indicating that Mn citrate did not serve as a substrate for the monocarboxylate or anion exchange transporters. On the other hand, Mn citrate uptake was found to be pH and proton dependent in b.End5 cells, suggesting carrier-mediated Mn citrate uptake. In addition, in situ perfusion experiments in Sprague Dawley rats indicated that Mn citrate uptake was inhibited by quercetin, which inhibits monocarboxylate and several other transporters. Therefore, involvement of a monocarboxylate transporter in Mn citrate uptake cannot be fully ruled out.

The investigators found some evidence supporting the involvement of calcium channels: (1) inhibition of Mn^{2+} uptake by calcium channel inhibitors; (2) inhibition of manganese uptake by adding calcium to the medium; and (3) increased uptake after depletion of intracellular calcium stores. However, in situ perfusion experiments in Sprague Dawley rats showed contradictory results that indicated that calcium channels may not be involved.

DISCUSSION

Yokel and Crossgrove have provided convincing evidence that manganese transport into the brain is carrier mediated. In contrast, they found that manganese transport out of the brain is not carrier mediated but occurs by diffusion only: manganese efflux was found to be slower than efflux of sucrose or dextran, sugar molecules that do not easily cross the blood–brain barrier. In experiments to identify the transporters for Mn influx, the investigators convincingly ruled out the involvement of the metal transporter DMT-1, which is specific for iron uptake. However, the results of experiments to show the involvement of calcium channels or monocarboxylate transporters in transport of Mn^{2+} and Mn citrate into the brain were inconclusive. The investigators confirmed that Mn is transported in association with transferrin. It is likely that multiple pathways of manganese transport operate in parallel, with several different carriers transporting different forms of manganese across the blood–brain barrier.

The finding of manganese efflux via diffusion rather than carrier-mediated transport has important implications for possible neurotoxicity resulting from chronic manganese exposure because it indicates that no mechanism exists to protect the brain against accumulation of manganese. As these investigators have shown, manganese is transported rapidly into the brain but much more slowly out of the brain, resulting in a potential for accumulation

with chronic exposure. These results support observations that manganese accumulated in brain tissue of individuals with liver dysfunction, who have high blood levels of manganese (Hauser et al 1996), and of occupationally exposed workers (Lucchini et al 2000), and that levels remained high years after exposed workers retired (Pal et al 1999). Chronic exposure to high levels of manganese causes irreversible damage to the nervous system, with symptoms persisting many years after exposure has ceased (Cotzias et al 1968). Some studies have found more subtle neurologic symptoms, such as decreased performance on neurobehavioral tests and poorer eye-hand coordination in workers (Lucchini et al 1995, 1999; Roels et al 1992). Similar subtle neurologic symptoms were observed in individuals exposed to manganese in ambient outdoor air; their blood levels of manganese were greater than 7.5 µg/L, significantly higher than the 0.6 to 1.0 µg/L blood levels observed in the general population (Hudnell 1999; Mergler et al 1999). Thus, Yokel and Crossgrove's results support the current understanding that the potential for manganese accumulation in the brain needs to be considered when assessing the risk resulting from exposure to manganese in the environment.

Yokel and Crossgrove reported that all three forms of Mn studied (Mn^{2+}, Mn citrate, and Mn transferrin) were readily taken up into the brain. The influx rates corresponded reasonably well with values determined by other researchers (Murphy et al 1991; Rabin et al 1993). The current study is novel in that the chemical species of Mn were carefully controlled in the in vivo experiments. The investigators confirmed transport of Mn transferrin across the blood–brain barrier. (Transferrin is known to effectively transport iron into the brain via a process called transferrin receptor-mediated endocytosis.) However, the relative importance of brain influx of manganese associated with transferrin, compared with influx of manganese via other transport mechanisms, is not entirely clear. Some previous studies (Davidsson et al 1989; Aschner et al 1999) suggested that this pathway may be more important than suggested by Yokel and Crossgrove's observations, in which uptake of Mn citrate seemed to dominate. Conversely, Malecki and colleagues (1999) concluded that transferrin seems to play a negligible role in manganese delivery to the brain. In addition, manganese transport into the brain via the olfactory bulb may play an important role (Dorman et al 2002), especially in transporting manganese associated with large particles that deposit in the nasal passages.

Yokel and Crossgrove investigated combined iron and manganese transport, but found that iron did not affect manganese uptake into the brain. These data contrast with observations that rats fed a diet with high iron concentrations showed reduced manganese uptake (Diez-Ewald et al 1968) as well as the observation that individuals with iron deficiency showed increased manganese uptake (Mena et al 1969; Roth and Garrick 2003). Chronic low dietary iron is associated with increased numbers of transferrin receptors, leading to enhanced iron uptake (Feelders et al 1999). In this situation, the increased number of transferrin receptors and low levels of iron would allow for more effective uptake of manganese. Possibly Yokel and Crossgrove did not observe an effect of iron on manganese uptake because they investigated short-term rather than long-term uptake. Alternatively, there may be influences of iron on manganese uptake from the gastrointestinal tract that are not manifest at the blood–brain barrier.

Yokel and Crossgrove reported that most manganese transported across the blood–brain barrier was in the form of Mn^{2+} and Mn citrate. The investigators found the highest rates of transport for Mn citrate and concluded that it was a major form of manganese transported into the brain. They also concluded that Mn^{2+} and Mn citrate may enter the brain by different carriers, or by the same carrier at different rates. The complexity of these transport mechanisms is further illustrated by the fact that manganese may rapidly respeciate from one form to another (Reaney et al 2002). For instance, Mn^{3+} may rapidly be converted to Mn^{2+}. Likewise, Mn citrate is expected to rapidly respeciate to other forms of manganese.

Manganese has been shown to accumulate in specific brain regions. For example, high levels of manganese have been observed in the basal ganglia of humans (Hauser et al 1996; Lucchini et al 2000). Loss of dopaminergic function in the striatum, which is part of the basal ganglia, is associated with the neurologic symptoms of Parkinson disease. Several symptoms observed in manganism are similar to those of Parkinson disease (for example, loss of motor control and slurred speech) and indicate similar loss of function of the basal ganglia. However, recent studies using magnetic resonance imaging have shown manganese accumulation specifically in the globus pallidus, which is rich in neurons containing γ-aminobutyric acid, rather than the striatum (Lucchini et al 2000). Animal studies have investigated manganese accumulation in specific brain regions after inhalation exposure; some studies found evidence for accumulation in the striatum (Roels et al 1997; Tjälve et al 1996) and in the globus pallidus (Normandin et al 2002). In the current study, Yokel and Crossgrove reported high uptake rates of Mn citrate into the cortex, cerebellum, caudate nucleus, and thalamus/hypothalamus. These differences in results among studies may be due in part to the difficulty of isolating small areas of the rat brain and obtaining enough tissue to run chemical analyses. Differentiating between

areas within the basal ganglia would be difficult because, for instance, the globus pallidus occupies a much smaller area than the striatum.

Other factors that could explain differences found in brain manganese accumulation between rats and humans may be the time scale assessed and the different uptake routes. Toxicokinetic studies such as the study by Yokel and Crossgrove assess uptake within minutes of administration. Distribution across the body and accumulation in brain takes place on a much longer time scale, ranging from weeks to years. In addition, the uptake routes in humans and rats are different. Rats are obligatory nose breathers, with much larger nasal passages and olfactory bulbs, affecting the amount of manganese taken up via the direct olfactory route into the brain. However, transporters and transport mechanisms across the blood–brain barrier in rats and humans are thought to be very similar. Therefore, Yokel and Crossgrove's findings on manganese transport across the blood–brain barrier in rats and cell lines should be relevant to humans.

The mechanisms of manganese accumulation in certain brain regions have not been fully elucidated. Higher uptake rates in certain brain regions could result from a higher number of transporters in those regions. Interestingly, Yokel and Crossgrove showed that uptake rates for the caudate region were lower than those for the cortex, which did not accumulate as much manganese as the caudate. This may again be in part because they studied uptake processes over very short time periods (minutes), whereas manganese accumulation takes place over months and years. The difficulty in relating short-term uptake to long-term accumulation is further illustrated by the fact that manganese concentrations in brain continue to increase for weeks after exposure has ceased (Newland et al 1987).

Manganese taken up by the olfactory bulb may travel via the neuronal axons to other brain areas. Manganese has been shown to cross the synaptic cleft between neurons, allowing transport throughout the brain (Tjälve et al 1996). In addition, after crossing the blood–brain barrier, manganese has been shown to enter astrocytes (see sidebar 1; Aschner et al 1992). Astrocytes incorporate manganese into the astrocyte-specific enzyme glutamine synthetase, which accounts for about 80% of brain manganese (Wedler and Denman 1984). Hence, several studies have focused on the role of astrocytes in manganese transport and accumulation (Aschner et al 1992; Malecki et al 1999). Yokel and Crossgrove's experiments were not designed to assess olfactory transport or uptake into astrocytes. However, the investigators showed high rates of manganese uptake into the choroid plexus, which may provide another route of entry into the brain. In the choroid plexus, manganese may cross the blood–cerebrospinal fluid barrier and thereby enter the cerebrospinal fluid, which flows through the brain ventricular system, reaching many brain areas. Whether the choroid plexus accumulates manganese or distributes it into the cerebrospinal fluid is unclear, leaving uncertainty about the importance of this pathway is for manganese entry into the brain.

After confirming carrier-mediated manganese transport into the brain, Yokel and Crossgrove performed several in vitro and in vivo experiments to investigate putative transporter candidates. They focused on several known transporters, such as DMT-1, which is involved in iron transport across the blood–brain barrier. Because of the interactions between iron and manganese uptake, the DMT-1 transporter would be a logical candidate for manganese transport, specifically in connection with transport via transferrin. Yokel and Crossgrove did not find evidence for the involvement of DMT-1, however, because manganese uptake in rats lacking and those expressing a functional DMT-1 transporter were the same. Yokel and Crossgrove also investigated the possible involvement of calcium transporters or monocarboxylate transporters but did not provide conclusive evidence for their involvement. In addition to the carriers investigated by Yokel and Crossgrove, others may be involved in manganese transport, such as the choline transporter (Lockman et al 2001), the dopamine reuptake carrier, or other neurotransmitter reuptake carriers (Ingersoll et al 1995). In part, the lack of conclusive evidence stems from a general lack of specificity of the pharmacologic agents used, a common challenge in this type of study. Approaches involving knockout mice or rats, in which specific carriers are nonfunctional, are recommended for future experiments. In conclusion, more research is needed to firmly identify the manganese transporters. Such information would greatly assist in characterizing transporter distribution in the brain and thus help us to understand the determinants of regional distribution of manganese across the brain and relate them to the neurotoxic consequences.

SUMMARY AND CONCLUSIONS

Yokel and Crossgrove have provided convincing evidence that manganese enters the brain via carrier-mediated transport, confirming and extending previous observations. They also are the first to have shown that manganese leaves the brain by diffusion only, a much slower process than carrier-mediated transport. Experiments conducted to identify the transporters involved in manganese uptake into the brain suggested that the divalent metal transporter DMT-1, which is specific for iron uptake, is not involved.

However, the identity of the putative manganese transporters remains elusive.

The finding that manganese transport out of the brain occurs via the slow process of diffusion, rather than via carrier-mediated transport, is important: it suggests that no mechanism exists to protect the brain from accumulating manganese from across the blood–brain barrier or via the olfactory bulb. This finding has important implications for neurotoxicity resulting from chronic manganese exposure. Although Yokel and Crossgrove studied manganese transport rates in rats, their observations may be relevant to humans because transport mechanisms at the blood–brain barrier are similar in rodents and humans. Their results support the current understanding that the potential for manganese accumulation in the brain should be considered when assessing risk from exposure to manganese in the environment. Future studies and risk assessments should also consider susceptible populations (such as people with iron deficiencies or liver disease) who may be at greater risk from increased manganese uptake. New research would be useful to confirm the lack of a carrier-mediated transport system for removing manganese from the brain and to address the relevance of these findings to humans.

ACKNOWLEDGMENTS

The Health Review Committee thanks the ad hoc reviewers for their help in evaluating the scientific merit of the Investigators' Report. The Committee is also grateful to Martha Richmond and Geoffrey Sunshine for their oversight of the study, to Annemoon van Erp and Matthew Jones for their assistance in preparing its Commentary, and to Genevieve MacLellan, Sally Edwards, Jenny Lamont, Melissa Harke, and Quentin Sullivan for their roles in publishing this Research Report.

REFERENCES

Agency for Toxic Substances and Disease Registry (US). 1994. Toxicological Profile for Zinc. US Department of Health and Human Services, Public Health Service, Atlanta GA.

Agency for Toxic Substances and Disease Registry (US). 2000. Toxicological Profile for Manganese. US Department of Health and Human Services, Public Health Service, Atlanta GA.

Agency for Toxic Substances and Disease Registry (US). 2002. Toxicological Profile for Copper; Draft for Public Comment. US Department of Health and Human Services, Public Health Service, Atlanta GA.

American Conference of Governmental Industrial Hygienists. 2003. 2003 TLVs and BEIs: Based on the Documentation of the Threshold Limit Values for Chemical Substances and Physical Agents & Biological Exposure Indices. ACGIH, Cincinnati OH.

Andersen ME, Gearhart JM, Clewell HJ III. 1999. Pharmacokinetic data needs to support risk assessments for inhaled and ingested manganese. Neurotoxicology 20:161–171.

Apostoli P, Lucchini R, Alessio L. 2000. Are current biomarkers suitable for the assessment of manganese exposure in individual workers? Am J Ind Med 37:283–290.

Aschner M, Gannon M, Kimelberg HK. 1992. Manganese uptake and efflux in cultured rat astrocytes. J Neurochem 58:730–735.

Aschner M, Vrana KE, Zheng W. 1999. Manganese uptake and distribution in the central nervous system (CNS). Neurotoxicology 20:173–180.

Carter JD, Ghio AJ, Samet JM, Devlin RB. 1997. Cytokine production by human airway epithelial cells after exposure to an air pollution particle is metal-dependent. Toxicol Appl Pharmacol 146:180–188.

Clayton CA, Pellizzari ED, Rodes CE, Mason RE, Piper LL. 1999. Estimating distributions of long-term particulate matter and manganese exposures for residents of Toronto, Canada. Atmos Environ 33:2515–2526.

Cotzias GC, Horiuchi K, Fuenzalida S, Mena I. 1968. Chronic manganese poisoning: Clearance of tissue manganese concentrations with persistance of the neurological picture. Neurology 18:376–382.

Couper J. 1837. On the effects of black oxide of manganese when inhaled into the lungs. Br Ann Med Pharmacy, Vital Stat Gen Sci 1:41–42.

Crump KS. 2000. Manganese exposures in Toronto during use of the gasoline additive, methylcyclopentadienyl manganese tricarbonyl. J Expos Anal Environ Epidemiol 10:227–239.

Davidsson L, Lonnerdal B, Sandstrom B, Kunz C, Keen CL. 1989. Identification of transferrin as the major plasma carrier protein for manganese introduced orally or intravenously or after in vitro addition in the rat. J Nutr 119:1461–1464.

Davis JM. 1998. Methylcyclopentadienyl manganese tricarbonyl: Health risk uncertainties and research directions. Environ Health Perspect 106(Suppl 1):191–201.

Diez-Ewald M, Weintraub LR, Crosby WH. 1968. Interrelationship of iron and manganese metabolism. Proc Soc Exp Biol Med 129:448–451.

Dorman DC, Brenneman KA, McElveen AM, Lynch SE, Roberts KC, Wong BA. 2002. Olfactory transport: A direct route of delivery of inhaled manganese phosphate to the rat brain. J Toxicol Environ Health A 65:1493–1511.

Dreher KL, Jaskot RH, Lehmann JR, Richards JH, McGee JK, Ghio AJ, Costa DL. 1997. Soluble transition metals mediate residual oil fly ash induced acute lung injury. J Toxicol Environ Health 50:285–305.

Environmental Protection Agency (US). 1984. Health Assessment Document for Manganese. Final Report. EPA/600/8-83-013F. Office of Health and Environmental Assessment, Cincinnati OH.

Environmental Protection Agency (US). 1994. Reevaluation of Inhalation Health Risks Associated with Methylcyclopentadienyl Manganese Tricarbonyl (MMT) in Gasoline. EPA/600/R-94/062. Office of Research and Development, Washington DC.

Environmental Protection Agency (US). 2003. Integrated Risk Information System: Manganese (CASRN 7439-96-5) (last updated 3/10/03). *www.epa.gov/iris/subst/0373.htm*. Accessed 8/6/03.

Feelders RA, Kuiper-Kramer EP, van Eijk HG. 1999. Structure, function and clinical significance of transferrin receptors. Clin Chem Lab Med 37:1–10.

Furchner JE, Richmond CR, Drake GA. 1966. Comparative metabolism of radionuclides in mammals: 3. Retention of manganese-54 in the mouse, rat, monkey and dog. Health Phys 12:1415–1423.

Greger JL. 1999. Nutrition *versus* toxicology of manganese in humans: Evaluation of potential biomarkers. Neurotoxicology 20:205–212.

Greger JL, Davis CD, Suttie JW, Lyle BJ. 1990. Intake, serum concentrations, and urinary excretion of manganese by adult males. Am J Clin Nutr 51:457–461.

Gunter TE, Miller LM, Gavin CE, Eliseev R, Salter J, Buntinas L, Alexandrov A, Hammond S, Gunter KK. 2004. Determination of the oxidation states of manganese in brain, liver, and heart mitochondria. J Neurochem. In press.

Hauser RA, Zesiewicz TA, Martinez C, Rosemurgy AS, Olanow CW. 1996. Blood manganese correlates with brain magnetic resonance imaging changes in patients with liver disease. Can J Neurol Sci 23:95–98.

Hudnell HK. 1999. Effects from environmental Mn exposures: A review of the evidence from non-occupational exposure studies. Neurotoxicology 20:379–397.

Ingersoll RT, Montgomery EB Jr, Aposhian HV. 1995. Central nervous system toxicity of manganese: I. Inhibition of spontaneous motor activity in rats after intrathecal administration of manganese chloride. Fundam Appl Toxicol 27:106–113.

Institute of Medicine (US). 2003. Dietary Reference Intakes for Vitamin A, Vitamin K, Arsenic, Boron, Chromium, Copper, Iodine, Iron, Manganese, Molybdenum, Nickel, Silicon, Vanadium, and Zinc. National Academy Press, Washington DC.

Kaiser J. 2003. Manganese: A high-octane dispute. Science 300:926–928.

Kandel ER, Schwartz JH, Jessell TM (eds). 1991. Principles of Neural Science, 3rd edition. Appleton & Lange, Norwalk CT.

Krieger D, Krieger S, Jansen O, Gass P, Theilmann L, Lichtnecker H. 1995. Manganese and chronic hepatic encephalopathy. Lancet 346:270–274.

Levy BS, Nassetta WJ. 2003. Neurologic effects of manganese in humans: A review. Int J Occup Environ Health 9:153–163.

Liccione JJ, Maines MD. 1988. Selective vulnerability of glutathione metabolism and cellular defense mechanisms in rat striatum to manganese. J Pharmacol Exp Ther 247:156–161.

Lockman PR, Roder KE, Allen DD. 2001. Inhibition of the rat blood-brain barrier choline transporter by manganese chloride. J Neurochem 79:588–594.

Loranger S, Zayed J. 1994. Manganese and lead concentrations in ambient air and emission rates from unleaded and leaded gasoline between 1981 and 1992 in Canada: A comparative study. Atmos Environ 28:1645–1651.

Lucchini R, Albini E, Placidi D, Gasparotti R, Pigozzi MG, Montani G, Alessio L. 2000. Brain magnetic resonance imaging and manganese exposure. Neurotoxicology 21:769–775.

Lucchini R, Apostoli P, Perrone C, Placidi D, Albini E, Migliorati P, Mergler D, Sassine M-P, Palmi S, Alessio L.

1999. Long term exposure to "low levels" of manganese oxides and neurofunctional changes in ferroalloy workers. Neurotoxicology 20:287–297.

Lucchini R, Selis L, Folli D, Apostoli P, Mutti A, Vanoni O, Iregren A, Alessio L. 1995. Neurobehavioral effects of manganese in workers from a ferroalloy plant after temporary cessation of exposure. Scand J Work Environ Health 21:143–149.

Malecki EA. 2001. Manganese toxicity is associated with mitochondrial dysfunction and DNA fragmentation in rat primary striatal neurons. Brain Res Bull 55:225–228.

Malecki EA, Devenyi AG, Beard JL, Connor JR. 1999. Existing and emerging mechanisms for transport of iron and manganese to the brain. J Neurosci Res 56:113–122.

Mena I, Horiuchi K, Burke K, Cotzias GC. 1969. Chronic manganese poisoning: Individual susceptibility and absorption of iron. Neurology 19:1000–1006.

Mergler D, Baldwin M, Bélanger S, Larribe F, Beuter A, Bowler R, Panisset M, Edwards R, de Geoffroy A, Sassine M-P, Hudnell K. 1999. Manganese neurotoxicity, a continuum of dysfunction: Results from a community based study. Neurotoxicology 20:327–342.

Murphy VA, Wadhwani KC, Smith QR, Rapoport SI. 1991. Saturable transport of manganese(II) across the rat blood-brain barrier. J Neurochem 57:948–954.

National Institute for Occupational Safety and Health (US). 2003. NIOSH Pocket Guide to Chemical Hazards (NPG). NIOSH 97-140. NIOSH, Cincinnati OH.

National Research Council (US). 1980. Drinking Water and Health. Vol 3, pp 331–337. National Academy Press, Washington DC.

Needleman HL. 1993. The current status of childhood low-level lead toxicity. Neurotoxicology 14:161–166.

Newland MC, Cox C, Hamada R, Oberdorster G, Weiss B. 1987. The clearance of manganese chloride in the primate. Fundam Appl Toxicol 9:314–328.

Normandin L, Panisset M, Zayed J. 2002. Manganese neurotoxicity: Behavioral, pathological, and biochemical effects following various routes of exposure. Rev Environ Health 17:189–217.

Occupational Safety and Health Administration (US). 1998. Table Z-1 Limits for Air Contaminants. Regulations (Standards 29 CFR). Part 1910.1000 Table Z-1. *www.osha.gov/pls/oshaweb/owadisp.show_document?p_table=STANDARDS&p_id=9992*. Accessed 8/7/03.

Pal PK, Samii A, Calne DB. 1999. Manganese neurotoxicity: A review of clinical features, imaging and pathology. Neurotoxicology 20:227–238.

Pellizzari ED, Clayton CA, Rodes CE, Mason RE, Piper LL, Fort B, Pfeifer G, Lynam D. 1999. Particulate matter and manganese exposures in Toronto, Canada. Atmos Environ 33:721–734.

Pellizzari ED, Clayton CA, Rodes CE, Mason RE, Piper LL, Fort B, Pfeifer G, Lynam D. 2001. Particulate matter and manganese exposures in Indianapolis, Indiana. J Expos Anal Environ Epidemiol 11:423–440.

Rabin O, Hegedus L, Bourre J-M, Smith QR. 1993. Rapid brain uptake of manganese(II) across the blood-brain barrier. J Neurochem 61:509–517.

Reaney SH, Kwik-Uribe CL, Smith DR. 2002. Manganese oxidation state and its implications for toxicity. Chem Res Toxicol 15:1119–1126.

Roels HA, Ghyselen P, Buchet JP, Ceulemans E, Lauwerys RR. 1992. Assessment of the permissible exposure level to manganese in workers exposed to manganese dioxide dust. Br J Ind Med 49:25–34.

Roels H, Lauwerys R, Buchet JP, Genet P, Sarhan MJ, Hanotiau I, de Fays M, Bernard A, Stanescu D. 1987. Epidemiological survey among workers exposed to manganese: Effects on lung, central nervous system, and some biological indices. Am J Ind Med 11:307–327.

Roels H, Meiers G, Delos M, Ortega I, Lauwerys R, Buchet JP, Lison D. 1997. Influence of the route of administration and the chemical form ($MnCl_2$, MnO_2) on the absorption and cerebral distribution of manganese in rats. Arch Toxicol 71:223–230.

Roth JA, Garrick MD. 2003. Iron interactions and other biological reactions mediating the physiological and toxic actions of manganese. Biochem Pharmacol 66:1–13.

Ter Haar GL, Griffing ME, Brandt M, Oberding DG, Kapron M. 1975. Methylcyclopentadienyl manganese tricarbonyl as an antiknock: Composition and fate of manganese exhaust products. J Air Pollut Control Assoc 25:858–860.

Tjälve H, Henriksson J, Tallkvist J, Larsson BS, Lindquist NG. 1996. Uptake of manganese and cadmium from the nasal mucosa into the central nervous system via olfactory pathways in rats. Pharmacol Toxicol 79:347–356.

Vitarella D, Wong BA, Moss OR, Dorman DC. 2000. Pharmacokinetics of inhaled manganese phosphate in male

Sprague-Dawley rats following subacute (14-day) exposure. Toxicol Appl Pharmacol 163:279–285.

Wedler FC, Denman RB. 1984. Glutamine synthetase: the major Mn(II) enzyme in mammalian brain. Curr Top Cell Regul 24:153–169.

Wood G, Egyed M. 1994. Risk Assessment for the Combustion Products of Methylcyclopentadienyl Manganese Tricarbonyl (MMT) in Gasoline. Health Canada, Ottawa, Ontario, Canada.

World Health Organization. 1981. Environmental Health Criteria 17: Manganese. WHO, Geneva, Switzerland.

World Health Organization. 1986. Diseases Caused by Manganese and its Toxic Compounds. Early Detection of Occupational Diseases. WHO, Geneva, Switzerland.

World Health Organization. 2000. Air Quality Guidelines for Europe, 2nd edition. WHO Regional Publications, European Series 91. WHO, Regional Office for Europe, Copenhagen, Denmark.

RELATED HEI PUBLICATIONS

Report Number	Title	Principal Investigator	Date*
Research Reports			
117	Peroxides and Macrophages in Toxicity of Fine Particulate Matter	DL Laskin	2003
112	Health Effects of Acute Exposure to Air Pollution	ST Holgate	2003
	Part I. Healthy and Asthmatic Subjects Exposed to Diesel Exhaust		
	Part II. Healthy Subjects Exposed to Concentrated Ambient Particles		
111	Effect of Concentrated Ambient Particulate Matter on Blood Coagulation Parameters in Rats	C Nadziejko	2002
110	Particle Characteristics Responsible for Effects on Human Lung Epithelial Cells	AE Aust	2002
107	Emissions from Diesel and Gasoline Engines Measured in Highway Tunnels	AW Gertler	2002
	Part I. Real-World Particulate Matter and Gaseous Emissions from Motor Vehicles in a Highway Tunnel	D Grosjean	2002
	Part II. Airborne Carbonyls from Motor Vehicle Emissions in Two Highway Tunnels	L Kobzik	2001
106	Effects of Combined Ozone and Air Pollution Particle Exposure in Mice	GD Leikauf	2001
105	Pathogenomic Mechanisms for Particulate Matter Induction of Acute Lung Injury and Inflammation in Mice	R Vincent	2001
104	Inhalation Toxicology of Urban Ambient Particulate Matter: Acute Cardiovascular Effects in Rats		2001
102	Metabolism of Ether Oxygenates Added to Gasoline	J-Y Hong	
	Human Cytochrome P450 Isozymes in Metabolism and Health Effects of Gasoline Ethers	W Dekant	
	Biotransformation of MTBE, ETBE, and TAME After Inhalation or Ingestion in Rats and Humans	JM Benson	
	MTBE Inhaled Alone and in Combination with Gasoline Vapor: Uptake, Distribution, Metabolism, and Excretion in Rats	P Gerde	2001
101	Epithelial Penetration and Clearance of Particle-Borne Benzo[*a*]pyrene	G Oberdörster	2000
96	Acute Pulmonary Effects of Ultrafine Particles in Rats and Mice	JJ Godleski	2000
91	Mechanisms of Morbidity and Mortality from Exposure to Ambient Air Particles	T Burbacher	1999
89	Reproductive and Offspring Developmental Effects Following Maternal Inhalation Exposure to Methanol in Nonhuman Primates		
	Part I. Methanol Disposition and Reproductive Toxicity in Adult Females		
	Part II. Developmental Effects in Infants Exposed Prenatally to Methanol	MA Medinsky	1997
77	Pharmacokinetics of Methanol and Formate in Female Cynomolgus Monkeys Exposed to Methanol Vapors	GM Pollack	1996
74	Maternal-Fetal Pharmacokinetics of Methanol		

Continued

* *Reports published since 1990.*
Copies of these reports can be obtained from the Health Effects Institute and many are available at www.healtheffects.org.

RELATED HEI PUBLICATIONS

Report Number	Title		Date*
Research Reports (*Continued*)			
73	Developmental Neurotoxicity of Methanol Exposure by Inhalation in Rats	B Weiss	1996
68	Pulmonary Toxicity of Inhaled Diesel Exhaust and Carbon Black in Chronically Exposed Rats		
	Part I. Neoplastic and Nonneoplastic Lung Lesions	JL Mauderly	1994
	Part II. DNA Damage	K Randerath	1995
	Part III. Examination of Possible Target Genes	SA Belinsky	1995
42	Effects of Methanol Vapor on Human Neurobehavioral Measures	MR Cook	1991
Special Reports			
	Revised Analyses of Time-Series Studies of Air Pollution and Health		2003
	Reanalysis of the Harvard Six Cities Study and the American Cancer Society Study of Particulate Air Pollution and Mortality: A Special Report of the Institute's Particle Epidemiology Reanalysis Project		2000
	Particulate Air Pollution and Daily Mortality: The Phase I Report of the Particle Epidemiology Evaluation Project		
	Phase I.A. Replication and Validation of Selected Studies		1995
	Phase I.B. Analyses of the Effects of Weather and Multiple Air Pollutants		1997
	The Potential Health Effects of Oxygenates Added to Gasoline: A Review of the Current Literature		1996
	Automotive Methanol Vapors and Human Health: An Evaluation of Existing Scientific Information and Issues for Future Research		1987
HEI Communications			
9	Evaluation of Human Health Risk from Cerium Added to Diesel Fuel		2001
8	The Health Effects of Fine Particles: Key Questions and the 2003 Review (Report of the Joint Meeting of the EC and HEI)		1999
5	Formation and Characterization of Particles: Report of the 1996 HEI Workshop		1996
HEI Research Program Summaries			
	Research on Diesel Exhaust and Other Particles		2003
	Research on Particulate Matter		1999
	Research on Air Toxics		1999
	Research on Oxygenates Added to Gasoline		1997
HEI Perspectives			
	Understanding the Health Effects of Components of the Particulate Matter Mix: Progress and Next Steps		2002
	Airborne Particles and Health: HEI Epidemiologic Evidence		2001

** Reports published since 1990, with exceptions.*
Copies of these reports can be obtained from the Health Effects Institute and many are available at www.healtheffects.org.

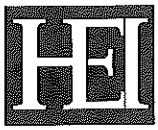

HEALTH
EFFECTS
INSTITUTE

Charlestown Navy Yard
120 Second Avenue
Boston MA 02129-4533 USA
+1-617-886-9330
www.healtheffects.org

RESEARCH
REPORT

Number 119
January 2004